Recommendations for the Formulation of Grazing in Marine Biogeochemical and Ecosystem Models

Tyler Rohr[1], Anthony J. Richardson[2,3], Andrew Lenton[4,5], Elizabeth Shadwick[1,4,5]

[1]Australian Antarctic Partnership Program, Hobart, TAS, Australia
[2]School of Mathematics and Physics, The University of Queensland, St Lucia, Queensland, Australia
[3]Commonwealth Scientific and Industrial Research Organisation (CSIRO) Oceans and Atmosphere, BioSciences Precinct (QBP), St Lucia, Queensland, Australia
[4]Commonwealth Scientific and Industrial Research Organisation (CSIRO) Oceans and Atmosphere, Hobart, TAS, Australia
[5]Centre for Southern Hemisphere Oceans Research, Hobart, TAS, Australia

Key Points:

- We review the derivation of the functional response equations, unified across all common response types and parameter schemes, which should benefit a range of marine models.
- Zooplankton grazing parameter values vary by 3 to 4 orders of magnitude with inconsistent allometric relationships, both in models and experiments.
- The apparent mean functional response, averaged across sufficient sub-grid scale heterogeneity, begins to resembles the shape and parameter sensitivity of a type III Michaelis-Menten response even when a local type II disk response is prescribed.
- We recommend a type II disk response in smaller scale, finer resolution models but a type III Michaelis-Menten response in larger scale, coarser resolution models.
- We recommend considering a wide range of $K_{1/2}$ values, particularly low ones.

Corresponding author: Tyler Rohr, tyler.rohr@csiro.au

Abstract

For nearly a century, functional reizes beingponse curves, which describe how predation rates vary with prey density, have been a mainstay of ecological modelling. While originally derived to describe terrestrial interactions, they have been adopted to characterize aquatic systems in marine biogeochemical, size-spectrum, and population models. However, marine ecological modellers disagree over the qualitative shape of the curve (e.g. Type II vs. III), whether its parameters should be mechanistically or empirically defined (e.g. disk vs. Michaelis-Menten scheme), and the most representative value of those parameters. As a case study, we focus on marine biogeochemical models, providing a comprehensive theoretical, empirical, and numerical road-map for interpreting, formulating, and parameterizing the functional response when used to prescribe zooplankton specific grazing rates on a single prey source. After providing a detailed derivation of each of the canonical functional response types explicitly for aquatic systems, we review the literature describing their parameterization. Empirical estimates of each parameter vary by over three orders of magnitude across 10 orders of magnitude in zooplankton size. However, the strength and direction of the allometric relationship between each parameter and size differs depending on the range of sizes considered. In models, which must represent the mean state of different functional groups, size spectra or in many cases the entire zooplankton community, the range of parameter values is smaller, but still varies by two to three orders of magnitude. Next, we conduct a suite of 0-D NPZ simulations to isolate the sensitivity of phytoplankton population size and stability to the grazing formulation. We find that the disk parameterizations scheme is less sensitive to it's parameterization than the Michaelis-Menten scheme, and quantify the range of parameters over which the Type II response, long known to have destabilizing properties, introduces dynamic instabilities. Finally, we use a simple theoretical model to show how the mean apparent functional response, averaged across sufficient sub-grid scale heterogeneity, diverges from the local response. Collectively, we recommend using a type II disk response for models with smaller scales and finer resolutions but suggest that a type III Michaelis-Menten response may do a better job of capturing the complexity of all processes being averaged across in larger-scale and coarser-resolution models, not just local consumption and capture rates. While we focus specifically on the grazing formulation in marine biogeochemical models, we believe these recommendations are robust across a much broader range of population and ecosystem models that use functional response curves.

1 Introduction

In the late 1950s, Buzz Holling began studying the predation of sawfly cocoons by small mammals (Holling, 1959a) to better understand how predation rates varied with prey density, a relationship coined a decade earlier as the functional response (Solomon, 1949). Holling observed that individual predators consumed more prey at higher prey densities, but found that this relationship was not necessarily linear or consistent across species. Over the course of three seminal papers, Holling developed a theoretical framework to describe how different assumptions about the rates at which predators captured and consumed their prey could explain observed nonlinearities and variability in the shape of functional response curve (Holling, 1959a, 1959b, 1965). Using this mechanistic approach, Holling derived three qualitatively distinct response types to describe differences in predator-prey interactions and their associated rates. In the ensuing decades, these equations have been further generalized (Real, 1977, 1979) and cemented into the bedrock of ecological modelling (Beardsell et al., 2021; Denny, 2014).

Although the functional response was originally developed for terrestrial applications (Holling, 1959a), the equations are also common in marine ecological modelling (Evans & Parslow, 1985; Fasham, 1995; Franks, Wroblewski, & Flierl, 1986). In the ocean, the functional response equations are now routinely used to link trophic dynamics in ma-

rine biogeochemical (Law et al., 2017; Moore, Lindsay, Doney, Long, & Misumi, 2013), size spectrum (Heneghan et al., 2020), and population models (Alver, Broch, Melle, Bagøien, & Slagstad, 2016). They are used to simulate both the rate at which heterotrophic zooplankton graze on autotrophic phytoplankton (Evans & Parslow, 1985; Franks et al., 1986) as well as the transfer of mass and energy further up the food chain in ecosystem (Butenschön et al., 2016) and fisheries models (Maury, 2010; Tittensor et al., 2018, 2021).

However, there remains a great deal of uncertainty surrounding the formulation of the functional response. For example, trade offs between the ecological veracity and numerical stability of different response types (Gismervik, 2005; Morozov, 2010; Morozov, Arashkevich, Reigstad, & Falk-Petersen, 2008) have led to disagreement over which is best suited for rapidly growing, easily perturbed, microbial systems common in marine ecology (Fasham, 1995; Flynn & Mitra, 2016; Gentleman & Neuheimer, 2008). Even amongst mathematically identical curves, there is not a consensus on how to define their parameters, no less prescribe them. While some modellers opt for a parameter scheme that mirrors the Michaelis–Menten (Michaelis & Menten, 1913) and Monod (Monod, 1949) equations developed to describe enzyme kinetics and bacterial growth rates (Aumont & Bopp, 2006; Dutkiewicz et al., 2015; Moore et al., 2013; Vichi, Pinardi, & Masina, 2007), others use a parameter scheme that mirrors the disk equation (Holling, 1959b, 1965) developed by Holling to describe terrestrial interactions (Fasham, 1995; Laws, Falkowski, Smith, Ducklow, & McCarthy, 2000; Oke et al., 2013; Schartau & Oschlies, 2003b). While the parameters used in the Michaelis–Menten scheme are overtly empirical, those used in the disk scheme are theoretically mechanistic. Disagreement over which parameter set to use can confuse inter-model comparisons and influence the parameter space considered in optimization schemes, especially when there are no robust observations to bound them.

Here, we focus on the formulation of grazing in marine biogeochemical models, which are a critical component of coupled earth system models used to simulate climate (Eyring et al., 2016; Flato et al., 2013; Taylor, Stouffer, & Meehl, 2012) and are often used to drive fisheries models (Maury, 2010; Tittensor et al., 2018, 2021). These models are increasingly under constrained and over parameterized (Doney, 1999; Matear, 1995; Schartau et al., 2017; Ward, Friedrichs, Anderson, & Oschlies, 2010). Accurately representing grazing is critical to both climate and ecosystem models, as it mediates the biological transport of carbon fixed via net primary production (Behrenfeld, Doney, Lima, Boss, & Siegel, 2013; Laufkötter et al., 2015) and transported to higher trophic levels via secondary production (Brander, 2007; Scherrer et al., 2020). Still, despite the growing recognition that biogeochemical models are highly sensitive to the grazing formulation (Adjou, Bendtsen, & Richardson, 2012; T. Anderson, Gentleman, & Sinha, 2010; Chenillat, Rivière, & Ohman, 2021; Fasham, 1995; Flynn & Mitra, 2016; Fussmann & Blasius, 2005; Gentleman & Neuheimer, 2008; Gross, Ebenhöh, & Feudel, 2004), it remains challenging to constrain global zooplankton dynamics using a limited number of simplified equations, state variables, and parameters. Most biogeochemical models represent only 1-2 zooplankton functional groups, but parameters inferred empirically vary considerably across zooplankton species, size and age (Hansen, Bjørnsen, & Hansen, 1997; Hirst & Bunker, 2003). Allometric models can vary parameters across size classes, but measured allometric relationships are not always robust (Hansen et al., 1997). Even once parameters are chosen, global simulations cannot be easily validated because we lack the required spatial resolution in observed distributions of zooplankton biomass and their associated grazing parameters (but see Moriarty, Buitenhuis, Le Quéré, and Gosselin (2013); Moriarty and O'Brien (2012)). Moreover, equations modellers must parameterize are empirical and theoretical simplifications and may not be adequate to represent the mean-state of diverse communities grazing in fundamentally different ways distributed heterogeneously across a patchy ocean.

Depending on the model, zooplankton diets range from a single generic phytoplankton to a complex portfolio of multiple phytoplankton, smaller zooplankton, and detri-

tus. When multiple prey are available, the distribution of grazing across them is determined by one of many multiple-prey response functions, which can take into account both the relative distribution of prey options and their intrinsic desirability (Fasham, Ducklow, & McKelvie, 1990). These equations, which are typically extensions of the single-prey response functions, have been reviewed in detail by Gentleman, Leising, Frost, Strom, and Murray (2003). Here, we focus on the single-prey response functions, which are a prerequisite for understanding the multiple-prey response functions and often describe their implied behavior when only one prey option is available. While many modern models use a multiple-prey response (Aumont, Ethé, Tagliabue, Bopp, & Gehlen, 2015; Stock et al., 2020; Totterdell, 2019; Yool et al., 2021), zooplankton grazing with a single-prey response remains common in many state-of-the-art CMIP6-class earth system models (Christian et al., 2021; Hajima et al., 2020; Law et al., 2017; Long et al., 2021; Tjiputra et al., 2020)

By combining theory, empirical data, and numerical models, we consolidate existing information and new results to develop a comprehensive guide for how the single-prey functional response is employed in marine ecological models to represent grazing. We begin by presenting a unified review of how each functional response and its associated parameter schemes are derived, providing detailed insights into how they relate to each other from first principles (**Section 2**). Next we review the mathematical influence of different grazing formulations on population stability (**Section 3**) and survey the literature to assess the range of parameter values that have been estimated empirically and used prescriptively in models (**Section 4**). Then we conduct a suite of simulations to isolate the sensitivity of phytoplankton population size and stability to the parameterization of the functional response using four different combinations of response type (i.e. II vs. III) and parameter scheme (i.e. disk vs. Michaelis-Menten; **Section 5**). Finally, we use a simple theoretical model to examine the influence of sub-grid scale heterogeneity on the shape of the functional response (**Section 6**). This work culminates with a set of recommendations for the formulation of grazing based on the evidence presented (**Section 7**). These recommendations are tailored to the single-prey representation of grazing in marine biogeochemical models, but are broadly applicable to much wider usage of the functional response across marine and terrestrial applications.

2 Derivation of the grazing formulation

The rate at which prey is grazed by zooplankton is generally expressed as the grazing rate (G) in units of prey concentration lost per unit time (e.g. $\frac{mmolC}{m^3 d}$). Here, we generally refer to prey as phytoplankton, but all results are relevant to grazing on any generic single prey (e.g. bacteria, detritus, or other zooplankton). The grazing rate is equal to the product of the ambient zooplankton concentration, $[Z]$, and the zooplankton specific grazing rate (g), often referred to as the ingestion rate (Franks et al., 1986; Gentleman & Neuheimer, 2008), which describes the concentration of phytoplankton grazed per unit zooplankton per unit time, reducing to units of one over time (e.g. $1/d$), such that

$$G = g[Z]. \tag{1}$$

To account for the intuitive fact that grazing is less successful when phytoplankton are scarce, the zooplankton specific grazing rate, g, must vary with the ambient phytoplankton concentration, $[P]$, particularly when $[P]$ is low. The mathematical formula that describes these relationships is know as the functional response.

Buzz Holling originally derived the functional response by assuming there was a fixed time interval, T, over which predator and prey were exposed (e.g. same location, same time, predator is awake), and that predators were assumed to exclusively be cap-

turing (e.g. searching, encountering, hunting, attacking) (T_{cap}) or consuming (e.g. killing, handling, processing, eating, digesting) prey (T_{con}) during this interval (Holling, 1959a), such that

$$T = T_{cap} + T_{con}. \tag{2}$$

The canonical type I, II, and III functional responses (**Fig. 1a**) were consequently derived (**Fig. 1b**) from different assumptions (**Fig. 1c**) about the efficiency of the capture and consumption processes, the associated total time needed to capture and consume a given amount of prey, and how those rates and times vary with prey density (see **Table 1** for a catalogue of terms). However, prey density was originally expressed in discrete units of prey over a given circular area (or disk). Here, we instead provide a derivation of the type I (**Section 2.2**), II (**Section 2.3**), and III (**Section 2.4**) responses explicitly for aquatic systems, with units of concentration ($mmolC/m^3$) for phytoplankton and zooplankton communities and days (d) for time. Further, we show how each functional response can be described by two sets of parameters: the disk scheme in which the consumption and capture processes are explicitly prescribed and mechanistically defined, and the Michaelis-Menten scheme, in which the maximum grazing rate and half saturation concentration of the curve are explicitly prescribed and empirically defined. Note, many of these equations have been derived in various forms and various contexts before (Aksnes & EGGE, 1991; Caperon, 1967). Here, we present them together, specifically in the context of zooplankton grazing, with careful attention to how they relate theoretically and mathematically to each other and first principles.

For each derivation, consider some concentration of phytoplankton, $[P_G]$ ($mmolC/m^3$), that is grazed (i.e. captured and consumed) by the ambient zooplankton community, $[Z]$ ($mmolC/m^3$), over the fixed grazing (or exposure) interval, T (d), at a grazing rate of $G = \frac{[P_G]}{T}$ and a zooplankton specific (i.e. considering the amount of predator present) grazing rate of $g = \frac{[P_G]}{[Z]T}$. To derive each functional response type, $g([P])$, we must solve for g ($1/d$) in terms of the ambient phytoplankton population, $[P]$ ($mmolC/m^3$), considering their respective assumptions regarding capture and consumption rates.

2.1 Type 0 response

A type 0 functional response is described by a straight horizontal line in which a zooplankton specific grazing rate is invariant to the ambient phytoplankton population ($g([P]) = constant$, **Fig. 1**; magenta). A type 0 response is not ecologically realistic for any species, nor does it appear in any models, but for pedagogical purposes assumes that the capture process is unaffected by prey scarcity and that the consumption process is negligible.

2.2 Type I response

A type I functional response is described by a straight line (Holling, 1959b), in which the zooplankton specific grazing rate ($g([P])$) increases linearly with the ambient phytoplankton concentration (**See Fig. 1**; black). Ecologically, a type I response assumes that zooplankton capture prey faster when it is more abundant and that the time needed to consume it is negligible compared with the time needed to capture it ($T_{cap} >> T_{con}$). Accordingly, zooplankton can spend all of their time capturing prey, such that

$$T = T_{cap}. \tag{3}$$

a.

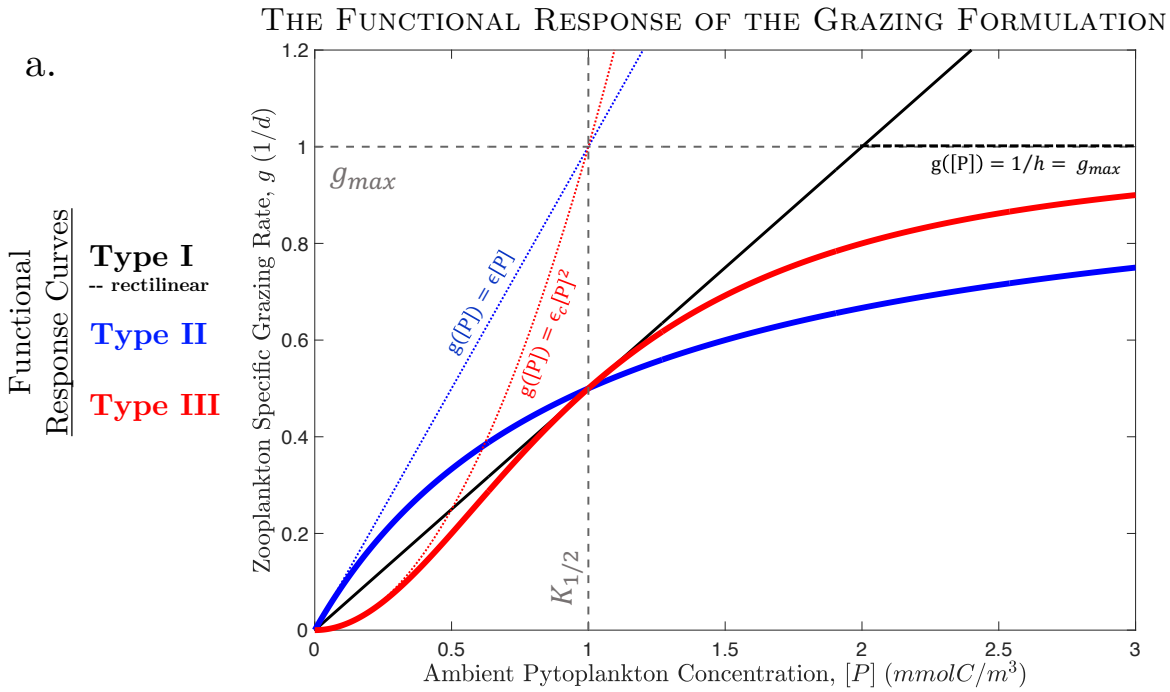

b.

	Type I	**Type II**	**Type III**
Capture Rate	$E = \epsilon[\mathrm{P}]$	$E = \epsilon[\mathrm{P}]$	$E = \epsilon[\mathrm{P}] = \epsilon_c[P]^2$
Theoretical Assumptions	**Zooplankton** capture prey easier (faster) when there is more	Zooplankton capture prey easier (faster) when there is more	Zooplankton learn to be more efficient hunters when exposed to more prey
Consumption Time	$h = 0$	$h = 1/g_{max}$	$h = 1/g_{max}$
Theoretical Assumptions	**Zooplankton** take no time consuming prey and spend all their time capturing.	Zooplankton spend a fixed amount of time consuming each phytoplankton.	Zooplankton spend a fixed amount of time consuming each phytoplankton.
Mass Balance of Time (for derivation)	$\mathrm{T} = \underset{\text{Capturing}}{\frac{[P_G]}{\epsilon[\mathrm{P}][\mathrm{Z}]}} + \underset{\text{Consuming}}{0}$	$\mathrm{T} = \underset{\text{Capturing}}{\frac{[P_G]}{\epsilon[\mathrm{P}][\mathrm{Z}]}} + \underset{\text{Consuming}}{\frac{\mathrm{h}[P_G]}{[\mathrm{Z}]}}$	$\mathrm{T} = \underset{\text{Capturing}}{\frac{[P_G]}{\epsilon_c[\mathrm{P}]^2[\mathrm{Z}]}} + \underset{\text{Consuming}}{\frac{\mathrm{h}[P_G]}{[\mathrm{Z}]}}$
Disk Formulation	$\mathrm{g} = \epsilon[\mathrm{P}]; \quad [P] < \frac{g_{max}}{\epsilon}$ (rectilinear) $\mathrm{g} = g_{max}; \quad [P] > \frac{g_{max}}{\epsilon}$	$\mathrm{g} = \frac{g_{max}\epsilon[P]}{g_{max} + \epsilon[P]}$	$\mathrm{g} = \frac{g_{max}\epsilon_c[P]^2}{g_{max} + \epsilon_c[P]^2}$
Michaelis-Menten Formulation	$\mathrm{g} = \frac{g_{max}}{2K_{1/2}}[\mathrm{P}]; \quad [P] < 2K_{1/2}$ (rectilinear) $\mathrm{g} = g_{max}; \quad [P] > 2K_{1/2}$	$\mathrm{g} = \frac{g_{max}[P]}{K_{1/2} + [P]}$	$\mathrm{g} = \frac{g_{max}[P]^2}{K_{1/2}^2 + [P]^2}$
Parameter Relationship	$\epsilon = g_{max}/2K_{1/2}$	$\epsilon = g_{max}/K_{1/2}$	$\epsilon_c = g_{max}/K_{1/2}^2$

Figure 1. The functional response of the grazing formulation. **a.** The zooplankton specific grazing rate (or ingestion rate) as a function of prey density, known as the the functional response curve is plotted for a type I, II, and III response, along with **b.** a description of their associated attributes, assumptions, and formulations. Each response type is parameterized such that the maximum specific grazing rate, g_{max}, and the half saturation concentration, $K_{1/2}$, are equal to one. Note, this requires different parameters for the disk parameter scheme. Dashed lines in **a.** show what each response reduces to at low and high prey densities.

Variable	Notation	Conceptual Units	Reduced Units	Relevant Relationships	Description
Phytoplankton concentrations	$[P]$, $[P_G]$, $[P_{Cap}]$, $[P_{Con}]$	$[P]$	$\frac{mmolC}{m^3}$	$[P_G] = GT = g[Z]T$ $[P_G] = [P_{Cap}] = [P_{Con}]$	Concentration of ambient, grazed (i.e. captured and consumed), captured, and consumed phytoplankton over the exposure period, respectively
Zooplankton concentration	$[Z]$	$[Z]$	$\frac{mmolC}{m^3}$	-	Concentration of zooplankton biomass
Functional response	g([P])	$\frac{[P]}{[Z]time}$	$\frac{1}{d}$	$g([P]) = \epsilon[P]$ (I) $= \frac{g_{max}}{2K_{1/2}}[P]$ (I-Rect) $g([P]) = \frac{g_{max}\epsilon[P]}{g_{max}+\epsilon[P]}$ (II) $= \frac{g_{max}[P]}{K_{1/2}+[P]}$ $g([P]) = g_{max}(1-e^{-\lambda[P]})$ (II-Iv) $g([P]) = \frac{g_{max}\epsilon_c[P]^2}{g_{max}+\epsilon_c[P]^2}$ (III) $= \frac{g_{max}[P]^2}{K_{1/2}^2+[P]^2}$	Functional description of how the zooplankton specific grazing rate varies with the phytoplankton concentration
Half saturation concentration	$K_{1/2}$	$[P]$	$\frac{mmolC}{m^3}$	$K_{1/2} = \frac{g_{max}}{2\epsilon}$ (II-R) $K_{1/2} = \frac{g_{max}}{\epsilon}$ (II) $K_{1/2} = \frac{-ln(.5)}{\lambda}$ (II-Iv) $K_{1/2} = \sqrt{\frac{g_{max}}{\epsilon_c}}$ (III)	Phytoplankton concentration where $g = \frac{g_{max}}{2}$
Maximum grazing rate	g_{max}	$\frac{[P]}{[Z]time}$	$\frac{1}{d}$	$g_{max} = \frac{1}{h}$	Rate of phytoplankton consumption per unit zooplankton when food replete
Grazing rate	G	$\frac{[P]}{time}$	$\frac{mmolC}{m^3 d}$	$G = \frac{[P_G]}{T}$ $G = g[Z]$	Rate at which phytoplankton are grazed by zooplankton
Phytoplankton specific grazing loss rate	l	$\frac{[P]}{[P]time}$	$\frac{1}{d}$	$l = \frac{G}{[P]}$	Phytoplankton specific rate at which phytoplankton are lost to grazing
Zooplankton specific grazing rate (i.e. ingestion rate)	g	$\frac{[P]}{[Z]time}$	$\frac{1}{d}$	$g = \frac{G}{[Z]}$	Zooplankton specific rate at which phytoplankton are grazed. The way in which g varies with $[P]$ is the functional response
Clearance rate	Cl	$\frac{[P]}{[P][Z]time}$	$\frac{m^3}{mmolCd}$	$Cl = \frac{G}{[P][Z]}$ $Cl = \frac{g}{[P]}$	Phytoplankton specific rate at which phytoplankton are grazed per unit zooplankton
Exposure period	T	$time$	d	$T = T_{cap} + T_{con}$	Fixed period over which zooplankton and phytoplankton are exposed
Capture period	T_{cap}	$time$	d	$T_{Cap} = \frac{[P_G]}{[Z]\epsilon[P]}$	Time spent capturing phytoplankton
Consumption period	T_{con}	$time$	d	$T_{Con} = 0$ (I) $T_{Con} = \frac{h[P_G]}{[Z]}$ (II,III)	Time spent consuming phytoplankton
Capture rate	C	$\frac{[P]}{time}$	$\frac{mmolC}{m^3 d}$	$C = \frac{[P_{cap}]}{T_{Cap}}$ $C = E[Z]$ (II) $C = \epsilon_c[Z]^2$ (III)	Rate at which phytoplankton are captured by the zooplankton
Zooplankton specific capture rate	E	$\frac{[P]}{[Z]time}$	$\frac{1}{d}$	$E = \frac{C}{[Z]}$ $E = \epsilon[P]$	Specific rate at which phytoplankton are captured per unit zooplankton
Prey capture efficiency	ϵ	$\frac{[P]}{[P][Z]time}$	$\frac{m^3}{mmolC\,d}$	$\epsilon = \epsilon_c[P]$ (III) $\epsilon = \lambda g_{max}$ (II-Iv)	Rate at which the zooplankton specific capture rate increases with the ambient phytoplankton concentration
Prey capture efficiency coefficient	ϵ_c	$\frac{[P]}{[P]^2[Z]time}$	$\frac{m^6}{mmolC^2\,d}$	-	Rate at which the prey capture efficiency increases with the ambient phytoplankton concentration
Consumption time	h	$\frac{[Z]time}{[P]}$	d	-	Time it takes for one unit of zooplankton to eat one unit of phytoplankton
Consumption rate	$\frac{1}{h}$	$\frac{[P]}{[Z]time}$	$\frac{1}{d}$	-	Rate of phytoplankton consumption per unit zooplankton
Ivlev parameter	λ	$\frac{1}{[P]}$	$\frac{m^3}{mmolC\,d}$	-	Used to parameterize Ivlev equation, which is qualitatively similar to a type II

Table 1. List of terms relevant to the derivation, parameterization and context of the functional response. Conceptual units distinguish between phytoplankton and zooplankton concentration and are not reduced.

The time, T_{cap} (d), that it takes to capture some concentration of phytoplankton, $[P_{Cap}]$ $(mmolC/m^3)$, can be related to the capture rate, C $(\frac{mmolC/m^3}{d})$, or the concentration of phytoplankton captured per unit time, by the equation

$$T_{cap} = \frac{[P_{Cap}]}{C}. \tag{4}$$

The capture rate can then be decomposed into the product of the ambient zooplankton concentration, $[Z]$ $(mmolC/m^3)$, and the zooplankton specific capture rate, E $(1/d)$, which describes the concentration of phytoplankton captured per unit zooplankton per unit time, such that

$$C = E[Z]. \tag{5}$$

Depending on the zooplankton in question, the zooplankton specific capture rate, E $(1/d)$, can represent a passive encounter rate (e.g. filter feeding) or an active search and attack rate (e.g. hunting), but does not include the time required to consume phytoplankton once captured. Either way, E $(1/d)$ is assumed to increase linearly with the ambient phytoplankton concentration, $[P]$ $(mmolC/m^3)$, to account for the fact that zooplankton are stochastically more likely to encounter and capture phytoplankton at higher ambient phytoplankton concentrations. The rate (per unit phytoplankton) at which the zooplankton specific capture rate increases with the ambient phytoplankton concentration can be considered the prey capture efficiency, ϵ $(\frac{1}{(mmolC/m^3)d})$, such that

$$E = \epsilon[P]. \tag{6}$$

The prey capture efficiency can be thought of as the fraction of the ambient phytoplankton concentration captured per unit zooplankton per unit time, in which units of $\frac{(mmolC/m^3)}{(mmolC/m^3)^2 d}$ reduce to $\frac{1}{(mmolC/m^3)d}$, and reflects the efficiency with which zooplankton can capture their prey. Note that the prey capture efficiency is variously referred to as the prey capture rate (Schartau & Oschlies, 2003b), attack rate (Gentleman & Neuheimer, 2008), affinity, and maximum clearance rate. It is also qualitatively similar to the search area defined by Holling (1959b), but not identical for concentration-based rates.

Substituting **eqs. 5 & 6** into **eq. 4** yields,

$$T_{cap} = \frac{[P_{Cap}]}{\epsilon[P][Z]}. \tag{7}$$

Next, we can substitute T_{cap} for T because of our assumption that no time is needed for zooplankton to consume phytoplankton (i.e. $T_{con} = 0$), and substitute $[P_{Cap}]$ for $[P_G]$ because the entire concentration of phytoplankton lost to grazing, $[P_G]$, must first be captured, $[P_{Cap}]$. Finally, we solve for the rate at which phytoplankton are grazed by the zooplankton community ($G = gZ = \frac{[P_G]}{T}$) as a function of $[P]$,

$$G([P]) = \frac{[P_G]}{T} = \epsilon[P][Z], \tag{8}$$

and divide by [Z] to yield the zooplankton specific grazing rate, g $(1/d)$, as a function of the ambient phytoplankton concentration $[P]$, such that,

$$g([P]) = \frac{[P_G]}{T[Z]} = \epsilon[P]. \tag{9}$$

Eq. 9 is the type I functional response, wherein $g([P])$ increases linearly with the ambient phytoplankton concentration, $[P]$, at a rate described by the prey capture efficiency, ϵ. This type of response is akin to a food-limited system in which it takes much longer to find and capture prey than it takes to consume it, and is analogous to the classic Lotka-Voltera equations (Lotka, 1910; Volterra, 1927) used to describe simple predator-prey dynamics. Note that here the grazing rate is identical to the capture rate ($G = C$) and the zooplankton specific grazing rate is identical to the zooplankton specific capture rate ($g = E = \epsilon[P]$). This is because the entire grazing process is assumed to be described by the capture process; however, this is not the case for higher order functional responses, in which zooplankton are assumed to spend a non-trivial amount of time consuming phytoplankton in addition to capturing them.

A standard type I response may be characteristic of passive filter feeders (Jeschke, Kopp, & Tollrian, 2004), but can overestimate the zooplankton specific grazing rate of mesozooplankton such as copepods (Gentleman & Neuheimer, 2008) by over an order of magnitude compared to observations (Frost, 1972; Hansen et al., 1997) because it does not account for predator satiation at high prey densities. To account for predator satiation, the type I response can be extended to a rectilinear response (Chen, Laws, Liu, & Huang, 2014; Frost, 1972; Hansen, Bjørnsen, & Hansen, 2014; Mayzaud, Tirelli, Bernard, & Roche-Mayzaud, 1998), in which $g([P])$ reaches some maximum rate, g_{max} (d^{-1}) such that

$$\begin{aligned} g([P]) &= \epsilon[P] \qquad \text{if} \quad [P] < \frac{g_{max}}{\epsilon} \\ g([P]) &= g_{max} \qquad \text{if} \quad [P] > \frac{g_{max}}{\epsilon}, \end{aligned} \tag{10}$$

where $\frac{g_{max}}{\epsilon}$ ($\frac{mmolC}{m^3}$) describes the prey concentration required to reach the maximum zooplankton specific grazing rate, g_{max}, for a given prey capture efficiency, ϵ.

Solving for $[P]$ when $g([P]) = \frac{g_{max}}{2}$ returns the half saturation concentration, $K_{1/2} = \frac{g_{max}}{2\epsilon}$. Note that parameterizing **eq. 10** with $K_{1/2}$ allows one to explicitly define the location of satiation using a single variable (as opposed to $\frac{g_{max}}{2\epsilon}$); however, changing $K_{1/2}$ with a fixed g_{max} necessarily alters the slope of the response, ϵ, and therefore implicitly alters assumptions about the prey capture efficiency.

2.3 Type II response

A type II functional response assumes a more gradual transition to satiation by employing a rectangular hyperbola with downward concavity (Holling, 1959b), in which the zooplankton specific grazing rate ($g([P])$) saturates towards a maximum asymptote at high phytoplankton concentrations (**See Fig. 1**; blue). Ecologically, a type II response assumes that zooplankton capture prey faster when it is more abundant and that a fixed, non-trivial, amount of time is needed to consume it ($T_{con} > 0$), allowing for gradual predator satiation as the prey density increases and more time is needed to consume it (Jeschke et al., 2004). Note, all assumptions about the capture process and zooplankton specific capture rate ($E = \epsilon[P]$) from the type I response are held.

The time it takes to consume the captured phytoplankton is parameterized by the consumption time, h (d), also commonly referred to as the handling time (Holling, 1959b, 1965), which is assumed to be equal to the fixed amount of time it takes for one unit of zooplankton to eat one unit of phytoplankton. The total time, T_{con} (d), needed for consumption of the entire captured phytoplankton concentration, $[P_{Cap}]$ ($mmolC/m^3$), by the ambient zooplankton concentration, $[Z]$ ($mmolC/m^3$), can then be expressed as the consumption time, h, multiplied by the ratio of the concentration of phytoplankton cap-

tured relative to the ambient concentration of zooplankton capturing them ($\frac{[P_{Cap}]}{[Z]}$), such that

$$T_{con} = \frac{h[P_{Cap}]}{[Z]}. \tag{11}$$

Remembering that all phytoplankton grazed must first be captured (i.e. $[P_G] = [P_{Cap}]$) and substituting T_{cap} and T_{con} into **eq. 2** yields

$$T = T_{cap} + T_{con} = \frac{[P_G]}{\epsilon[P][Z]} + \frac{h[P_G]}{[Z]}. \tag{12}$$

Solving for the concentration of phytoplankton lost to grazing, $[P_G]$, yields the aquatic analogue to the familiar disk equation, originally derived by Holling (1959b) for terrestrial predation on a planar disk,

$$[P_G] = \frac{\epsilon[P][Z]T}{1 + \epsilon h[P]}, \tag{13}$$

where dividing by T returns the grazing rate,

$$G = \frac{[P_G]}{T} = \frac{\epsilon[P][Z]}{1 + \epsilon h[P]}, \tag{14}$$

and dividing again by Z returns the zooplankton specific grazing rate, which is the type II functional response,

$$g([P]) = \frac{[P_G]}{[Z]T} = \frac{\epsilon[P]}{1 + \epsilon h[P]}. \tag{15}$$

Note that by factoring out $\epsilon[P]$ from the denominator and rearranging **eq. 15** as

$$g([P]) = \frac{1}{\frac{1}{\epsilon[P]} + h}, \tag{16}$$

it becomes clear that when food is limiting the type II disk equation reduces to a type I linear Lotka-Voltera functional response with a slope equal to the prey capture efficiency (**Fig. 1a;** dashed blue line). If the consumption rate ($\frac{1}{h}$) is much faster than the zooplankton specific capture rate ($E = \epsilon[P]$), such that $\frac{1}{h} >> \epsilon[P]$ or equivalently $h << \frac{1}{\epsilon[P]}$, then **eqs. 15 & 16** reduce to $g([P]) = \epsilon[P]$ (i.e. **eq. 9**). This occurs when the consumption time, h, is very fast (i.e. type I, **Section 2.1.1**), or the phytoplankton concentration, $[P]$, is very low (i.e. a food-limited system).

Alternatively, we see that **eqs. 15 & 16** saturate towards $g([P]) = 1/h$ when the consumption rate ($\frac{1}{h}$) is much slower than the zooplankton specific capture rate ($E = \epsilon[P]$), such that $\frac{1}{h} << \epsilon[P]$ or equivalently $h >> \frac{1}{\epsilon[P]}$ (**Fig. 1a**; dashed black line). This is typical of a food replete system (high $[P]$), where more food is captured as soon as the previous prey item has been consumed. The maximum grazing rate, g_{max} $(1/d)$, can now be defined by the consumption rate, or one over the consumption time, such that $g_{max} = \frac{1}{h}$. Note, however, g_{max} is approached slowly in a type II response, and $g([P])$ is still only 80% of g_{max} even when $[P] > 4K_{1/2}$.

The disk equation (**eq. 13**) can be simplified by substituting the parameter $g_{max} = \frac{1}{h}$ into **eq. 15** and multiplying by $\frac{g_{max}}{g_{max}}$ to arrive at

Type II (disk)

$$g([P]) = \frac{g_{max}\epsilon[P]}{g_{max} + \epsilon[P]}. \tag{17}$$

Henceforth, this will be referred to as the disk parameter scheme. Note, the formulation of the disk equation used here differs from the traditional form (**eq. 14**) because we replaced the handling time with its reciprocal (g_{max}), making it easier to compare with the Michaelis–Menten form of the equation (see below).

Equation 17 can be rewritten as the familiar Michaelis–Menten equation originally derived for enzyme kinetics (Michaelis & Menten, 1913) (or Monod equation derived for bacterial growth (Monod, 1949)) by defining the half-saturation concentration, $K_{1/2}$ ($mmolC/m^3$), in terms of parameters g_{max} and ϵ. Setting $g([P]) = \frac{g_{max}}{2}$ and solving for $[P]$, we find,

$$[P] = K_{1/2} = \frac{g_{max}}{\epsilon}. \tag{18}$$

Substituting $\epsilon = \frac{g_{max}}{K_{1/2}}$ into **eq. 17** and rearranging yields the familiar form,

Type II (Michaelis–Menten)

$$g([P]) = \frac{g_{max}[P]}{K_{1/2} + [P]}. \tag{19}$$

Henceforth, this will be referred to as the Michaelis–Menten parameter scheme. Note, that in the Michaelis–Menten formulation $g([P])$ still reduces to g_{max}, or $\frac{1}{h}$, when $[P] >> K_{1/2}$ and to $\frac{g_max}{K_{1/2}}$, or (**eq. 18**), when $[P] << K_{1/2}$.

Eq. 19 is mathematically identical to **eq. 17**. That is, for all parameter sets $\{g_{max}, \epsilon\}$, there exists a parameter set $\{g_{max}, K_{1/2}\}$ that can identically describe $g([P])$. As with the type I response (**eq. 10**), the difference is that $\{g_{max}, \epsilon\}$ are ecologically independent, while $\{g_{max}, K_{1/2}\}$ more directly define the shape of the curve. For example, increasing g_{max} in **eq. 17** does not affect the prey capture efficiency, ϵ, but it does increase the half-saturation concentration. This makes sense ecologically, as it should require a higher phytoplankton concentration for a faster consumption time (i.e. higher g_{max}) to become limiting, given a constant prey capture efficiency. On the other hand, increasing g_{max} in **eq. 19** does not change the location of $K_{1/2}$, but implicitly assumes that the prey capture efficiency, ϵ, increases in order to maintain a constant $K_{1/2}$.

Note, another common formulation that is qualitatively similar to the type II response is the Ivlev equation (Ivlev, 1961), where

$$g([P]) = g_{max}(1 - e^{-\lambda[P]}) \tag{20}$$

(T. Anderson et al., 2010; C. A. Edwards, Batchelder, & Powell, 2000; Franks & Chen, 2001; Shigemitsu et al., 2012). However, the Ivlev formulation is strictly empirical and cannot be derived mechanistically, but is qualitatively similar to the type II response (**See Fig. 1a**; cyan). All else being equal, the Ivlev equation will yield slower grazing rates below the half saturation concentration and faster grazing rates above the half saturation concentration. As noted elsewhere (Aldebert & Stouffer, 2018; T. Anderson et al., 2010; Gentleman et al., 2003), the half saturation point and prey capture efficiency can be related to the Ivlev parameter, λ ($\frac{1}{mmolC/m^3}$), as

$$K_{1/2} = \frac{-ln(0.5)}{\lambda}$$
$$\epsilon = \lambda g_{max} \tag{21}$$

2.4 Type III response

A type III functional response is described by a sigmoidal curve (Jeschke et al., 2004), in which the zooplankton specific grazing rate ($g([P])$) increases quadratically at low phytoplankton concentrations and approaches saturation much faster at high ones (**Fig. 1**; red). Ecologically, a type III response further assumes that the prey capture efficiency, ϵ ($\frac{1}{(mmolC/m^3)d}$), increases with prey density. That is, the zooplankton specific capture rate, $E = \epsilon[P]$, does not just increase due to a stochastic increase in the likelihood of encountering phytoplankton as the ambient phytoplankton concentration increases, but zooplankton additionally become more efficient grazers as well, capturing an increasing fraction of the ambient phytoplankton concentration. Consequently, specific grazing rates increases quadratically at low $[P]$ and approach saturation much faster than at high $[P]$.

Mathematically, this change in behavior can be represented by assuming the prey capture efficiency, ϵ ($\frac{1}{(mmolC/m^3)d}$), is a function of the ambient phytoplankton concentration, $[P]$. In a type III response this function is assumed to be linearly proportional to some prey capture efficiency coefficient, ϵ_c ($\frac{1}{(mmolC/m^3)^2 d}$), such that,

$$\epsilon = \epsilon_c[P], \tag{22}$$

and

$$E = \epsilon_c[P]^2. \tag{23}$$

By assuming that the prey capture efficiency, ϵ, increases linearly with the phytoplankton concentration at a rate described by the prey capture efficiency coefficient, ϵ_c, we are in turn assuming that the zooplankton specific grazing rate, E, increases quadratically with the phytoplankton population (i.e. $E = \epsilon_c[P]^2$). Note that higher order functional responses can be achieved by modifying the relationship between the prey capture efficiency and the phytoplankton concentration (e.g. $\epsilon = \epsilon_c[P]^2$).

Following the same derivation as **Section 2.3**, but now using **eq. 23** instead of **eq. 6** to define the specific capture rate, yields the disk parameterization of the type III functional response,

Type III (disk)
$$g([P]) = \frac{g_{max}\epsilon_c[P]^2}{g_{max} + \epsilon_c[P]^2}. \tag{24}$$

As for the type II response, g([P]) reduces to the zooplankton specific capture rate ($E = \epsilon_c[P]^2$) at low phytoplankton densities (**Fig. 1a**; dashed red line) and saturates towards the consumption rate ($1/h$) at very high phytoplankton densities (**Fig. 1a**; dashed black line). Now, however, because the zooplankton specific capture rate, E, is described by a quadratic function of $[P]$, the functional response, $g(P)$, is sigmoidal in shape (**Fig. 1a**).

The prey capture efficiency, ϵ, in **eq. 17** has been replaced with the prey capture efficiency coefficient, ϵ_c, in **eq. 24**, which describes how ϵ varies with $[P]$. Units of ϵ_c are

non-intuitive, but can be considered as the fraction of the phytoplankton population captured per unit zooplankton, per unit phytoplankton, per unit time, which reduces to $\frac{1}{(mmolC/m^3)^2 d}$.

Finally, following identical logic to the type II response, **eq. 24** can be transformed to the Michaelis–Menten function by setting $g([P])$ equal to $\frac{g_{max}}{2}$, solving for $[P]$ to find $K_{1/2}$, and substituting the ensuing value of $K_{1/2}$ into **eq. 24**. The result is the Michaelis–Menten parameterization of the type III functional response,

Type III (Michaelis–Menten)

$$g([P]) = \frac{g_{max}[P]^2}{K_{1/2}^2 + [P]^2}, \tag{25}$$

where,

$$K_{1/2} = \sqrt{\frac{g_{max}}{\epsilon_c}}. \tag{26}$$

Note that the Michaelis-Menten parameter scheme employs the same parameters in each response type ($K_{1,2}, g_{max}$), while the disk scheme requires a slightly different parameter set in a type II (ϵ, g_{max}) and III (ϵ_c, g_{max}) response.

Finally, note that where we refer to the disk and Michaelis–Menten parameterization of the type III response, throughout the literature they are often referred to as the 'Holling Type III' and 'Sigmoidal Type III' response, respectively. We use the former nomenclature to clarify that both functions are sigmoidal in shape and because it allows us to refer to the parameter scheme generically without specifying the response type. Throughout the review, this is semantically useful for comparisons between parameter schemes that are agnostic to response type.

3 Stability of the grazing formulation

Past studies have shown that the shape of these theoretical relationships, when embedded into models and integrated forward in time, influences the dynamical stability of the system, and in turn the propensity for phytoplankton extinction (Adjou et al., 2012; Dunn & Hovel, 2020; J. Steele, 1974) and excitation (i.e. blooms) (Hernández-García & López, 2004; Malchow, Hilker, Sarkar, & Brauer, 2005; Truscott & Brindley, 1994; Truscott, Brindley, Brindley, & Gray, 1994). In particular, Gentleman and Neuheimer (2008) have shown how the stabilizing influence of the grazing formulation is determined by the sign of the first derivative of the clearance rate ($\frac{dCl}{d[P]}$). The clearance rate (Cl) is equal to the the functional response ($g([P])$) normalized by the ambient phytoplankton concentration (i.e. $Cl = g([P])/[P]$). This is equivalent to the phytoplankton specific loss rate to grazing per unit zooplankton (see **Table 1**) or in other words, the volume of water completely cleared of phytoplankton per unit time, per unit zooplankton (Gentleman & Neuheimer, 2008). Ecologically, higher clearance rates imply individual zooplankton are either spending less time consuming their prey or more efficiently capturing it.

Gentleman and Neuheimer (2008) showed how clearance rates vary with prey density in different functional response types (see their **Fig. 2**). In a type I functional response, clearance rates are constant because it is assumed that the prey capture efficiency (ϵ) is constant and the consumption time is negligible (thus constant). In a type II response, clearance rates decrease with increasing prey density because the consumption rate is no longer assumed negligible, meaning the more zooplankton graze, the more time they need to consume their food, leaving less time to capture it. In a type III response clearance rates first increase, then decrease with prey density based on the balance between increasing consumption time and increasing prey capture efficiency.

The stabilizing influence of the functional response is negative, or destabilizing, when clearance rates decrease with increasing prey density ($\frac{dCl}{d[P]} < 0$). In turn, growing (decaying) phytoplankton populations are subject to decreasing (increasing) per capita grazing pressure, creating a destabilizing feedback that amplifies changes in phytoplankton growth (decay) and increases the likelihood of excitation (extinction). This occurs when the functional response has downward concavity, such that a type II response has a destabilizing influence at all prey densities, while a type III response has a destabilizing influence only above $K_{1/2}$ (Gentleman & Neuheimer, 2008). The stabilizing influence of the functional response is positive, or stabilizing when clearance rates increase with increasing prey density ($\frac{dCl}{d[P]} > 0$). In turn, growing (decaying) phytoplankton populations are subject to increasing (decreasing) per capita grazing pressure, creating a stabilizing feedback that buffers changes in phytoplankton growth (decay) and decreases the likelihood of excitation (extinction). This occurs when the functional response has upward concavity, such that a type III response has stabilizing influence below $K_{1/2}$ (Gentleman & Neuheimer, 2008). A type I response, in which clearance rates are constant ($\frac{dCl}{d[P]} = 0$), has no first order influence on stability.

The parameterization of the functional response can influence stability in two ways. First, increasing g_{max} or decreasing $K_{1/2}$ both increase the curvature of the response, which directly increases its stabilizing or destabilizing influence. Thus, a type II response with a higher g_{max} or lower $K_{1/2}$ is more destabilizing at all prey densities. However, a type III response is more destabilizing above $K_{1/2}$ but more stabilizing below $K_{1/2}$. This is illustrated clearly in Figure 5 of Gentleman and Neuheimer (2008), which tracks the first derivative of clearance rates ($\frac{dCl}{d[P]}$). Second, the parameterization of the functional response can influence stability indirectly by applying stronger or weaker grazing pressure, which in turn drives the size of the phytoplankton population and thus the position on the curve at which $\frac{dCl}{d[P]}$ is considered. For example, if using a type III response with a lower $K_{1/2}$, the functional response will have a more destabilizing influence on all phytoplankton populations above $K_{1/2}$, but faster grazing rates associated with the lower $K_{1/2}$ value make it more difficult for population levels to exceed $K_{1/2}$, such that the overall outcome may be increasing the stabilizing influence of the response. Note, in a disk scheme, $K_{1/2}$ is not parameterized directly and its location varies with both parameters.

4 Parameters of the grazing formulation

Constrained by computational resources and parsimony, biogeochemical models are limited in the number of zooplankton functional groups they can include, making it difficult to select parameters that accurately represent the mean state of natural variability across the diverse zooplankton they are trying to simulate. We combine data from two extensive reviews by Hansen et al. (1997) and Hirst and Bunker (2003) to show how the values of 119 empirically estimated sets of grazing parameters vary across zooplankton size and species (**Fig. 2**; filled markers; **Fig. 3a-c**). We then compare them to the values used in 40 modelling studies that have over 70 unique grazing formulations (**Table 2**; **Fig. 2**; empty markers; **Fig. 3d-f**). Of the 40 models surveyed, 28 include only one zooplankton group, meaning they must represent the mean behavior of all global zooplankton with a single set of parameters. Those that include multiple zooplankton have the flexibility to imply different traits for different functional groups by selecting different parameters. However, functional group resolution is still very limited, with only one model including more than three (Stock, Powell, & Levin, 2008). To determine if the values used in models are ecologically realistic approximations of the mean state, it is essential to understand how empirical estimates vary and how models attempt to either capture or average out this variability.

The most common partitioning of zooplankton functional groups in models is allometric (i.e. by size). Accordingly, we have binned all observed and modelled zooplank-

ton based on body volume, with nanozooplankton defined as $< 10^3 \mu m^3$ ($\sim$ nanoflagellates), microzooplankton defined as $10^3 - 10^6 \mu m^3$ ($\sim$ dinoflagellates, rotifers and ciliates), mesozooplankton defined as $10^6 - 10^9 \mu m^3$ ($\sim$ copepods, meroplankton larvae and cladocerans) and macrozooplankton as $> 10^9 \mu m^3$ (none reported). In the models the same size classes are assigned based on the relative prey portfolio or other specified descriptions of each zooplankton functional group. For example, in a model with 2 zooplankton functional groups nominally called 'small' and 'large' and prescribed to preferentially graze on small phytoplankton and diatoms, we would categorize these as 'micro' and 'meso', respectively. The 'nano-' and 'macro-' designations were only given when more than two zooplankton were included or they were classified explicitly as such in the study. Models with one generic, unspecified zooplankton were left unclassified.

For consistent comparison between models and empirical studies, we converted all units to $mmolC/m^3$ for prey density and $1/d$ for rates. In Hirst and Bunker (2003) $K_{1/2}$ was reported in chlorophyll units and converted with a C:Chl ratio of 50:1 (T. Anderson et al., 2010). In Hansen et al. (1997), $K_{1/2}$ was reported in ppm, and converted assuming a carbon density of 0.12 gC/cm^3, consistent with the range of carbon densities in phytoplankton (Menden-Deuer & Lessard, 2000). Different conversion factors would shift the absolute values of $K_{1/2}$ reported here, but not the size of their range or strength of their correlations with size. In modelling studies that used a currency other than carbon, units were converted assuming a fixed Redfield ratio of 106:16:1, unless otherwise stated in the study. Finally, **eqs. 18 & 26** were used to convert between Michaelis-Menten and disk parameters and **eq. 21** was used to determine the initial slope (i.e. ϵ) and half saturation concentration (i.e. $K_{1/2}$) of Ivlev responses. Note, the maximum clearance rates reported in Hansen et al. (1997) are synonymous with ϵ once units have been converted.

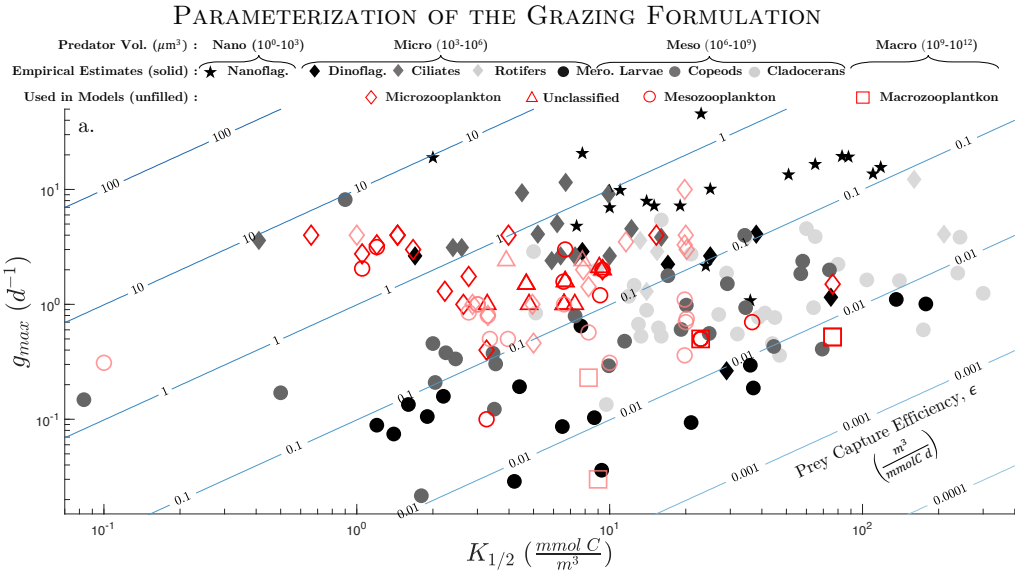

Figure 2. Parameters of the grazing formulation. **a.** Empirical estimates of parameters for >60 zooplankton species (Hansen et al., 1997; Hirst & Bunker, 2003) are plotted with filled markers. Parameters for different zooplankton functional groups from 40 modelling studies (**Table 2**) are plotted with red empty markers. Light red markers denote formulations with a multiple-prey response and parameters refer to the implied single-prey response when grazing exclusively on their most preferred prey. Contours for the corresponding prey capture efficiency (assuming type-II response) are overlaid.

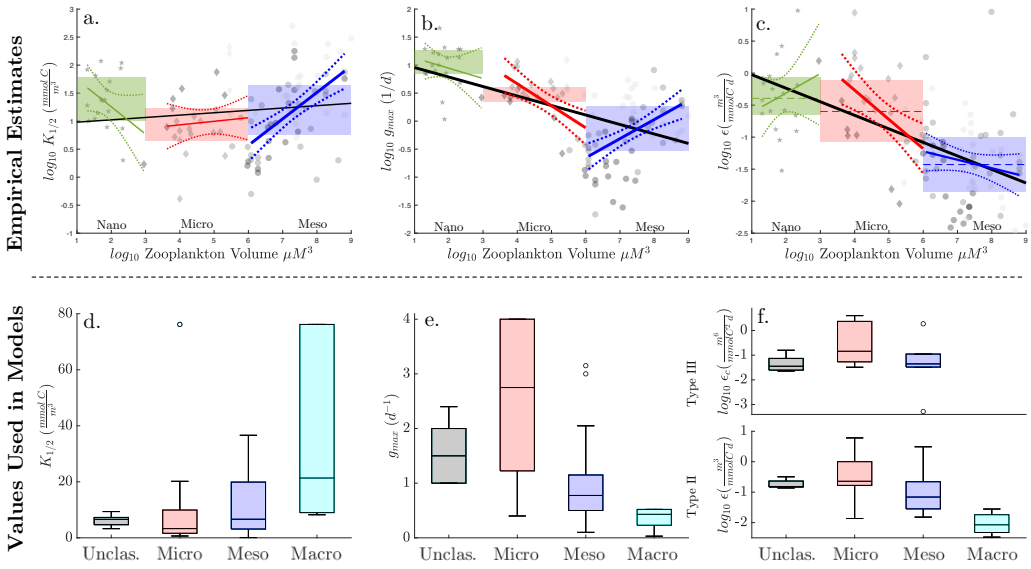

Figure 3. Allometric Relationships. **a-c.** Empirical estimates of all grazing parameters are plotted against zooplankton size and subdivided into size classes. Marker shapes are consistent with species in **Fig. 2**. The interquartile range (IQR) is overlaid for each size class along with a log-linear regression and 95% confidence intervals. A log-linear regression is shown for the complete data set as well (black). Statistically significant correlations have thicker line widths and detailed statistical information is provided in **Table 3a**. **d-f.** Box plots of each grazing parameter in models for each size class. Note, macrozooplankton and nanozooplankton are not included for empirical and model plots, respectively, because less than two of each were surveyed. Additionally, ϵ_c is not shown for the empirical values because all empirical estimates were fit to a type II response.

4.1 Empirical estimates

Grazing parameters for a myriad of different zooplankton have been estimated empirically via laboratory incubation and dilution experiments. In these studies, specific grazing rates were measured at different prey concentrations and then fit to a type II response function. Together, reviews by Hansen et al. (1997) and Hirst and Bunker (2003) describe 119 empirical estimates of over 20 functional groups, derived from data on over 200 species. Looking across all surveyed zooplankton, the values of each grazing parameter vary by over three orders magnitude, with $K_{1/2}$ ranging from .08-499 $mmolC/m^3$, g_{max} ranging from 0.02-45.6 d^{-1}, and ϵ ranging from .003-9.5 $\frac{m^3}{mmolCd}$ (**Fig. 2**). While some of this variability can be explained statistically by the large variability in zooplankton size ($10-10^9 \mu m^3$), the strength of the allometric relationship differs with both the parameter in question and whether you are considering all samples or just a subset within a certain size class (**Fig. 3; Table 3**).

Consistent with Hansen et al. (1997), when considering the entire, combined data set there is a statistically significant allometric relationship between zooplankton size and both g_{max} (**Fig. 3b**; black regression) and ϵ (**Fig. 3c**; black regression). This decrease in the parameters that describe consumption and capture rates, respectively, is consistent with the conventional wisdom that grazing rates decrease with predator size (Moloney & Field, 1989; Peters & Downing, 1984; Saiz & Calbet, 2007; Wirtz, 2013). However, as in Hansen et al. (1997), $K_{1/2}$ values from the combined data set do not exhibit a statistically significant allometric relationship (**Fig. 3a**; black regression), contradicting the

notion that $K_{1/2}$ should increase with increasing predator size (Ray et al., 2011). This can be explained because $K_{1/2}$ is not an independent, physiological parameter, but rather a mathematical description of the curve, relating the other two parameters that mechanistically describe consumption (i.e. g_{max}) and capture (i.e. ϵ) rates (see **Section 2**). While all parameters are estimated here empirically, only ϵ and g_{max} reflect independent trait-based differences in grazing behaviour. Therefore, if g_{max} and ϵ both decrease with zooplankton size, grazing rates will decrease at low and high concentrations such that the half-saturation concentration may increase, decrease, or remain largely unaltered, depending of the relative changes. The net effect when considered across all zooplankton sizes is a flat and not statistically significant (**Table 3a**).

Similarly, when grouped into discrete size classes, the mean, median and interquartile range (IQR) of g_{max} and ϵ decrease monotonically from nanozooplankton (**Fig. 3; green**) to microzooplankton (red) to mesozooplankton (blue), while those of $K_{1/2}$ do not (**Table 3b**). Instead the median value of $K_{1/2}$ decreases from 23 $mmolC/m^3$ in nanozooplankton to 8.9 $mmolC/m^3$ in microzooplankton but then increases to 18.1 $mmolC/m^3$ in mesozooplankton. Of the three parameters, binning by size class does the best job of explaining variability in distributions of g_{max}, which has the smallest coefficient of variability (i.e. std/mean) of all parameters in all size classes. Moreover, using a two sample t-test at the 95% confidence level, g_{max} is the only parameter in which the mean value in adjoining size classes are statistically different from one another. For ϵ, only nano- and mesozooplankton have statistically different means, although the difference between micro- and mesozooplankton is nearly significant (p=0.1) and may become so if the binning bounds were adjusted. For $K_{1/2}$, the range of values in each size class varies by over two order of magnitude and largely overlaps. In turn, there is no statistically significant difference between the mean $K_{1/2}$ value within any two size classes, even nano- and microzooplankton which differ by ~ 6 orders of magnitude in volume. Together, empirical estimates of g_{max} appear better constrained by size class than $K_{1/2}$, or even ϵ, suggesting that consumption rates are better correlated than capture rates with zooplankton size class.

However, these trait-based correlations become more complex when looking at variability within a given size class, rather than across them (**Fig. 3a-c; Table 3a**). Nanozooplankton parameter values are the most poorly constrained by size. When considered in isolation, there is no statistically significant relationship between any of their empirically derived grazing parameters and size (**Fig. 3a-c; green**). Microzooplankton parameter values, on the other hand, are the best constrained by size. Both g_{max} (**Fig. 3b; red**) and ϵ (**Fig. 3c; red**) exhibit a robust, statistically significant, inverse relationship with size, with a higher coefficient of determination (r^2) than in any other size class. In turn, the correlation between $K_{1/2}$ and size is flat and not statistically significant (**Fig. 3b; red**). This is consistent with decreasing capture and consumption rates that combine to lower mean grazing rates but not systematically modify $K_{1/2}$. Mesozooplankton parameter values are also fairly well constrained by size, but in a qualitatively different way. When exclusively considering mesozooplankton (**Fig. 3a-c; blue**), $K_{1/2}$ and g_{max} both exhibit a statistically significant positive relationship with size, while the relationship with ϵ is flatter and not statistically significant. This suggests that consumption rates in mesozooplankton actually increase with size while capture rates are invariant, leading to an apparent increase in the $K_{1/2}$ (see **eq. 18**). Critically though, this increase in $K_1/2$ is associated with faster, not slower, grazing on average.

The most common partitioning in models with multiple zooplankton is into two micro- and mesozooplankton groups (**Table 2**). Nanozooplankton on the other hand only appear in one surveyed (**Table 2**). When considering exclusively empirical variability in micro- and mesozooplankton, ignoring nanozooplankton, there is a statistically significant correlation with size for all three parameters. Similar to when considering all zooplankton, g_{max} and ϵ both decrease with size; however, with nanozooplankton removed, the decline in g_{max} is flatter and less significant (i.e. lower p-value) while the decline in

ϵ is steeper and more significant (**Table 3a**). In turn, there is now also a statistically significant increase in $K_{1/2}$ with size. Additionally, if only considering the IQR of $K_{1/2}$, there is statistically significant difference in the means value in micro- and mesozooplankton.

Accordingly, in biogeochemical models using two discrete zooplankton state variables to simulate the mean state of micro- and mesozooplankton, it appears the mesozooplankton class should have slower consumption (i.e. g_{max}) and capture rates (i.e. ϵ) than microzooplankton. Further, the empirically observed increase in $K_{1/2}$ means that the decrease in ϵ should be disproportionately larger than that of g_{max}. However, in different model configurations one may wish to vary different parameters in different ways, depending on the range and resolution of what you are simulating. For example, a size-spectrum model of exclusively microzooplankton may wish to decrease both capture and consumption rates with size, whereas a size spectrum model of exclusively mesozooplankton may wish to increase consumption rates with size and leave capture rates constant.

Finally, it is important to note that the way in which these trait-based correlations can be prescribed depends on the parameter scheme. For example, to increase consumption rates without increasing capture rates in a Michaelis-Menten scheme one must increase g_{max} and $K_{1/2}$ or else otherwise increase ϵ implicitly as well. This would inadvertently overestimate grazing rates at low prey densities. However, to increase consumption and capture rates in a Michaelis-Menten scheme one must still increase g_{max} but the change in $K_{1/2}$ depends on the intended relative difference in the two properties. In any scenario, all parameters should be computed and considered explicitly to confirm if the correct behavior is being implied at low and high prey densities.

4.2 Values used in models

Over 70 independent grazing formulations from 40 modelling studies were surveyed (**Table 2, Fig. 2**; empty markers) to gauge the range of commonly prescribed parameter values and investigate if they vary in a manner consistent with the natural variability measured empirically (**Sec. 4.1**). A large sampling of prominent modelling studies, from canonical 0-dimensional theoretical work (Evans & Parslow, 1985; Franks et al., 1986), through slightly more sophisticated NPZD models (Fasham, 1995; Fasham et al., 1990), to state-of-the-art CMIP6 earth system models (Aumont et al., 2015; Christian et al., 2021; Hajima et al., 2020; Law et al., 2017; Long et al., 2021; Stock et al., 2020; Tjiputra et al., 2020; Totterdell, 2019; Yool et al., 2021) were included. Surveyed models were assessed to determine if their selection of parameter values is representative of the mean state of empirically estimated values and if variability therein is consistent with the observed allometric variability (**Fig. 3d-f; Table 3c**) or varies with other aspects of the grazing formulation (**Table 3d**).

Of the 40 models surveyed, 26 include a zooplankton group that grazes with a single-prey response, including 5 of 9 IPCC CMIP6 earth system models. This amounts to 40 of the 70 unique grazing formulations. The others graze on multiple prey (**Table 2**; grey rows & **Figure 3**; light red markers) and use a $K_{1/2}$ parameter that is fundamentally different from that of the single-prey response (Gentleman et al., 2003). In multiple-prey response functions, $K_{1/2}$ refers to the half saturation 'concentration' of the total, preference-weighted prey pool, which is not a one-to-one function of the prey distribution. In **Table 2**, we report this value in parenthesis, but focus our analysis on the implied $K_{1/2}$ for the single-prey response for each zooplankton group when grazing exclusively on their preferred prey. Gentleman et al. (2003) describe in detail how this value can be calculated algebraically from the reduced multiple-prey response based on both innate prey preferences (i.e. constants) and assumptions about whether preferences can vary with the relative distribution of prey (i.e. switching vs. no switching; Fasham et al. (1990)). Although the apparent $K_{1/2}$ for a given prey item will increase in the presence of other

Reference	Dimensions (# Z, P tracers)	Location	Zooplankton Functional Group	Grazing Formulation (Single Prey Response)			
				Resp. Type	Parameter Scheme	$K_{1/2}$ $(mmolC/m^3)$	g_{max} $(1/d)$
Wroblewski (1977)	2 $(1P1Z)^N$	coastal upwelling	macro	II	Ivlev	76.18	.52
Evans and Parslow (1985)	0 $(1P1Z)^N$	N. Atlantic	-	II^{th}	M-M	7.28	1
Franks et al. (1986)	0 $(1P1Z)^N$	-	meso	II	Ivlev	2.25-45.7	0.16-1.5
Fasham et al. (1990)	0 $(1P1Z)^N$	Bermuda	meso	II	M-M	6.6 (6.6)	1
Frost (1993)	1 $(1P1Z)^C$	Station P	micro	II^{th}	M-M	2.23	1.01-1.6
Truscott and Brindley (1994)	0 $(1P1Z)^N$	coastal (red tide)	meso	III	M-M	36.6	0.7
Fasham (1995)	0 $(1P1Z)^N$	Station P	- -	II III	disk disk	6.6 3.82	1 1
Franks and Chen (1996)	2 $(1P1Z)^N$	Georges Bank	meso	II	Ivlev	22.9	.5
Franks and Walstad (1997)	2 $(1P1Z)^N$	-	meso	II	Ivlev	22.9	.5
Denman and Peña (1999)	1 $(1P1Z)^N$	Station P	micro	III	M-M	2.64	1
Edwards et al. (2000)	2 $(1P1Z)^N$	coastal upwelling	micro macro	II II	Ivlev Ivlev	15.3 22.9	4 0.5
Franks and Chen (2001)	3 $(1P1Z)^N$	Georges Bank	meso	II	Ivlev	22.9	.5
Denman and Peña (2002)	1 $(1P2Z)^N$	Station P	micro meso	III III	M-M M-M	4.96 (4.96) 3.96 (3.96)	1 0.5
Leising et al. (2003)	0 $(1P1Z)^N$	HNLC equatorial Pacific	micro micro micro micro	II II^{th} II III	M-M M-M M-M M-M	0.66 1.45 3.98 1.45	4 4 4 4
Newberger et al. (2003) **Spitz et al. (2003)**	0 $(1P1Z)^N$ 2 $(1P1Z)^N$	coastal upwelling	micro macro	II II	Ivlev Ivlev	76.18 76.18	1.5 0.52
Schartau and Oschlies (2003b)	3 $(1P1Z)^N$	N. Atlantic	-	III	disk	6.67	1.58
Aumont and Bopp (2006) (PISCES)	3 $(2P2Z)^C$	global	micro meso	II II	M-M M-M	20 (20) 20 (20)	4 0.7
Gentleman and Neuheimer (2008)	0 $(1P1Z)^N$	-	-	III, II, II, II^{th}	M-M, M-M Ivlev, M-M	4.68	1.5
Stock et al. (2008)	0 $(3P4Z)^N$	Low, Mid, High Productivity	nano($100\mu m$) micro($1e4\mu m$) meso($1e6\mu m$) macro($1e8\mu m$)	II II II II	M-M M-M M-M M-M	20 (20) 20 (20) 20 (20) 20 (20)	10 3.3 1.1 0.6
Sinha et al. (2010) (PLANKTOM5.2)	3 $(3P2Z)^C$	global	micro meso	II II	M-M M-M	11.6 (15) 0.1 (0.26)	3.5 0.31
T. Anderson et al. (2010)	3 $(3P2Z)^C$	global	micro meso	I, II, II, III	M-M, M-M, Ivlev, M-M	1 (1) 3 (3)	4 1
Adjou et al. (2012)	0 $(2P1Z)^N$	Station P	-	II, III	M-M, disk	6.6	1
Kriest et al. (2012)	3 $(1P1Z)^P$	global	-	III	M-M	9.38	2
Shigemitsu et al. (2012) (MEM)	1 $(2P3Z)^N$	N. Pacific	micro meso	II^{th} II^{th}	Ivlev Ivelv	3.38 3.28	.4 0.1, 0.4
Dunne et al. (2013) (TOPAZ)	3 (1P0Z)	global	allometric	-	-	-	0.19
Tjiputra et al. (2013) (NORESM1)	3 $(1P1Z)^P$	global	-	II	M-M	4.8	1
Hauck et al. (2013) (REcoM2)	3 $(2P1Z)^N$	global	*micro* *meso*	III III	M-M M-M	3.9 (3.9) 7.8 (3.9)	2.4 2.4
Moore et al. (2013) (BEC)	3 $(3P1Z)^C$	global	*micro* *meso*	III III	M-M M-M	1.05 1.05	2.05 2.75
Oke et al. (2013) (WOMBAT)	3 $(1P1Z)^N$	global	-	III	disk	9.1	2.1
Dutkiewicz et al. (2015) (Darwin)	3 $(8P2Z)^P$	global	micro meso	III III	M-M M-M	2.86 (2.86) 3.01 (2.86)	1 1
Le Quéré et al. (2016) (PlanktTOM10)	3 $(6P3Z)^C$	global	micro meso macro	II II II	M-M M-M M-M	5 (10) 10 (10) 9 (9)	0.46 0.31 0.03
Law et al. (2017) (WOMBAT)	3 $(1P1Z)^N$	global	-	III	disk	6.57	1.58
Totterdell (2019) (diat-HadOCC)	3 $(2P1Z)^N$	global	*micro* *meso*	II II	M-M M-M	3.3 (3.3) 3.3 (3.3)	0.8 0.8
Stock et al. (2020, 2014) (COBALTv2, COBALT)	3 $(3P3Z)^N$	global	micro meso macro	II II II	M-M M-M M-M	8.28 (8.28) 8.28 (8.28) 8.28 (8.28)	1.42 0.57 0.23
Christian et al. (2021) (CANOE)	3 $(2P2Z)^C$	global	micro meso	II II	Ivlev Ivlev	2.77 2.77 (2.77)	1.75 0.85
Yool et al. (2021, 2013) (MEDUSA2.0)	3 $(2P2Z)^N$	global	micro meso	III III	M-M M-M	7.65 (5.3) 3.36 (1.88)	2 0.5
Long et al. (2021) (MARBL)	3 $(3P1Z)^C$	global	*micro* *meso*	II II	M-M M-M	1.2 1.2	3.3 3.15
Hajima et al. (2020) (MIROC)	3 $(2P1Z)^N$	global	*micro* *meso*	II II	disk disk	9.36 9.36	2 2
Aumont et al. (2015) (PISCESv2)	3 $(2P2Z)^C$	global	micro meso	II II	M-M M-M	20 (20) 20 (20)	3 0.75
Tjiputra et al. (2020) (NORESM2)	3 $(1P1Z)^P$	global	-	II	M-M	9.76	1.2

Table 2. The parameterization of the grazing formulation in biogeochemical models. The model currency (C,N, or P) is noted in the superscript in column 1 and units of $K_{1/2}$ are converted to carbon where required using a Redfield ratio of 106:16:1 (C:N:P) if not noted in the study. The $K_{1/2}$ relationship algebraically relates the mathematical half saturation concentration ($g(P) = g_{max}/2$) to the parameters specified in the model when not parameterized explicitly. Different zooplankton size classes have separate rows. Values from a given study separated by commas indicate different simulations. Models with a multiple prey response are highlighted in grey and reported $K_{1/2}$ values refer to the implied single-prey response when grazing exclusively on their most preferred prey. In parentheses is the $K_{1/2}$ prescribed for bulk ingestion on the total preference weighted prey field. Models with one zooplankton tracer that grazes separately on two phytoplankton groups with two distinct single-prey responses (i.e. specific grazing rates on one prey group are not effected by the concentration of the other) are considered to have a single-prey response and two implicit zooplankton groups. Implicit functional groups are italicized.

a) Empirical Estimates: Trait-based Correlation with Size

Size Class	$K_{1/2}$			g_{max}			ϵ		
	p	r^2	b	p	r^2	b	p	r^2	b
All Sizes n=119	0.12	0.02	0.04	10^{-11}	0.31	-0.17	10^{-13}	0.37	-0.21
Nano. & Micro. n = 49	0.06	0.07	-0.10	10^{-7}	0.44	-0.24	0.01	0.12	-0.13
Micro & Meso. n=94	10^{-4}	0.13	0.17	0.01	0.06	-0.11	10^{-8}	0.29	-0.27
Nanozooplankton n=19	0.1	0.15	-0.47	0.41	0.04	-0.18	0.35	0.05	0.30
Microzooplankton n=30	0.68	.008	0.06	10^{-4}	0.33	-0.39	10^{-3}	0.29	-.046
Mesozooplankton n=64	10^{-6}	0.29	0.47	10^{-5}	0.23	0.34	0.18	0.03	-0.13

b) Empirical Estimates: Sample Statistics by Size Class

Size Class	$K_{1/2}$ $(mmolC/m^3)$				g_{max} $(1/d)$				ϵ $(m^3/mmolC/d)$			
	mean	med.	range	IQR	mean	med.	range	IQR	mean	med.	range	IQR
All zooplankton n=119	40	16	$8.3e^{-2}$ 500	6.4 43	3.7	1.6	$2.1e^{-2}$ 46	0.46 3.8	0.49	$8.4e^{-2}$	$3.4e^{-3}$ 9.5	$2.1e^{-2}$ 0.27
Nanozooplankton n=19	37	23	1.7 120	10 62	13	10	1.1 46	7.0 19	1.1	0.40	$3.0e^{-2}$ 9.5	0.22 0.85
Microzooplankton n=30	25	8.9	0.41 210	4.5 17	3.6	3.0	0.11 12	2.2 4.1	0.71	0.25	$9.1e^{-3}$ 8.8	$9.0e^{-2}$ 0.78
Mesozooplankton n=64	45	18	$8.0e^{-2}$ 500	5.8 45	1.3	0.77	$2.0e^{-2}$ 8.2	0.29 1.8	0.24	$4.0e^{-2}$	$3.4e^{-3}$ 9.1	$1.0e^{-2}$ 0.10

c) Values Used in Models: Sample Statistics by Size Class

Size Class	$K_{1/2}$ $(mmolC/m^3)$				g_{max} $(1/d)$				ϵ $(m^3/mmolC/d)$ *				ϵ_c $(m^6/mmolC^2/d)$ **			
	mean	med.	range	IQR	mean	med.	range	IQR	mean	med.	range	IQR	mean	med.	range	IQR
All Zoo. (n=70,47*,23**)	11	6.6	0.1 76	3.3 11.6	1.7	1.1	$3.0e^{-2}$ 10	0.7 2.4	0.56	0.15	$3.3e^{-3}$ 6.1	$3.2e^{-2}$ 0.32	0.50	0.04	$5.0e^{-4}$ 4	$3.3e^{-2}$ 0.14
Uncat. (n=14,5*,9**)	6.3	6.6	3.3 9.4	4.7 7.3	1.5	1.5	1.0 2.4	1.0 2.0	0.19	0.15	0.14 0.32	0.15 0.24	$5.6e^{-2}$	$3.5e^{-2}$	$2.3e^{-4}$ 0.16	$2.5e^{-4}$ $7.5^{5e^{-4}}$ 4
Nanozoo. (n=1,1*,0**)	20	20	-	-	10	10	-	-	0.51	0.51	-	-	-	-	-	-
Microzoo. (n=25,18*,7**)	9.1	3.3	0.66 76	1.6 9.9	2.4	2.8	0.40 4.0	1.2 4.0	0.96	0.23	$1.4e^{-2}$ 6.1	0.17 1.0	1.2	0.14	$3.2e^{-2}$ 4.0	$6.1e^{-2}$ 2.3
Mesozoo. (n=24,17*,7**)	10	6.6	0.10 37	3.1 20	1.0	0.78	0.10 3.2	0.5 1.2	0.44	$6.9e^{-2}$	$1.5e^{-2}$ 3.1	$2.9e^{-2}$ 0.22	0.31	$4.4e^{-2}$	$5.0e^{-4}$ 1.9	$3.3e^{-2}$ 0.11
Macrozoo. (n=6,6*,0**)	35	21	8.3 76	9 76	0.37	0.43	$3.0e^{-2}$ 0.52	0.23 0.52	$1.2e^{-2}$	$9.9e^{-3}$	$3.3e^{-3}$ $2.8e^{-2}$	$4.7e^{-3}$ $1.8e^{-2}$	-	-	-	-

d) Values Used in Models: Sample Statistics by Grazing Formulation

Grazing Formulation	$K_{1/2}$ $(mmolC/m^3)$				g_{max} $(1/d)$				ϵ $(m^3/mmolC/d)$ *				ϵ_c $(m^6/mmolC^2/d)$ **			
	mean	med.	range	IQR	mean	med.	range	IQR	mean	med.	range	IQR	mean	med.	range	IQR
Type III (n=23,0*,23**)	6.0	4.0	1.0 37	3.0 6.7	1.7	1.6	0.5 4.0	1 2.1	-	-	-	-	0.50	$4.4e^{-2}$	$5.0e^{-4}$ 4	$3.3e^{-2}$ 0.14
Type II (≠Ivlev) (n=35,35*,0**)	8.9	7.3	0.1 20	3.5 11	1.9	1.2	$3.0e^{-2}$ 10	0.8 3.1	0.72	0.20	$3.3e^{-3}$ 6.1	0.10 0.49	-	-	-	-
Ivlev (n=12,12*,0**)	29	23	2.7 76	3.3 50	0.97	0.51	0.1 4.0	0.5 1.2	$8.5e^{-2}$	$1.5e^{-2}$	$4.7e^{-3}$ 0.44	$1.4e^{-2}$ 0.13	-	-	-	-
Michaelis-Menten (n=49,32*,17**)	7.8	5.0	0.10 37	12.8 9.2	1.9	1.2	$3.0e^{-2}$ 10	0.79 3.0	0.77	0.19	$3.3e^{-2}$ 6.1	$8.0e^{-2}$ 0.54	0.66	0.11	$5.0e^{-4}$ 4.0	$3.8e^{-2}$ 0.58
disk (n=9,3*,6**)	7.1	6.6	3.2 9.4	6.6 9.2	1.5	1.6	1.0 2.1	1.0 2.0	0.19	0.21	0.15 0.21	0.17 0.21	0.04	$3.6e^{-2}$	$2.3e^{-2}$ $9.3e^{-2}$	$2.5e^{-2}$ $3.6e^{-2}$
Single Prey (n=40,27*,13**)	13	6.6	0.66 76	2.7 9.8	1.8	1.5	0.1 4.0	1.0 2.4	0.75	0.18	$4.7e^{-3}$ 6.1	$1.6e^{-2}$ 0.55	0.52	$3.6e^{-2}$	$5.0e^{-4}$ 2.5	$2.5e^{-2}$ 0.57
Multiple Prey (n=30,20*,10**)	9.3	7.8	0.1 20	3.3 20	1.6	1.0	$3.0e^{-2}$ 10	0.5 2.4	0.29	0.15	$3.3e^{-3}$ 3.1	$3.6e^{-2}$ 0.23	0.5	$7.0e^{-2}$	$3.3e^{-2}$ 3.1	$3.6e^{-2}$ 0.23

Table 3. Statistics from empirically estimated and modelled grazing parameters. **a.** The p-value (p), coefficient of determination (r^2), and slope (b) are displayed for a linear regression fit between the log_{10} of zooplankton size (μm^3) and the log_{10} of $K_{1/2}$, g_{max}, and ϵ. Data included in each model is limited to the size class(es) specified in the left column. Statistically significant relationship ($p<0.05$) are highlighted in blue for positive correlations ($b>0$) and red for negative correlations ($b<0$). **b,c,d.** Sample statistics are shown for **b.** empirical values sorted by size classes and **c,d.** model values sorted by size class and other attributes of the grazing formulation. The IQR referes to the Inter-quartile range (i.e. middle 50%). Statistics for ϵ do not include any type III responses and statistics for ϵ_c do not include any type II or Ivlev response. ϵ_c is not shown for the empirical data as a type II response was always assumed.

prey options, we consider the implied $K_{1/2}$ for the single-prey response as it is informative as to how modellers assume zooplankton behave in optimal conditions, grazing exclusively on their preferred prey.

Overall, the full range of grazing parameters used in models varies considerably (**Fig. 2; empty red markers**). $K_{1/2}$ and g_{max} both vary by over two orders of magnitude, from 0.1-76 $mmol\ C/m^3$ and 0.03-10 $1/d$, respectively. When converted into a disk parameter scheme the range is even larger, with ϵ in type II (and Ivlev) response functions spanning more than 3 orders of magnitude, from $3.3{*}10^{-3}$ to 6.1 $\frac{m^3}{mmolCd}$, and ϵ_c in type III response functions spanning nearly 4 orders of magnitude, from $5.2{*}10^{-4}$ to 4 $\frac{m^6}{mmol^2Cd}$. Considering that these values are used to represent the mean state of many zooplankton, they might be expected to vary substantially less than empirical estimates, which should be expected to span a large range of natural variability. However, the range of model values for each parameter exceeds the interquartile range of empirical estimates (**Table 3b,c**), suggesting that some models may be using unreasonably high or low parameter values. This is especially true for model values of ϵ, which exceed the interquartile range of empirical estimates by an order of magnitude in both directions. Moreover, the mean of model and empirical distributions are not statistically similar ($p>0.05$; 2-sample t-test) for any parameter. However, this comparison may be biased by intended differences in the zooplankton functional groups being modelled.

Breaking down the model values by size class gives a better indication of how representative model values are of empirically estimates (**Fig. 3d-f**; **Table 3b,c**). Focusing on microzooplankton and mesozooplankton, the most commonly simulated size classes, the range of $K_{1/2}$, g_{max}, and ϵ for both size classes falls within the range, but beyond the interquartile range, of their respective empirical estimates. However, relative differences between the two size classes are generally consistent with observations. Statistically, modelled consumption (g_{max}; **Fig. 3e**) and capture (ϵ, ϵ_c; **Fig. 3f**) rates both decline with zooplankton size and do so in a manner that increases $K_{1/2}$ (**Fig. 3d**).

In particular, variability in g_{max} across the two size classes is well aligned with the observations (**Fig. 3b,e**; **Table 3b,c**). The median value (and interquartile range) of g_{max} decreases from 2.75 (1.2-4) in microzooplankton to 0.78 (0.5-1.15) in mesozooplankton models, compared to from 3.0 (2.2-4) to 0.77 (0.3-1.8) in the empirically measured values. Moreover, there is no statistical difference between the mean of the model and empirical distributions of g_{max} in either simulated size class. Unsurprisingly, both sets of model and empirical values reported here are consistent with values of 2-4 $1/d$ and 1 $1/d$, respectively, reported elsewhere throughout the literature (C. A. Edwards et al., 2000; Gismervik, 2005; Lancelot et al., 2005; Leising, Gentleman, & Frost, 2003; Strom & Morello, 1998).

However, allometric variability in capture rates, either prescribed directly by ϵ (**Fig. 3c,f**) and ϵ_c or indirectly by $K_{1/2}$ (**Fig. 3a,d**), is less consistent with observations. The median value (and IQR) of ϵ decreases from 0.27 (.17-1.79) to 0.14 (.04-.37) in models, compared to from 0.25 (.09-0.78) to .04 (.01-.09) in the empirically measured values. This smaller drop in ϵ between size classes in the models is consistent with a smaller increase in $K_{1/2}$ than observed. The median value (and IQR) of $K_{1/2}$ increases from 3.3 (1.6-9.9) to 6.6 (3-9.9) in models, compared to from 8.9 (4.5-17) to 18 (5.8-45) in the empirically measured values (**Table 3b,c**). In turn, the relative decrease in mesozooplankton grazing at low prey concentrations (where capture rates dominate) may be underestimated in models. This is likely happening because most models that include micro- and mesozooplankton use a Michaelis-Menten parameter scheme and vary g_{max} between size classes but not $K_{1/2}$ (**Table 2**). While this is consistent with the allometric relationships measured across the full range of zooplankton, it may not be when focusing explicitly on the difference between micro- and mesozooplankton (**Sec 4.1; Table 3a**). In turn, models that vary both g_{max} and $K_{1/2}$ (e.g. T. Anderson et al. (2010)) may be more realistic than those that fix $K_{1/2}$ across size.

While the clearest source of variability between model values is justifiably allometric, we additionally checked for differences associated with attributes of the grazing formulation (**Table 3d**). The only statistically significant difference related to the grazing formulation was between capture rates prescribed in Ivlev response types compared to those in Holling type III, or even type II, responses. The mean $K_{1/2}$ used in zooplankton simulated with an Ivlev response was nearly 5x larger (29 $mmolC/m^3$) than that used in a type III response (6.0), and over 3x larger than that used in a qualitatively similar type II response (8.0). Although a disproportionate number of zooplankton simulated with a Ivlev response are described as macrozooplankton (50%), mean $K_{1/2}$ values for micro- (24) and mesozooplankton (15) simulated with an Ivlev response are also much higher than the average value used in non-Ivlev type II response functions (7.8 & 9.6, respectively). This suggests that $K_{1/2}$ may be systematically overestimated in Ivlev responses, perhaps because the Ivlev parameter is further abstracted from any mechanistically meaningful value or intuitive characteristic of the curve. Finally, there was no statistically significant difference between the mean of any parameter value when comparing those used in Michaelis-Menten versus disk parameter schemes or when comparing single-prey response types with the implied single prey response from multi-prey response types.

5 Sensitivity of the grazing formulation

To isolate the sensitivity of phytoplankton population dynamics to the functional response and its parameterization, we extend the sensitivity analysis conducted by Gentleman and Neuheimer (2008). We use an identical, idealized, 0-dimensional Nutrient-Phytoplankton-Zooplankton (NPZ) box model to that of Gentleman and Neuheimer (2008), and earlier Franks et al. (1986). This model assumes that phytoplankton (P) grow via uptake of external inorganic nutrients (N) and are lost to zooplankton (Z) grazing and mortality. Nutrients are returned to the inorganic pool via phytoplankton mortality, zooplankton mortality and sloppy grazing. Phytoplankton growth follows nutrient limited Michaelis-Menten kinetics (Michaelis & Menten, 1913) and both phytoplankton and zooplankton mortality terms are linear. Mass transfer between N, P and Z pools is described by

$$\begin{aligned}
\frac{dN}{dt} &= (1-\alpha)g([P])Z - \mu_{max}\frac{N}{K_N+N}P + m_pP + m_zZ, \\
\frac{dP}{dt} &= \mu_{max}\frac{N}{K_N+N}P - g([P])Z - m_pP, \\
\frac{dZ}{dt} &= \alpha g([P])Z - m_zZ,
\end{aligned} \tag{27}$$

where α is the grazing efficiency, μ_{max} is the phytoplankton maximum specific growth rate, K_N is the nutrient uptake half saturation constant, m_p is the phytoplankton mortality rate, m_z is the zooplankton mortality rate, and $g([P])$ is the grazing formulation (i.e. **eq. 17, 18, 24, or 25**). The model is not forced with seasonality in light, mixing or other environmental conditions, such that μ_{max} is constant and phytoplankton growth is determined only by nutrient availability. Non-grazing parameters and initial conditions (**Table 4b**) are identical to Gentleman and Neuheimer (2008), but converted to carbon units using a stoichiometric ratio of C:N = 106:16.

Gentleman and Neuheimer (2008) used this model to assess the change in dynamical stability when switching between a type II and III response or doubling/halving $K_{1/2}$ and g_{max}. In addition to testing both response types, we go on to test both parameter schemes (disk, Michaelis-Menten) and a much larger range of grazing parameters. This allows for the comparison of gradients across the parameter space between four different grazing formulations (i.e. Type II-disk, Type III-disk, Type II-Michaelis-Menten, Type

a. The Grazing Formulation

	Response Type	Parameter Scheme	Parameters	Sensitivity Range
$g([P])$	II	disk	ϵ g_{max}	$0.01-10$ $\frac{m^3}{mmolCd}$ $0.1-45$ d^{-1}
	III	disk	ϵ_c g_{max}	$0.01-10$ $\frac{m^6}{mmolC^2d}$ $0.1-45$ d^{-1}
	II	Michaelis-Menten	$K_{1/2}$ g_{max}	$100-0.1$ $\frac{mmolC}{m^3}$ $0.1-45$ d^{-1}
	III	Michaelis-Menten	$K_{1/2}$ g_{max}	$100-0.1$ $\frac{mmolC}{m^3}$ $0.1-45$ d^{-1}

b. Other Parameters and Initial Conditions

	Parameter	Value	Sensitivity Range
α	Grazing efficiency	0.7	0.35, 1.0
μ_{max}	Phytoplankton maximum specific growth rate	2 d^{-1}	1, 4 d^{-1}
m_P	Phytoplankton mortality rate	0.1 d^{-1}	.05, 0.2 d^{-1}
m_Z	Zooplankton mortality rate	0.2 d^{-1}	0.1, 0.4 d^{-1}
K_N	Nutrient uptake half-saturation constant	6.6 $\frac{mmolC}{m^3}$	3.3, 13.2 $\frac{mmolC}{m^3}$
N_0	Nutrient density initial condition	10.6 $\frac{mmolC}{m^3}$	5.3, 21.2 $\frac{mmolC}{m^3}$
P_0	Phytoplankton density initial condition	1.3 $\frac{mmolC}{m^3}$	0.65, 2.6 $\frac{mmolC}{m^3}$
Z_0	Zooplankton density initial condition	1.3 $\frac{mmolC}{m^3}$	0.65, 2.6 $\frac{mmolC}{m^3}$

Table 4. List of **a.** grazing formulations and **b.** other parameters and initial conditions used for the NPZ (**eq. 27**) sensitivity analysis in **Section 5**.

III-Michaelis-Menten; see **Table 4a**). Within each grazing formulation, we consider a range of $\log_{10}$-spaced values spanning nearly 3 orders of magnitude for both parameters (**Table 4a**). These ranges are all within the range of empirical estimates (**Fig. 2; Table 3b**). Note that corresponding grid cells in each panel of **Figs. 5** & **6** do not equate to identical functional response curves; identical parameter values used in different response types or parameter schemes will yield differently shaped curves and thus different dynamics. Instead, when comparing panels, we consider differences in gradients across the parameter space.

All 784 combinations of parameters values for each functional response (i.e. 3136 total tests) were integrated for 5 years, after which the system either reached steady state, quasi state-state (repeating limit cycles), or numerical instability. Integrating any further did not meaningfully change our results. We analyse the final year of each integration, which was long enough to capture limit cycles that had a period of anywhere from weeks to months. We then assessed how the choice of response type, parameter scheme, and parameter values influences prescribed grazing rates (**Section 5.1**) and in turn drives the size (**Section 5.2**) and stability (**Section 5.3**) of the phytoplankton population. The sensitivity of our results to non-grazing parameters and initial conditions is also examined (**Table 4b**; **Section 5.4**).

5.1 Sensitivity of grazing rates

Modellers can prescribe faster grazing rates by increasing ϵ, ϵ_c, and/or g_{max} in a disk parameter scheme, or decreasing $K_{1/2}$ and/or increasing g_{max} in a Michaelis-Menten parameter scheme. Note that while ϵ and g_{max} modify the curve in the same direction when using a disk formulation, $K_{1/2}$ and g_{max} modify it in opposite directions when using a Michaelis-Menten formulation, meaning that modellers must ensure parameter changes do not inadvertently cancel out if modifying both in the same direction. Moreover, the sensitivity of the shape of the curve and associated grazing rates to these parameters varies with the parameter scheme, response type, and the prey density (or location on the curve) in question. To illustrate this, we have provided a schematic showing how proportional changes in different parameters modify the curve in different ways at low and high $[P]$ values (**Fig. 4**). We then quantify these changes by computing the mean grazing rates prescribed at low and high $[P]$ values for all curves defined across the entire parameter space (**Fig. 5**).

When using a disk scheme (**Fig. 4**, green), regardless of response type, grazing rates are determined almost entirely by prey capture rates when food is scarce (Low $[P]$; **Fig. 4**, middle row) and by consumption rates when food is replete (High $[P]$; **Fig. 4**, bottom row). This is a direct consequence of the underlying theory, but not necessarily obvious from the terms 'attack' or 'capture rate'. In turn, g_{max} has almost no bearing on the shape of the curve at low $[P]$ (**Fig. 4f, h**) and ϵ (or ϵ_c) has little influence on the shape of the curve at high $[P]$; (**Fig. 4i, k**). Moving from a type II (**Fig. 4**, left side) to III (**Fig. 4**, right side) response switches the description of prey capture rates from a linear to quadratic function of $[P]$ (see **Section 2**), which decreases the sensitivity of grazing rates to ϵ_c (relative to ϵ), especially at low $[P]$ (**Fig. e, g**).

When using a Michaelis-Menten parameter scheme (**Fig. 4**, magenta), grazing rates are proportionally, but inversely, affected by changes in $K_{1/2}$ compared to ϵ in a disk scheme (**Fig. 4a, e, i**), leading to the dark green overlapping curves in the left-most panel of **Fig. 4**. This occurs because $K_{1/2}$ is equal to $\frac{g_{max}}{\epsilon}$, or equivalently $\frac{1}{\epsilon h}$ (see **Sec. 2.3**), and g_{max} (and its reciprocal, h) are held constant. However, in a type III response, grazing rates are substantially more sensitive to $K_{1/2}$ than ϵ_c, (**Fig. 4c, g, k**), particularly at low prey densities (**Fig. 4g**). Moreover, in both a type II and III response, the Michaelis-Menten scheme is dramatically more sensitive to g_{max} at low prey densities (**Fig. 4f, h**). This is because faster (slower) prey capture rates and thus a larger prey capture efficiency are implicitly required for the curve to saturate at a faster (slower) grazing rate with the same half saturation concentration.

Computing the mean grazing rate across low ($0-0.5\ \frac{mmolC}{m^3}$) and high ($10-15\ \frac{mmolC}{m^3}$) phytoplankton concentrations ($[P]$) for all grazing formulations considered in our sensitivity analysis (**Table 4**) confirms these trends (**Fig. 5**). In a type II disk formulation, grazing rates at low $[P]$ are almost entirely unaffected by g_{max}, especially when ϵ is low (**Fig. 5a**), whereas grazing rates at high $[P]$ are almost entirely driven by g_{max}, especially when ϵ is large (**Fig. 5b**). Introducing the concavity of a Type III response increases this disparity. In turn, the mean grazing pressure at low $[P]$ increases with ϵ_c but is effectively invariant across 3 orders of magnitude change in g_{max} (**Fig. 5c**). Alternatively, mean grazing rates at high $[P]$ are almost entirely described by g_{max} unless ϵ_c is so low that our definition of 'high $[P]$' no longer falls above the half saturation point of the curve (**Fig. 5d**).

Using a Michaelis-Menten scheme increases the sensitivity of grazing rates to both parameters (**Fig. 5e-h**), such that g_{max} has much more influence at low $[P]$ (**Fig. 5e, g**) and $K_{1/2}$ has more influence at high $[P]$ (**Fig. 5f, h**). However, in a type III response, grazing rates are still more sensitive to $K_{1/2}$ than g_{max} at low $[P]$ (**Fig. 5g**) and more sensitive to g_{max} than $K_{1/2}$ at high $[P]$ (**Fig. 5h**). Increased parameter sensitivity in the Michaelis-Menten scheme means that a greater variety of curve shapes and associated grazing rates can be described with an equivalent range of parameter values, albeit with lower resolution. This means that there should be more variability in model output derived from equivalent changes in Michaelis-Menten versus disk parameters.

In other words, in a Michaelis-Menten scheme a smaller range of parameters can test the same range of curves, but many intermediate options with be skipped.

5.2 Sensitivity of phytoplankton population size

The mean size of the phytoplankton population, $\overline{[P]}$, (**Fig. 6**, left column) is largely driven by the shape of the functional response at low phytoplankton concentrations and unaffected by the curve as it begins to saturate at high phytoplankton concentrations. For example, $\overline{[P]}$ is 14% lower in type II than analogously parameterized type III responses (i.e. same $K_{1/2}$ and g_{max}), despite the fact that a type II response takes much longer to reach maximum grazing rates (i.e. saturation), and prescribes slower grazing at all prey concentrations above $K_{1/2}$. This disparity increases to 58% when only considering

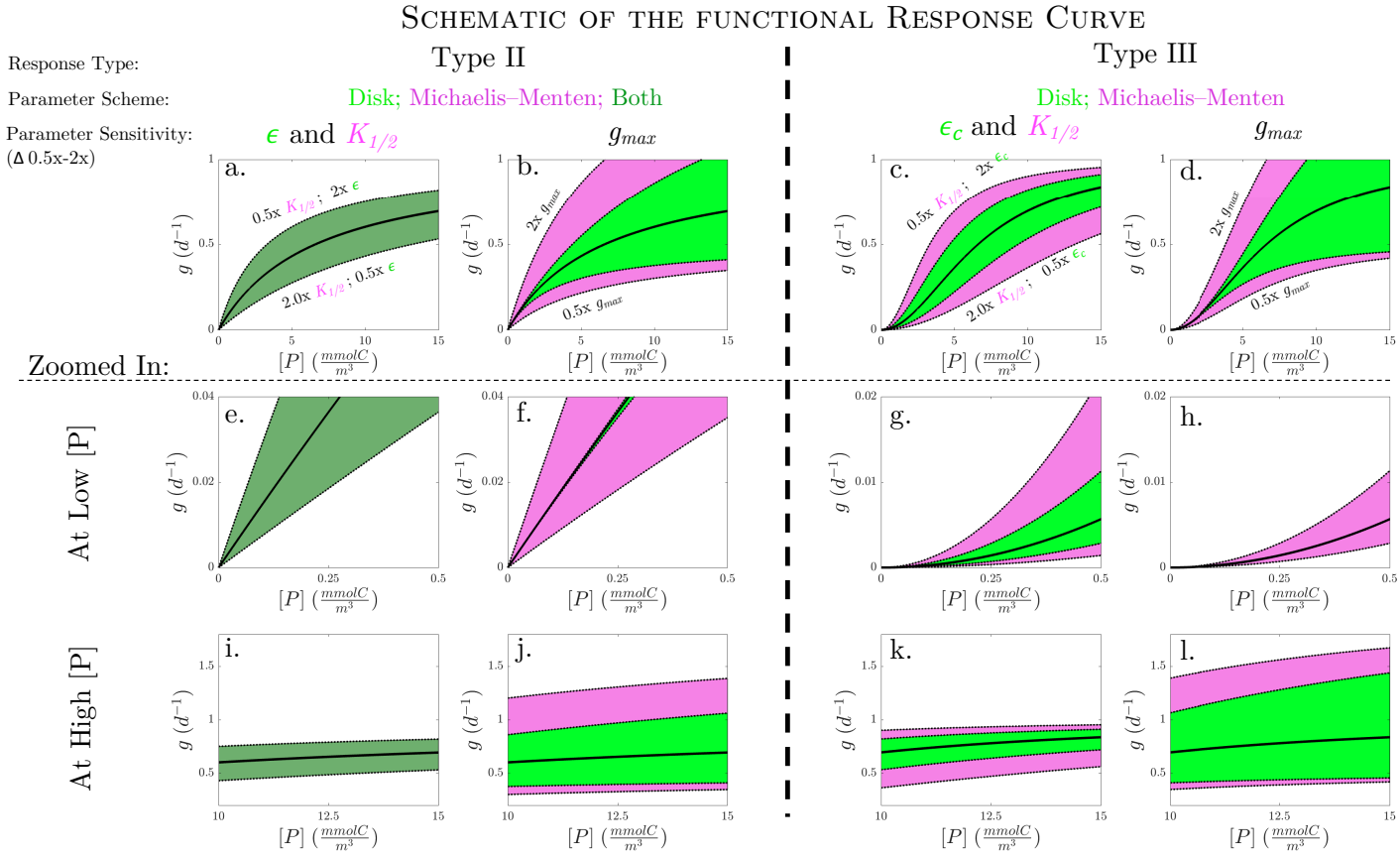

Figure 4. Schematic of the functional response curve. A type II (**a,b**) and III (**c,d**) response curve is plotted in black with colored windows depicting how the curve varies with proportional changes to its parameters. Initial parameters were chosen such that the disk and Michaelis-Menten parameter schemes yield mathematical identical curves ($g_{max} = 1$, $K_{1/2} = 6.625$). Colored windows show how the curve varies when its parameters are individually halved (0.5x) or doubled (2x) within a disk (green) or Michaelis-Menten (magenta) parameter scheme. The shaded region depicts the range of curves encompassing a 0.5x-2x change in the associated parameter. Close ups of the same curves are shown below for (**e-h**) low and (**i-l**) high phytoplankton concentrations. Annotations in Row 1 show which curves correspond to which parameter modification. Note the dark green shading in (**a,e & i**) indicates a complete overlap in the variability window for both parameter schemes.

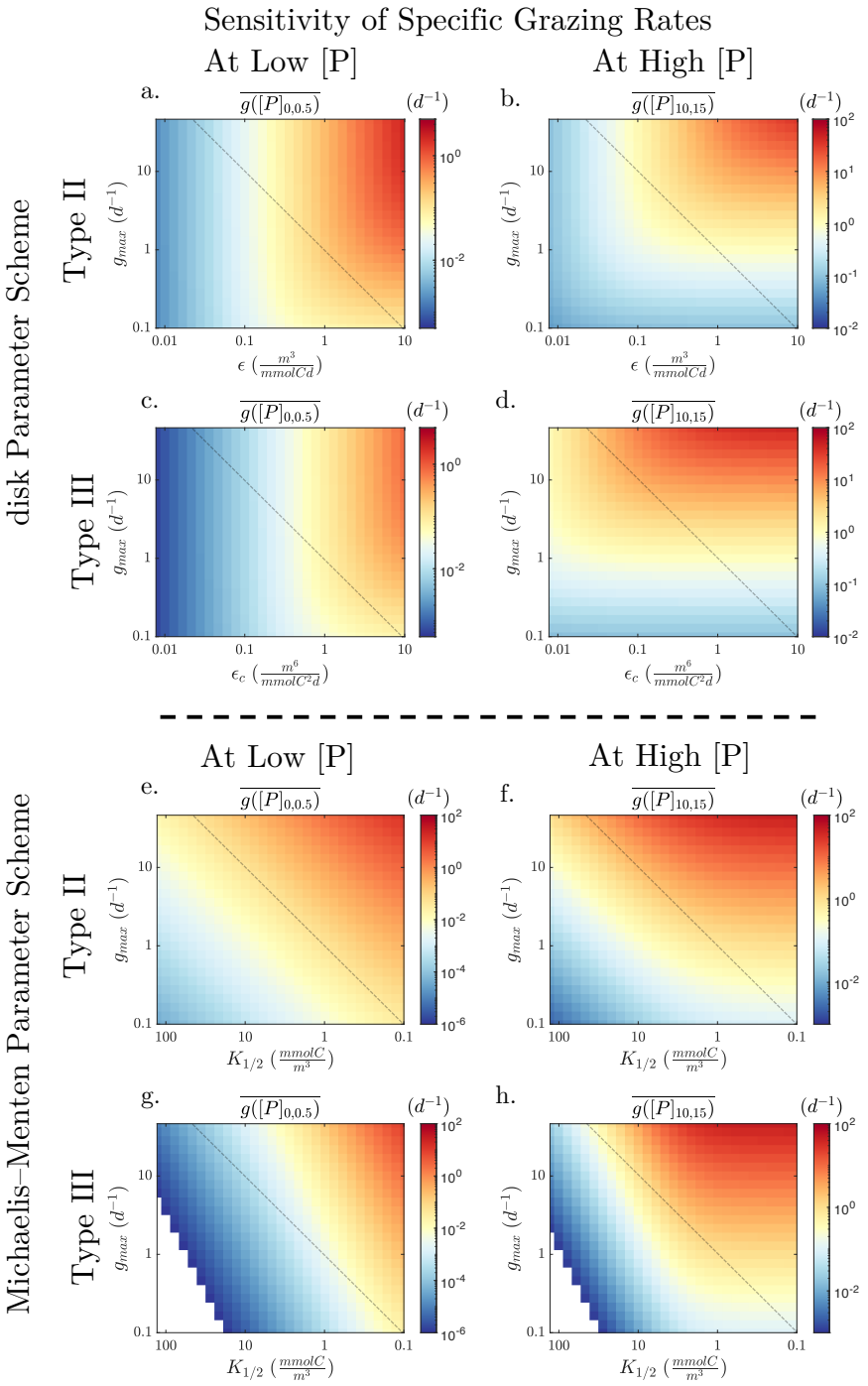

Figure 5. Sensitivity of specific grazing rates. Variability in the mean zooplankton specific grazing rate averaged across (**a, c, e, g**) low ($[P] < 0.5\frac{mmolC}{m^3}$) and (**b, d, f, h**) high ($10 < [P] < 15\frac{mmolC}{m^3}$) phytoplankton concentrations ($[P]$) is shown as a function of the parameters of the functional response curve using a (**a, b, e, f**) Type II and (**c, d, g, h**) Type III response type, as well as a (**a-d**) disk and (**e-h**) Michaelis-Menten parameter scheme. The range of low and high $[P]$ correspond to the zoomed in panels of the schematic in **Fig. 4**. A dashed log 1:1 line is included to assess the relative parameter sensitivity.

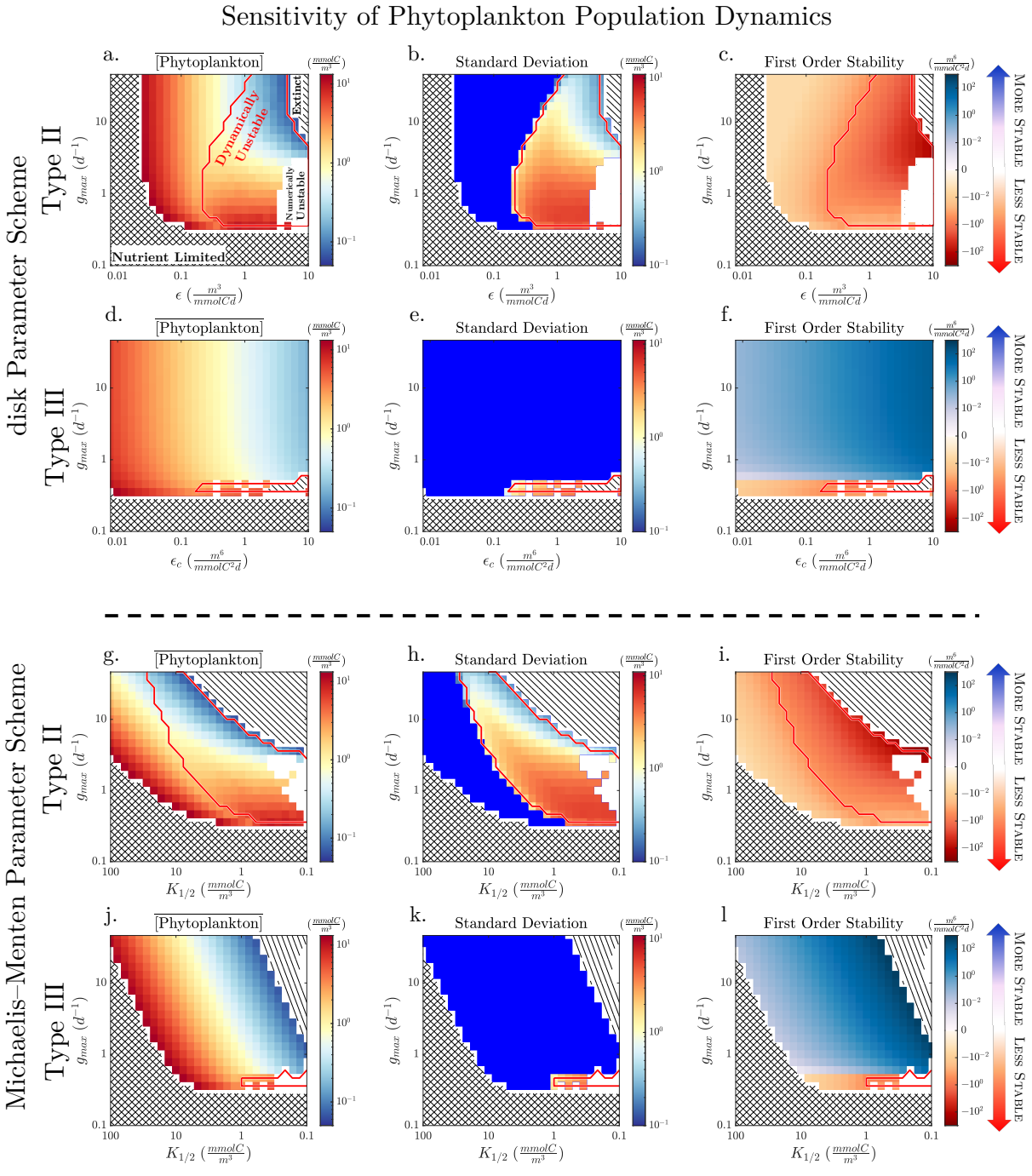

Figure 6. Sensitivity of phytoplankton population dynamics. Variability in the (**a, d, g, j.** mean annual phytoplankton concentration, (**b, e, h, k.** standard deviation, and (**c, f, i, l.** First Order Stability of the solution are plotted against the parameterization of the functional response curve using a (**a-c, g-j.** Type II and (**d-f, j-l.** Type III response type as well as a (**a-f.** disk and (**g-l.** Michaelis-Menten parameter scheme. Parameter schemes that yield complete nutrient utilization or phytoplankton extinction are hatched out with cross or single lines, respectively. Dynamically unstable regions are bounded with a red contour, while dynamically stable solutions have a near-zero standard deviation and appear blue in **b, e, h, k.** Numerically unstable regions are plotted in white. Note that the dynamics and stability of the disk and Michaelis-Menten parameter schemes are identical when their parameters overlap (i.e. $\epsilon = g_{max}/K_{1/2}$ or $\epsilon_c = g_{max}/K_{1/2}^2$)

stable solutions that have neither gone extinct nor reached complete nutrient limitation (see **Section 5.3**). This occurs because $\overline{[P]}$ dynamics are more sensitive to grazing when prey $[P]$ is low and a type II response imposes faster grazing than its type III analogue below $K_{1/2}$.

The out-sized importance of the grazing rates at low $[P]$ is even more noticeable in the type III response. Considering all dynamically solutions, $\overline{[P]}$ has a much stronger correlation with mean grazing rates at low $[P]$ ($r^2 = 0.97$) than high $[P]$ ($r^2 = -0.53$). Accordingly, the sensitivity of $\overline{[P]}$ to the grazing formulation qualitatively mirrors the sensitivity of mean grazing rates at low $[P]$ to the grazing formulation (**Fig. 5, 6**, left columns). Ecologically, this implies that the size of phytoplankton populations is limited by zooplankton capture rates, which dominate when prey is scarce, not consumption rates, which dominate when prey is abundant and the zooplankton community is more likely to be larger and capable of exerting strong grazing pressure, regardless of the speed of zooplankton specific grazing rates.

In turn, $\overline{[P]}$ is most sensitive to the parameterization of the response curve when the response type and parameter scheme allow for those parameters to most efficiently describe the bottom of the response curve. This means $\overline{[P]}$ is less sensitive to the parameterization of the functional response in a disk than Michaelis-Menten parameter scheme. For example, phytoplankton in a type III disk scheme only experienced extinction or complete nutrient utilization in 20% of the tested parameter space (**Fig. 6d**), compared to 40% when using a type III Michaelis-Menten scheme (**Fig. 6j**). The size of the intermediate solution space will vary with other parameter choices and the size of the nutrient pool; however, the fact remains that a smaller range of parameters is needed to span from extinction to complete nutrient utilization in a Michaelis-Menten than disk scheme. Similarly, when using a type III response, $\overline{[P]}$ is more sensitive to $K_{1/2}$ and ϵ_c than g_{max} in both parameter schemes because they more directly define the shape of the response curve when prey is scarce (**Fig. 4g, h**). The value g_{max} has almost no influence on the size of the phytoplankton population in a type III disk scheme.

5.3 Sensitivity of phytoplankton population stability

In the simplified NPZ model, with no seasonal forcing, phytoplankton populations tend to quickly reach a seasonally invariant steady state. However, if the destabilizing influence of the functional response is large enough, dynamically unstable oscillations (i.e. limit cycles) in the phytoplankton population can emerge. The magnitude of the destabilizing (or stabilizing) influence of the grazing formulation is determined by both the curvature the functional response as well as the prognostic feedback of grazing on the phytoplankton population, which determines its the position on the curve. We approximate the magnitude of this stabilizing influence with the First Order Stability (**Fig. 6c, f, i, l**), defined as the first derivative of clearance rates (see **Sec. 3**) calculated at the mean phytoplankton concentration in year 5 of the solution. Larger negative values, for example, mean that the grazing formulation has a more destabilizing influence on the mean phytoplankton population, but does not necessarily determine if the system is dynamically unstable, as other stabilizing processes could dominate.

To determine if the system is dynamically unstable, we investigated whether oscillations emerged. The strength of these oscillations was approximated by the standard deviation of the phytoplankton population (**Fig. 6b, e, h, k**). The system was deemed stable if it reached roughly steady state by year five of the integration and exhibited a near-0 standard deviation (plotted in blue). The system was deemed dynamically unstable if the standard deviation in year 5 is greater than 0.5% of the total nutrient pool. The system was further deemed numerically unstable if Matlab's ode45 solver, a standard non-stiff integration technique, was unable to meet the integration tolerance without reducing the integration time-step below the smallest allowed. This occurs when the

initial slope of the functional response curve is exceedingly steep (i.e. high ϵ), allowing for large changes in grazing, even at slow integration time-steps, causing the solution to explode toward negative or positive infinity. Such solutions are theoretically attainable using a smaller time-step or more sophisticated stiff integration technique but are not necessary for our purposes. Here, we only flag the numerically parameter combinations as too stiff to be solved with a standard non-stiff integration technique at a reasonable time-step.

The phytoplankton population remains dynamically stable, with a near zero standard deviation (**Fig. 6b, e, h, k**, blue shading), when First Order Stability is positive or slightly negative (**Fig. 6c, f, i, l**). However, the phytoplankton population begins to oscillate, exhibiting much larger standard deviations, once First Order Stability becomes sufficiently negative. It is possible for a dynamically stable solution with negative First Order Stability to emerge if other stabilizing factors dominate the destabilizing influencing of the grazing formulation. First Order Stability, as defined here, is only a measure of the stabilizing (or destabilizing) influence of the grazing formulation and other factors can provide a stabilizing feedback on the phytoplankton population. In this model, these factors include nutrient limitation and the size of the zooplankton community, which both increasingly dampen phytoplankton population growth as phytoplankton biomass accumulates, even if specific grazing rates decline. In more complicated NPZ models other factors, including more complex closure schemes such as quadratic zooplankton mortality, can provide stability as well (A. M. Edwards & Yool, 2000; J. H. Steele & Henderson, 1992). Conversely, in this simple model, oscillations never occur when First Order Stability is positive, even when initial conditions are varied by 0.5-2x (**Table 4b**). However, it is possible that in longer simulations of more complex models with other destabilizing factors, they may.

When using a type II response (**Fig. 6**; rows 1 & 3), First Order Stability is always negative and the phytoplankton population in 53% of tested solutions was either dynamically unstable (37.5%, red contour), numerically unstable (5.5%, white), or extinct (10%, diagonal hash). Increasing g_{max} and decreasing $K_{1/2}$ both decrease stability; however, when using a Michaelis-Menten parameter scheme, the First Order Stability is, on average, ~ 5 times more sensitive to changes in $K_{1/2}$ than g_{max} due to its greater influence on the curvature of the functional response. In a disk scheme, however, First Order Stability is only 0.25 times more sensitive to ϵ than g_{max}, because both parameters influence the location of $K_{1/2}$. Because the stability of the population is much more sensitive to g_{max} than the size of the population, relatively small changes in g_{max} could trigger sudden instabilities with little warning.

When using a type III response (**Fig. 6**; rows 2 & 4), First Order Stability is rarely negative. Only 5.5% of tested solutions were dynamically (1.7%) or numerically (3.8%) unstable and less than 4% led to phytoplankton extinction. First Order Stability becomes increasingly stable with increasing g_{max} and decreasing $K_{1/2}$ because increasing grazing pressure drives $[P]$ below $K_{1/2}$, where the upward concavity of the response curve provides stability and protects against extinction. This holds even though decreasing $K_{1/2}$ simultaneously lowers the threshold for instability. There is only negative First Order Stability and oscillations in the phytoplankton population when both $K_{1/2}$ and g_{max} are very low. This occurs because as the g_{max} approaches the zooplankton mortality rate, zooplankton net population growth slows, decoupling $[P]$ and $[Z]$ and allowing $[P]$ to escape grazing pressure and exceed a low $K_{1/2}$ value.

5.4 Influence of other parameters

The sensitivity of phytoplankton population size to the grazing formulation does not appear to be qualitatively influenced by the selection of other non-grazing parameters or initial conditions (see **Table 4b**); however, these choices influence the size of the

stable solution space. Nutrient limitation is described by a type II Michaelis-Menten curve and thus has similar, but qualitatively opposite, stabilizing properties to the grazing formulation. The difference is that the saturation of nutrient uptake provides a negative, rather than positive, feedback on phytoplankton population growth. In turn, increasing the maximum phytoplankton specific division rates (μ_{max}) or decreasing the half saturation concentration for nutrient uptake (K_N) both increase the stability of the system and reduce the number of unstable solutions. On the other hand, our results agree with previous work that limiting zooplankton community growth by either increasing zooplankton mortality (m_Z) or reducing grazing efficiency (α) can increase the destabilizing influence of a type II (or Ivlev) response (Edwards et al., 2000a, b, GN08) (C. Edwards, Powell, & Batchelder, 2000; C. A. Edwards et al., 2000; Gentleman & Neuheimer, 2008). We go on to show that this can even occur in a type III response if $m_Z > \alpha g_{max}$ (**Fig. 6e,k**), thereby decoupling specific grazing rates from bulk grazing pressure (i.e. $g[Z]$). Reallocating the initial distribution of nutrients between the $[N]$, $[P]$, and $[Z]$ pools had little influence on stability. However, as similiarly shown by Franks and Chen (1996, 2001), increasing the total nutrient pool increases the number of unstable solutions by diminishing the stabilizing influence of nutrient limitation.

6 Sensitivity to sub-grid scale heterogeneity

Mechanistic derivations (**Sec. 2**) and empirical approximations (**Sec. 4**) of the functional response are based on communities that are spatially well-mixed. Therefore, the shape and sensitivity of the functional response is predicated on the assumption that a homogeneously distributed zooplankton community is grazing on a homogeneously distributed phytoplankton population. However, the ocean is notoriously patchy, with global plankton distributions highly heterogeneous at scales well below the typical resolution of even eddy-resolving ocean models (Ohman, 1990; Raymont, 2014). Phytoplankton and zooplankton communities are often log-normally distributed (J. Campbell, 1995; Druon et al., 2019), such that an increase in the mean plankton concentration is associated with a disproportionate increase in smaller areas of high productivity, surrounded by large swaths of lower productivity. In turn, the functional response used in global, or even coarse regional models, is likely to be implicitly averaged over substantial sub-grid scale heterogeneity.

Ideally, coarse models should strive to prescribe how mean specific grazing rates, $\overline{g}$, averaged across a grid-cell, vary with the grid-cell mean phytoplankton population, $\overline{[P]}$. However, this apparent mean functional response ($\overline{g([P])}$) can differ substantially from the local response of individual zooplankton ($g([P])$ when averaged across sufficient sub-grid scale heterogeneity. Notably, Morozov and Arashkevich (2008, 2010) have shown the emergence of upward concavity in $\overline{g([P])}$ when averaged across a 1-D water column model, even though $g([P])$ was prescribed with a type II response. These modelling studies were further supported by field work (Morozov et al., 2008) and led Morozov to advocate for the emergence of the type III response as a more appropriate representation of dynamics integrated vertically across the water column (Morozov, 2010). Critical to this finding were the conditions that: 1) The vertical distribution of prey becomes more heterogeneous as the mean state increases due to nonlinear effects of light attenuation and self-shading (Herman & Platt, 1983); and 2) Zooplankton can take advantage of this disparity through active vertical migration (Giske, Rosland, Berntsen, & Fiksen, 1997; Herman & Platt, 1983; Lampert, 2005). In turn, increasing the mean prey field coincides with: 1) An increase in the discrepancy between the depth-averaged prey concentration and that of high density layers; and 2) An increase in the relative proportion of zooplankton grazing in those high density layers. Together, this is capable of yielding an exponential increase in the mean grazing rate with the mean prey concentration (i.e. Type III), even if the local response is linear (i.e. Type II).

We further generalize these results by examining a simple non-dimensional system (or grid cell) composed of just two regimes: one fraction of high productivity water, and one fraction with low productivity water. Unlike Morozov and Arashkevich (2008), in which the biological rates in each vertical layer are explicitly linked via the active migration of zooplankton and the attenuation of light due to shelf-shading, our two fractions can be considered independent. This has the advantage of considering the effect of averaging across two distinct ecological niches in a coarse grid cell, rather than one tightly coupled system. This is an important distinction because because uncoupling the system decreases the degree of inherent non-linearity (e.g. in Morozov and Arashkevich (2008) increasing phytoplankton growth rates in one layer necessarily decrease growth rates in the layer below via shelf-shading). Further, general circulation models have much higher vertical (10 m) than horizontal resolution (10-100s km), most biogeochemical models already resolve self-shading, and future generation models may include active vertical migration as well (Archibald, Siegel, & Doney, 2019). Thus, future models may explicitly account for the mechanisms that lead to the emergence of a type III response in the vertical, but still implicitly average across a great deal of ecological heterogeneity horizontally. In this way our generalized 0-D representation may be a more useful analogue to a 3D grid-cell, as it is not tied to specific mechanisms that operate vertically. Our results show that averaging across a spatially patchy ocean fundamentally changes the shape of the apparent mean functional response, even without direct interaction between the oligotrophic and eutrophic parts of the grid cell. We show how this averaging can increase apparent mean capture rates, induce upward concavity at low $\overline{[P]}$, and increase the sensitivity of mean specific grazing rates to local consumption rates.

We assume a generic model grid cell is divided into two regimes, one fraction with high productivity eutrophic water, f_{eu} and one fraction with low productivity oligotrophic water, f_{ol} (f_{eu}+$f_{ol} = 1$). All zooplankton are assumed to graze according to the same local functional response, $g([P])$, but the sub-grid scale distributions of phytoplankton ($[P]_{eu}$, $[P]_{ol}$) and zooplankton ($[Z]_{eu}$, $[Z]_{ol}$) biomass are assumed to be heterogeneous and allowed to vary in time. The phytoplankton population is assumed to grow exponentially with a different growth rate in each region (μ_{ol}, μ_{eu}).

The concentration of zooplankton biomass in either region is assumed to be proportional to the distribution of phytoplankton. This is a similar assumption to that made by Morozov and Arashkevich (2010), who assume that zooplankton biomass co-varies with prey abundance across the water column. In the vertical, this assumption is well supported by observations of zooplankton aggregating in food-rich layers (Giske et al., 1997; Herman & Platt, 1983; Lampert, 2005). While it is difficult to observe individual lateral migration in the open ocean (Pearre, 2003), it is plausible that zooplankton, known to forage vertically between different depths based on the balance between predation risk and hunger (Pearre, 2003; Pierson, Frost, & Leising, 2013), may drift with currents for longer at depth between unsuccessful forays to the surface, before vertically migrating less and staying closer to the surface once they find food (Bandara, Varpe, Wijewardene, Tverberg, & Eiane, 2021). This would lead to a similar consolidation of zooplankton around horizontally distributed high-density prey patches. More importantly, active individual migration of zooplankton is not a necessary assumption here. In the work of Morozov and Arashkevich (2010) and Morozov and Arashkevich (2008), active migration was required to account for shifts in the zooplankton distribution because the short time scale considered precluded substantial population growth (note that many zooplankton - especially microzooplankton and some mesozooplankton and macrozooplankton - exhibit very little vertical migration). However, by considering two distinct ecological niches, assumed to exist in the same grid cell but implicitly averaged over larger space and time scales, the population of zooplankton needs only to be assumed to increase faster in regions with higher prey abundance (and thus higher grazing and growth rates) for the relative distribution of zooplankton to shift towards more eutrophic patches as the grid cell

mean prey concentration increases. Therefore, no assumptions regarding active migration are required.

The concentration of phytoplankton and zooplankton in either fraction of the grid cell ($R = eu, ol$) can then be computed at a given time as

$$[P]_R = [P]_{R,t=0}(1 + \mu_R)^t \tag{28}$$

$$[Z]_R = \theta \frac{[P]_R}{\overline{[P]}}, \tag{29}$$

where $[P]_{R,t=0}$ is the initial concentration and θ is the proportionality constant for zooplankton biomass. Finally, the apparent grid cell mean specific grazing rate, $\overline{g}$, and phytoplankton concentration, $\overline{[P]}$, can be calculated as

$$\overline{[P]} = (f_{eu}[P]_{eu} + f_{ol}[P]_{ol}) \tag{30}$$

$$\overline{g} = g([P]_{eu})\frac{[Z]_{eu}f_{eu}}{Z_{tot}} + g([P]_{ol})\frac{[Z]_{ol}f_{ol}}{Z_{tot}}, \tag{31}$$

where Z_{tot} is the sum of all zooplankton in the grid cell (i.e. $Z_{tot} = [Z]_{eu}*[f]_{eu}+[Z]_{ol}*f_{ol}$). Note that θ cancels out in **eq. 31**. The spatially-averaged, apparent mean functional response, $\overline{g([P])}$, can then be examined by plotting all values of $\overline{[P]}$ against $\overline{g}$ (**Fig. 7**).

We consider two scenarios. In the first scenario (**Fig. 7a, b**), all biology is assumed to be consolidated in the eutrophic fraction of the grid cell (i.e. $[P]_{ol,t=0}$, μ_{ol}, $[P]_{ol}$ and $[Z]_{ol}$ all equal 0). In this scenario it does not matter what the initial concentration or growth rate of phytoplankton in the euphotic region is because the relative distribution is constant (i.e. $[P]_{eu}f_{eu}/[P]_{Tot} = 1$) and the grid-cell mean specific grazing rate, $\overline{g}$, reduces to the local response, $g([P]_{eu})$. However, $\overline{[P]}$ is less than $[P]_{eu}$ as it is diluted by the oligotrophic fraction. We consider a local type II (**Fig. 7a**) and type III (**Fig. 7b**) response. In both cases, the qualitative shape of $\overline{g([P])}$ is consistent with the local response; however, there is a decrease in the half saturation concentration of $\overline{g([P])}$ which is proportional to the size of the euphotic fraction of the grid cell, such that $\overline{K_{1/2}} = f_{eu}K_{1/2}$. This occurs because all zooplankton are actually grazing on a phytoplankton concentration ($[P]_{eu}$) that is $1/f_{eu}$ larger than the grid cell mean. In turn, as biological productivity is consolidated into a smaller fraction of the grid cell, the apparent capture rate appears to increase (i.e. the initial slope of the curve steepens). However, this occurs not because local capture rates increase, but because zooplankton are grazing at saturation in a smaller area.

Note that unlike the results of Morozov and Arashkevich (2008) and Morozov and Arashkevich (2010), this deformation of the mean response does not require any assumptions about how the distribution of phytoplankton or zooplankton biomass varies with the mean concentration. This is not necessarily inconsistent with their findings that such conditions are required for the emergence of a type III mean response because here it is only the apparent parameters of the mean response, not the response type itself, that changes. However, it is clear that a much simpler set of assumptions, only that the ocean is patchy and a given grid-cell likely includes some swaths of relatively oligotrophic water, can lead to dramatic differences between the local and mean functional response.

In the second scenario (**Fig. 7c-f**) we assume that all water contains at least some biomass, but that phytoplankton population growth is faster in the eutrophic fraction. Here, phytoplankton biomass begins uniformly distributed with an initial concentration

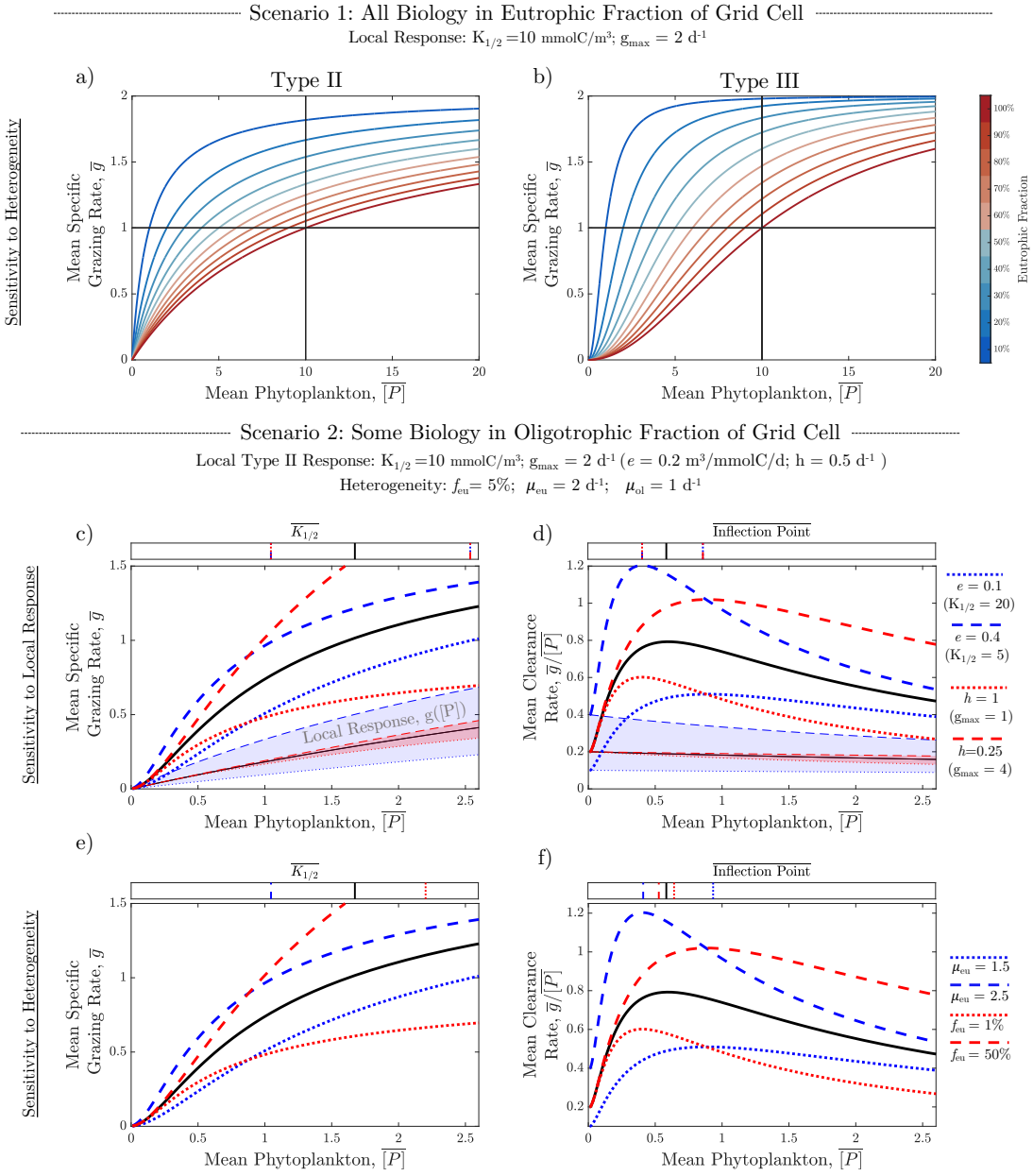

Figure 7. Influence of sub-grid scale heterogeneity. The spatially-averaged, apparent mean functional response is plotted for several simple examples of sub-grid scale heterogeneity. **a,b.** shows what happens if a **a.** type II or **b.** III local functional response is used but biological activity is consolidated in some fraction (see colorbar) of the grid cell, with nothing in the remaining fraction. Note, the darkest red line (f_{eu}=1) is equivalent to the local response. **c-f.** show what happens to **c,e.** the mean functional response and **d,f.** mean clearance rates (solid black lines) when the same local type II response is used but some phyto- and zooplankton growth is permitted in the oligotrophic fraction of the grid cell, but at a slower rate. Red and blue lines show the sensitivity of the mean functional response to changes in **c,d.** the local response parameters and **e,f.** degree of sub-grid scale heterogeneity. The sensitivity of the local response is shaded in the background of **c** & **d**. Above each subplot, the location of the half saturation concentration and inflection point of the mean response is noted with the corresponding line style.

of 0.01 $mmolC/m^3$, then grows exponentially at a rate of 2 d^{-1} in the eutrophic fraction and 1 d^{-1} in the oligotrophic fraction. Zooplankton biomass is still assumed proportional to phytoplankton. The eutrophic fraction of the grid cell is now assumed to be 5% and the local grazing response is a Type II disk response with $K_{1/2} = 10$ and $g_{max} = 2$. We find that even though all zooplankton graze locally with a type II response (**Fig. 7c; thin black line**), $\overline{g([P])}$ exhibits upward concavity at low $\overline{[P]}$ (**Fig. 7c; solid black line**), akin to a type III response. This is even clearer when looking at mean clearance rates ($\overline{g}/\overline{[P]}$). Unlike local clearance rates (**Fig. 7d; thin black line**) which decreases monotonically, mean clearance rates (**Fig. 7d; solid black line**) initially increase, providing the same stabilizing influence as the type III response (**Sec. 3**). Note, however, $\overline{g([P])}$ is a fundamentally different mathematical curve than the standard type III response. Its apparent mean half saturation constant ($\overline{K_{1/2}} = 1.7$) is substantially lower than that of the local response ($K_{1/2} = 10$) and unlike the standard type III response, $\overline{K_{1/2}}$ is no longer the location of the inflection point of the curve (i.e. transition from upward to downward concavity) which occurs before $\overline{K_{1/2}}$ in $\overline{g([P])}$ (**Fig. 7b,c**)

Still, it is important that the mean of many individual type II responses can yield the upward concavity associated with a type III response when averaged across heterogeneously distributed plankton populations. Similar to the conditions described by Morozov (2010), the reason for this is that phytoplankton growth is associated with a shift in the relative distribution of zooplankton into the eutrophic region where they can graze faster. This hinges on the assumption that more predators are likely to reside where there is more prey, but is agnostic to the specific mechanisms for how they get there (i.e. population growth vs. migration) or their time scales. In turn, as the mean grid cell phytoplankton concentration increases, the mean specific grazing rate will increase multiplicatively with an increasing proportion of zooplankton grazing at increasingly fast specific rates, leading to an exponential increase at low $\overline{[P]}$. Note that there was no upward concavity in Scenario 1, despite sub-grid scale heterogeneity. This is because the proportion of zooplankton grazing in the eutrophic region did not increase with $\overline{[P]}$. Therefore, for upward concavity to exist in the mean state, we must assume that zooplankton are more likely to aggregate where there is more prey, either because they are growing faster locally or because they are actively migrating. This is ecologically and numerically important because it can provide dynamical stability and refuge for low phytoplankton concentrations without invoking any associated change in the assumptions about the foraging behavior of individual zooplankton.

The exact shape of $\overline{g([P])}$ is a function of the local response (**Fig. 7c,d**) and the evolution of sub-grid scale plankton distributions (**Fig. 7e,f**). Alterations to the local capture rate (**Fig. 7c,d**; blue lines) and consumption time (red lines) show how modifications to the local response (thin lines; shaded area) do not directly translate to the mean response (thick lines). As with the local response, increasing (decreasing) capture rates (ϵ) or decreasing consumption times (h) both decrease the half saturation concentration, $\overline{K_{1/2}}$, of the mean response. However, $\overline{g([P])}$ is much more sensitive to changes in the consumption time compared to the local response. For the most part, $\overline{g}$ is more sensitive to changes in h (thick red lines) than ϵ (thick blue lines) at low $\overline{[P]}$, despite hardly any change to g at low $[P]$ (thin, shaded lines). This is possible because even at low $\overline{[P]}$, heterogeneously distributed zooplankton are predominately grazing at or near saturation in small patches, where rates of consumption, not capture, drive grazing.

Altering the distribution of plankton (**Fig. 7e,f**), either by increasing population growth rates in the eutrophic fraction (blue lines) or by changing the size of the eutrophic fraction (red lines) also has a pronounced effect on the shape of $\overline{g([P])}$. Increasing (decreasing) μ_{eu} has a qualitatively similar effect to decreasing (increasing) $K_{1/2}$ because it increases the disparity between eutrophic and oligotrophic plankton populations. Reducing sub-grid scale heterogeneity by increasing (decreasing) the size of f_{eu} lowers the inflection point and decreases (increases) the extent of upward concavity. At $f_{eu} = 50\%$,

$\overline{g([P])}$ begins to qualitatively resemble $g([P])$, but $\overline{K_{1/2}}$ is still 45% lower than $K_{1/2}$. Even when we reduced heterogeneity to 20% of the grid cell growing just 10% faster, $\overline{g([P])}$ still exhibited increasing clearance rates at very low $\overline{[P]}$. Together, it is clear that the shape of $\overline{g([P])}$ can dramatically diverge from $g([P])$ but the degree to which it does is sensitive to the degree of sub-grid scale heterogeneity.

Considering that the evolution of natural plankton distributions is much more complex than modelled here, a more sophisticated analysis is required to understand which curve best represents their mean state and how varying degrees of patchiness would modify the concavity and parameters of the apparent response. However, provided there is sufficient heterogeneity, when compared to the local response, it appears that $\overline{g([P])}$ should have faster capture rates, be more sensitive to consumption rates at low $\overline{[P]}$, and exhibit a larger degree of upward concavity at low $\overline{[P]}$, than does $g([P])$.

7 Recommendations for modellers

7.1 Functional Response Choice for Single-Prey Grazing

Biogeochemical models are largely split in their use of a type II (or Ivlev) or type III functional response (**Table 3**). Of all 70 surveyed grazing formulations, 23 use a type III and 35 use a type II (12 used an Ivlev). Of those that graze with a single-prey response the split is 13, 16, and 14 for type III, II and Ivlev, respectively. Mathematically, when parameterized with analogous parameters (i.e. the same $K_{1/2}$ and g_{max}), a type II response is more likely to exert stronger grazing pressure (**Sec. 5.2**) and produce dynamically unstable solutions (**Sec. 3, 5.3**) due to its downward concavity at low prey concentrations. Ecologically, the most realistic option likely depends on the model configuration and the system being simulated.

Models that use a type III response typically benefit from its stabilizing properties (Gentleman & Neuheimer, 2008). For example, many models require a type III response to produce realistic blooms rather than unstable oscillations (Hernández-García & López, 2004; Malchow et al., 2005; Morozov, 2010; Truscott & Brindley, 1994; Truscott et al., 1994). This is because the stabilizing properties of a type III response prevent the extinction of a very small wintertime phytoplankton seed population, while starving the zooplankton community, subsequently permitting a bloom at the onset of rapid changes in bottom-up growth conditions during spring stratification (Behrenfeld et al., 2013; Evans & Parslow, 1985).

However, stability is not a sufficient justification to use a type III response. Natural systems have been observed to exhibit dynamical instabilities (McCauley & Murdoch, 1987) and even when they do not, there are many plausible stabilizing factors that could dominate unstable predator-prey dynamics to dampen limit cycles and stabilize the system (C. A. Edwards et al., 2000; Gentleman & Neuheimer, 2008). For example, only half the parameter combinations tested here actually produced a dynamically unstable solution when using a type II response (**Fig. 6a,g**). This was because the destabilizing influence of the predator-prey dynamics (i.e. the First Order Stability; **Fig. 6c,i**) was weak enough to be dominated by the stabilizing influence of nutrient limitation, which buffers changes in the phytoplankton population by decreasing (increasing) division rates when the population is large (small). Similarly, other factors such as quadratic zooplankton mortality can create a negative feedback loop which stabilizes population dynamics despite the destabilizing influence of the grazing formulation. Selecting a response type that does not represent the true destabilizing (or stabilizing) influence of natural predator-prey dynamics could lead parameter optimization schemes to underestimating (or overestimating) the influence other stabilizing processes. Thus, the stabilizing influence of a type III response is only preferable if it is ecologically representative of the predator-prey dynamics it seeks to represent.

Ecologically, there is disagreement on whether a type II (Hansen et al., 1997; Hirst & Bunker, 2003; Jeschke et al., 2004) or type III (Chow-Fraser & Sprules, 1992; Frost, 1975; Gismervik & Andersen, 1997; Sarnelle & Wilson, 2008) response is more appropriate to represent the grazing behavior of individual zooplankton. Laboratory dilution experiments are often better fit empirically by a type II response (Hansen et al., 1997; Hirst & Bunker, 2003), while a type III response is typically justified by more complex behavior, such as changes in prey refugia, (Wang, Morrison, Singh, & Weiss, 2009), predator learning (Holling, 1965; van Leeuwen, Jansen, & Bright, 2007), predator effort, (Gismervik, 2005), or prey switching (Gentleman et al., 2003; Oaten & Murdoch, 1975; Uye, 1986). Unfortunately, this behavior is difficult to replicate in a lab (Leising et al., 2003) and large-scale field experiments are challenging and rare.

However, despite uncertainty in the true behavior of individual zooplankton in their natural environment, it is possible that a type III response is more representative of their mean state, even if individuals are assumed to exhibit a sub-grid scale type II response (**Sec. 6**). If plankton are assumed to be heterogeneously distributed and the relative distribution of the zooplankton community is assumed to co-vary with the phytoplankton population, then the mean grazing rate should generally exhibit some degree of upward concavity (**Fig. 6c,e**) and exert an associated stabilizing influence on mean population dynamics (**Fig. 6d, f**). Morozov (2010) found similar upward concavity in the mean dynamics of vertically distributed plankton and argued for a Holling type III response. However, it should be clarified that while the mean behavior of heterogeneous systems likely does exhibit some upward concavity, the function is not exactly sigmoidal in shape and is mathematically distinct from a type III disk response. Importantly, the mean response becomes destabilizing (i.e. downwardly concave) well before the half-saturation concentration of the local response (**Fig. 6a,b**) and varies with the degree of sub-grid scale heterogeneity (**Fig. 6c,d**) .

In turn, the most ecologically justifiable response type may depend on the resolution of the model in question. For high resolution, small scale models, or those representing systems known to be well-mixed, a type II response is likely to be the most appropriate. Even though laboratory incubations are unlikely to translate directly to zooplankton feeding behavior in the ocean (Dutkiewicz et al., 2015), there are insufficient observations of individual zooplankton grazing with type III dynamics to justify ignoring the many empirical estimates of a type II response (Hansen et al., 1997; Hirst & Bunker, 2003). However, a type III response may be a more ecologically realistic representation of the mean state of many zooplankton grazing locally with a type II response on a highly heterogeneous phytoplankton population. Therefore, for coarse-resolution, large-scale models (e.g. global earth system models) a type III response may be more appropriate.

7.2 Parameter Scheme for Single-Prey Grazing

Throughout the literature, the type II and type III functional responses appear in two distinct, but mathematically equivalent, forms (**Table 2**): the disk parameter scheme (**eq. 17, 24**) (Adjou et al., 2012; Fasham, 1995; Law et al., 2017; Oke et al., 2013; Schartau & Oschlies, 2003b) and the Michaelis–Menten parameter scheme (**eq. 19, 25**) (Aumont & Bopp, 2006; Dutkiewicz et al., 2015; Hauck et al., 2013; Le Quéré et al., 2016; Moore et al., 2013; Stock, Dunne, & John, 2014; Totterdell, 2019; Vichi et al., 2007). Both schemes can describe identical response curves given the right parameterization, but use different information to do so. The disk scheme uses ecologically meaningful quantities to mechanistically determine how grazing rates vary in well-mixed systems. On the other hand, the Michaelis–Menten scheme is an empirical description of the shape of the curve, with no theoretical basis.

This distinction would be irrelevant if we had infinite computational power to sample all parameter combinations and a complete set of observations with which to eval-

uate their skill. In this scenario, the optimized cost function (i.e. the agreement between model output and observations) would converge on a mathematically and dynamically identical functional response curve, regardless of whether a Michaelis–Menten or disk scheme was used. However, modern biogeochemical models include dozens of different parameters, many with a large spread of plausible values (e.g. **Section 4**), and computational limitations exist (Matear, 1995; Neelin, Bracco, Luo, McWilliams, & Meyerson, 2010). Therefore, it is not practical (or often possible) to test all parameter combinations. Moreover, these models are heavily under constrained (Doney, 1999; Matear, 1995; Schartau et al., 2017; Ward et al., 2010), meaning there are insufficient observations to identify a unique parameter set as optimal. Instead, parameter optimization routines must use limited information to decide which parameter sets to test to converge on the optimal solution. Unfortunately, these routines can yield the right result for the wrong reason (T. R. Anderson, 2005) and/or identify local rather than global minima/maxima (Ward et al., 2010), meaning that they do not always converge on the 'true' optimal solution.

Whether or not a specific search routine is successful (or computationally efficient) is often determined by the path it uses to search the parameter space. Often the direction of this path is determined by back-computing the partial derivatives of the cost function with respect to each parameter and then moving down the steepest gradient in parameter space (Kane et al., 2011). In other algorithms, movement across parameter space is more stochastic, mimicking the evolutionary process by selecting for optimal genomes (i.e. parameter sets) from a population of initial estimates and passing on their parameters (sometimes with mutations) to future 'generations' (Falls et al., 2022). Either way, if search schemes are 'pointed' in the wrong direction, say by a partial with a large magnitude or a mutation with strong fitness, then they may take much longer to compute or, worse, never converge on the 'true' optimal solution. It is therefore important to consider the influence of individual parameters on the model solution, as they can help steer parameter search routines.

Although g_{max} and $K_{1/2}$ in a Michaelis–Menten scheme and g_{max} and ϵ (or ϵ_c) in a disk scheme form the same basis, they are fundamentally different parameters. Thus, their partials with respect to the functional response, model solution, and cost function will be different, meaning they could point search algorithms in different directions. Therefore, even though it is plausible for an optimization scheme to converge on the same functional response regardless of parameter scheme (particularly in simpler models), it would be prudent to use the parameter scheme with partials that most accurately represent reality. This would presumably be more likely to 'point' in the 'right' direction and thus converge on the 'true' optimal solution in the most efficient manner. Thus it is useful to consider how the partials of both parameter schemes compare with what we would expect ecologically.

The most notable difference between the influence of the individual parameters of the functional response is that independent changes to g_{max} have a much more pronounced influence on the shape of $g([P])$ at low $[P]$ in the Michaelis–Menten scheme (**Section 5.1, 5.2**). This is because changing g_{max} in a Michaelis–Menten scheme implicitly changes the initial slope of the response curve (i.e. ϵ), while changing g_{max} in a disk scheme conserves the value of ϵ, but instead modifies the half saturation concentration (i.e. $K_{1/2}$) (**Section 2**). In turn, phytoplankton population growth, which is most sensitive to grazing at low concentrations, is much more responsive to changes to g_{max} in a Michaelis–Menten scheme than in a disk scheme, leading to entirely different model dynamics (**Section 5.3**). Therefore, the partial derivative of the cost function with respect to g_{max} could point the search algorithm in entirely different directions depending on which parameter scheme is used. The question is which direction is most ecologically realistic, or more specifically, should zooplankton specific grazing rates at saturation be related to those when food is scarce? We suggest that the answer depends on the system being simulated.

If the system in question is well-mixed, then it is reasonable to assume it generally conforms to the assumptions that underlie the disk parameter scheme and classic Holling-style predator-prey dynamics. In this case there there should be no relationship between grazing rates at very low and very high prey concentrations. This is because grazing is limited by capture rates (ϵ) when food is scarce versus consumption times ($h = 1/g_{max}$) when food is replete and these are assumed to be two physiologically distinct processes. Thus, a disk scheme will yield the theoretically correct partial with respect to g_{max}, in that it has fairly little influence on the model solution, particularly in oligotrophic (i.e low $[P]$) regions. The disk scheme has the added advantage of a strong theoretical basis, which allows modellers to directly prescribe biologically meaningful quantities. In general, this is the simplest way to reduce confusion amongst biologists and modellers and ensure that trait-based relationships are correctly parameterized between functional groups (see **Section 4**).

However, the theoretical integrity of the disk response may be limited to well-mixed systems and not necessarily represent the mean state of a patchy ocean, which coarse global models must implicitly average over. In **Section 6**, we demonstrated how when averaged across a patchy grid cell, decreasing local zooplankton consumption times can substantially increase the grid cell mean grazing rate at low mean $\overline{[P]}$, without actually influencing how zooplankton graze locally at low local $[P]$, where grazing rates remain dominated by capture rates (**Fig. 7c**). This is possible because a greater proportion of zooplankton are grazing at a prey density closer to saturation than the grid cell mean, which is diluted by large swaths of oligotrophic water, would suggest. In other words, the partial derivative of the apparent mean functional response with respect to g_{max} is qualitatively more consistent with that of a Michaelis–Menten rather than disk parameter scheme. In this case, the empirical nature of the Michaelis–Menten scheme is advantageous, as it is not constrained by mechanistic underpining of the disk response, allowing the individual influence of each parameter to capture a combination of the local grazing dynamics (as governed by the disk parameters) as well as the time-evolving subgrid scale distribution of zooplankton and phytoplankton. Therefore, when modelling the mean state of a sufficiently heterogeneous region, it may be more appropriate to use a Michaelis–Menten parameter scheme.

Additionally, another potential advantage of the Michaelis–Menten scheme is that population dynamics are more sensitive to proportional changes in its parameters, compared to the disk parameters, particularly for a type III response (**Section 5.2**). This is predominately because ϵ_c implicitly varies with the square of $K_{1/2}$ in a Michaelis-Menten scheme ($\epsilon_c = \frac{g_{max}}{K_{1/2}^2}$). In turn, the disk scheme is less sensitive to its parameterization, meaning it requires a larger range of parameters to be tested to cover the same range of solutions. For example, a conservative range of observed ϵ_c values, from .0001-1 $\frac{m^6}{mmolC^2 d}$, can span $K_{1/2}$ $\frac{mmolC}{m^3}$ values from 1-100 at a fixed g_{max} (see contours on **Fig. 2**). The trade off is increased precision in the disk scheme; however, the overwhelming lack of consensus on what these parameters actually are (**Section 4**), especially for the mean state of the entire ocean (Moriarty et al., 2013; Moriarty & O'Brien, 2012), suggests that it is more valuable to consider a wider, but lower resolution, set of parameters to avoid inadvertently constraining the parameter space, rather than trying to focus on an impossibly exact value. For example, the parameter search used by Schartau and Oschlies (2003a), who use a disk scheme to represent the mean state of relatively coarse grid cells, chose both parameter values at the boundary of their search space, suggesting a wider range might have found a better solution. Practically speaking, this problem could be addressed by careful conversion. Modellers using a disk scheme could sub sample a wider set of coarser resolution ϵ_c values in optimization search schemes; however, modellers must select a search range for dozens, if not hundreds, of parameters, and are less likely to mistakenly constrain the parameter space if using a Michaelis-Menten scheme, which has a narrower range of realistic parameters and more intuitive units.

Together, the mechanistic and empirical nature of the disk and Michaelis-Menten parameter schemes respectively can be used intentionally to the modellers' advantage, depending on whether they are trying to represent mechanistically the behavior of zooplankton in a well-mixed system or represent empirically the mean state of grazing at the mean phytoplankton concentration of a patchy grid cell. Thus a disk scheme can be used in smaller-scale, higher-resolution models, in which the biological attributes of zooplankton are relatively well understood. This allows known, measured values, of ϵ and h to be directly prescribed and reduces the chance of inadvertently mis-parameterizing their relationship in a Michaelis–Menten scheme. However, a Michaelis–Menten scheme may be more appropriate to represent the mean state of a patchy ocean in larger-scale, lower-resolution models, in which the true parameter values are not well known. This affords the empirical flexibility to account for differences in the system as a whole, not just the local dynamics. This may allow parameter optimization routines to search more efficiently for the 'true' apparent mean response, which is necessarily an empirical relationship averaged over the effects of many distinct processes, including local grazing behavior rates and any processes that modify plankton distributions (e.g. zooplankton migration, sub-mesoscale nutrient enhancement).

7.3 Parameter Search Range for Single-Prey Grazing

Given the uncertainty in empirically estimated parameter values, it is necessary to select what range of parameters to test in optimization routines. Although there is a high degree of variability in all parameter values (**Fig. 3; Table 3**), there is more uncertainty in the correct value of $K_{1/2}$, or associated attack rates in a disk scheme. Compared to $K_{1/2}$, the value of g_{max} is better constrained by size (**Sec. 4.1**), more consistent between models and observations (**Sec. 4.2**), and less influential on driving phytoplankton population dynamics (**Section 5.2**). In turn, parameter search schemes should favor testing a larger range of $K_{1/2}$ values than g_{max} values when resource limited. However, it is reasonable to ask how large a range is appropriate, lest implicitly imposing ecologically unrealistic prey capture rates or selecting values of fringe functional groups to represent the mean state. However, there are insufficient empirical, ecological, and mathematical arguments to heavily restrict the range of grazing parameters, and $K_{1/2}$ values as low as 0.1 ($\frac{mmolC}{m^3}$) and as high as 100 ($\frac{mmolC}{m^3}$) should be considered.

Empirically, reported estimates of $K_{1/2}$ and g_{max} fit to a type II response function by Hansen et al. (1997) and Hirst and Bunker (2003) combine to yield a range of ϵ that spans 4 orders of magnitude, from .003 to 10 $\frac{m^3}{mmolC\,d}$ (**Section 3.1**; **Fig. 2**). Moreover, if a type III response had been assumed, $K_{1/2}$ estimates would remain similar while the range of ϵ_c would increase to nearly 7 orders of magnitude, from .00001 to 21 $\frac{m^6}{mmolC^2\,d}$, or roughly 1 order of magnitude slower and 3 orders of magnitude faster than the range tested in the parameter optimization search of Schartau and Oschlies (2003a) ($0.00056 < \epsilon_c < .0364$). At the species level, the range of plausible $K_{1/2}$ values appears largely unconstrained by empirical estimates of ϵ_c.

Ecologically, we do not have a firm understanding of how a myriad of complex interactions combine across innumerable zooplankton species and evolve over time to yield a reasonable approximation of the mean state. For instance, juvenile zooplankton have faster metabolic rates (Clerc, Aumont, & Bopp, 2021) and graze with $K_{1/2}$ an order of magnitude smaller than adults (Hirst & Bunker, 2003; Richardson & Verheye, 1998), suggesting the apparent $K_{1/2}$ of the community could be substantially lower during spawning. On the other hand, most applications of the functional response assume an instantaneous response between increasing prey and faster grazing rates, while in reality there is likely a longer acclimation time as predators adapt to new conditions (Mayzaud & Poulet, 1978). Explicitly including acclimation times can destabilize the response in even the most stable configurations (i.e. type III, quadratic mortality; Gentleman and Neuheimer (2008)). However, one might consider implicitly including them by using larger $K_{1/2}$ values than

found in dilution experiments, suggesting that the zooplankton community is always adapted to a lower prey density than present. This could be useful for modelling bloom initiation, where time scales of prey accumulation are similar to that of predator acclimation (1-6 days), but fails to capture dynamics accurately at steady state or during bloom decline. Additionally, filter feeding meso- and macrozooplankton, such as salps and larvaceans, are typically common in low chlorophyll waters and have a much smaller $K_{1/2}$ than euphausiids and copepods that graze in high chlorophyll waters (Hansen et al., 1997; Hirst & Bunker, 2003). If species with slower $K_{1/2}$ values dominate in more productive ecosystems, such that $K_{1/2}$ increases with chlorophyll (Chen et al., 2014), that would effectively raise the apparent global mean $K_{1/2}$ value. In turn, the community-wide $K_{1/2}$ value probably varies spatially and temporally depending on the zooplankton community present and whether it is dominated by juveniles or adults, such that the mean state of a population with shifting age and species distributions could have an apparent $K_{1/2}$ value much different than any individual within.

Mathematically, it is not just the ecosystem complexity that is poorly resolved in models, but also its spatial heterogeneity. If the phytoplankton density the average zooplankton experiences is larger than the grid cell mean, which is averaged across many square kilometers of implicitly less productive water (J. Campbell, 1995; Druon et al., 2019) then the $K_{1/2}$ value of the mean response will appear much lower than the actual grazing rate of the zooplankton (**Fig. 7a, b**). This further increases the range of possible $K_{1/2}$ values below even the fastest prey capture rates inferred from dilution experiments with homogeneous phytoplankton concentrations.

Although the full range of empirically observed $K_{1/2}$ values (0.1-71 $mmolC/m^3$) is likely to be larger than the range of plausible values to represent the mean state, this only applies to the mean value of individuals in well-mixed incubation experiments. Uncertain ecological complexities and spatial heterogeneity both work to expand the range of $K_{1/2}$ values that plausibly could represent the mean state of myriad dynamics across a patchy ocean. We thus recommend testing a broad range of $K_{1/2}$ values, particularly on the lower end, in parameter optimization routines.

7.4 Recommendations for future models

Biogeochemical models are evolving to include an increasingly complex representation of phytoplankton, including dozens of functional groups (Follows & Dutkiewicz, 2011), variable composition (Smith et al., 2015), and the flexibility to adapt to changing environments (Anugerahanti, Kerimoglu, & Smith, 2021). With these changes should come similar advances in the representation of zooplankton and zooplankton grazing. Notably, it is essential that the mean parameterization of the zooplankton field be able to respond to the evolving phytoplankton field to reflect that different zooplankton eat different things and do so at different rates. Already, many modern models include multiple zooplankton functional groups (Le Quéré et al., 2016; Stock et al., 2020) and multiple-prey grazing response (Aumont et al., 2015; Yool et al., 2021). Moving forward, it is important to consider how insights into the single-prey response extend to more complex grazing schemes.

One concern is that the Michaelis-Menten form of the multi-prey response is over parameterized, requiring an extra parameter to describe the same equation as the corresponding disk form (Gentleman et al., 2003). In turn, the parameterization of the implied single-prey response cannot be prescribed directly, but becomes a function of prey preference and the preference weighted $K_{1/2}$ used for bulk ingestion. If not careful, this could confuse the interpretation of parameter values and lead modellers to prescribe unintended single-prey dynamics that may imply inappropriate relationships between functional groups. Despite recommendations to parameterize the attributes of the multi-prey response directly with a disk scheme (Gentleman et al., 2003), 29 of 30 multi-prey graz-

ing formulations surveyed here used a Michaelis-Menten scheme, and none used a disk (**Table 2**). To help assess if this has influenced their parameterization, we compared the implied single-prey response of micro- and meso-zooplankton grazing on their preferred prey and compared them to those directly parameterized in single-prey formulations. In multi-prey formulations the median implied single-prey $K_{1/2}$ value decreases from 7.7 in microzooplankton to 4.0 in mesozooplankton. This is qualitatively inconsistent with the observed relationship (**Table 3**) as well as single-prey formulations in which the median $K_{1/2}$ value increases from 2.4 in microzooplankton to 9.1 in mesozooplankton. This suggests the models using a Michaelis-Menten multi-prey response may be implying unintended allometric relationships between functional groups grazing in their optimal conditions and highlights that modeller's who select a Michaelis-Menten multi-prey response must carefully consider the implied relationships between parameter values.

Finally, future work is needed to better assess the shape of the apparent mean functional response, both in-situ and in models. Higher resolution general circulation models are known to modify local biogeochemical distributions via their representation of nutrient transport (Harrison, Long, Lovenduski, & Moore, 2018). While it is intractable to estimate the apparent mean functional response exactly, it would be useful to better understand its attributes with deliberate experiments designed to empirically average across high resolution biogeochemical models into coarser grid-cells representative of standard global earth system models. This may help constrain the functional response curve and range of parameter values beyond what has been observed for individual well-mixed zooplankton, and lead to a better understanding of how to represent unresolved processes across the entire system that could influence sub-grid scale heterogeneity.

7.5 Implications for other models

We focus on grazing in marine biogeochemical models, but these recommendations apply to a much broader range of marine and terrestrial ecological models. Most models in marine and terrestrial systems that involve predator-prey interactions use type I, type II or type III functional responses. We found that when trying to implicitly represent sub-grid scale heterogeneity, a type III (**Section 6.1**) Michaelis-Menten response (**Section 6.2**) parameterized with a lower than-expected $K_{1/2}$ value (**Section 6.3**) may be a more ecologically realistic way to describe the mean state of patchy predator and prey populations, even if individual interactions are best described by a type II disk response, parameterized with higher $K_{1/2}$ values. In the ocean, this would apply to most higher trophic levels simulated in size spectrum (Blanchard, Heneghan, Everett, Trebilco, & Richardson, 2017; Heneghan et al., 2020), population (Alver et al., 2016), ecosystem (Audzijonyte et al., 2019; Butenschön et al., 2016) and fisheries models (Maury, 2010; Tittensor et al., 2018, 2021). Fish, for instance aggregate in schools and feed on sparse, but consolidated, prey patches. These distributions are in turn reflected in global fishing effort (Kroodsma et al., 2018). On land, plants and animals are also patchy in time and space, with high prey concentrations rare. Most abundance data for marine and terrestrial species are overdispersed and/or have an excess of zeros, implying there is a long tail to the right of low abundances (H. Campbell, 2021). The mean state of any of these systems is likely best represented by a low-$K_{1/2}$, type III, Michael-Menten response; however, the range of possible $K_{1/2}$ considered should increase with the number of unique species, interactions, and stages of life history being averaged into individual pools.

On the other hand, well understood interactions in well mixed systems, may be better represented by a type II disk response, provided there is a low amount of implicit averaging at the species and spatial level. At the species level, this may include models of simple systems with fewer species, such as lakes or polar regions rather than rainforests or coral reefs, or models of more complex systems, but with many explicitly resolved predator groups. At the spatial level, this may include the oligotrophic gyres in the ocean and grasslands or boreal forests on the land. Still, modellers should consider how much im-

plicit averaging is baked into their model and consider if it warrants a more empirical approach before choosing a mechanistic framework (disk) or response type (II) better suited for homogeneously distributed systems.

8 Conclusions

In marine biogeochemical and ecological modelling, the transfer of carbon and nutrients between trophic groups, particularly from phytoplankton to zooplankton via grazing, is typically represented with one of two functional response curves. However, we find that there is little consensus across biogeochemical models regarding: **I)** which response type to use (II vs. III); **II)** whether to describe that curve with mechanistic (disk scheme) or empirical parameters (Michaelis-Menten scheme); and **III)** what parameter values to use.

We examine the single-prey formulation of the functional response in systematic detail to provide theoretical clarity, assess the agreement between observed parameters and those used in models, examine the sensitivity of the response to its parameterization, and explore how the shape of the curve changes when averaged explicitly over sub-grid scale heterogeneity. Considering these issues collectively, we recommend using a type II disk response in models with smaller scales, finer resolution, and or well understood ecological interactions. However, we suggest that a type III Michaelis-Menten response may be more appropriate for models with larger scales, coarser resolution, and more complex ecological and physical processes implicitly being averaged across. In both scenarios, a large range of parameter values should be tested in parameter optimization schemes as the interquartile range of empirically observed values spans roughly an order of magnitude for all parameters, and the full range spans 3-4. Moreover, averaging across sub-grid scale heterogeneity could lead to $K_{1/2}$ values well below the mean of empirically estimated values obtained from experiments in well-mixed solutions. These recommendations are specifically tailored to the single-prey grazing formulation in marine biogeochemical models, but also apply to any effort to describe the mean state of multiple interactions across coarse grid cells with populations assumed to have heterogeneous sub-grid cell distributions.

Data Access

All Matlab code required to run all four NPZ models and compute the relevant diagnostics from **Section 5** (PO_Rohr_NPZ_Models.m) and run the theoretical experiments on sub-grid scale heterogeneity from **Section 6** (PO_Rohr_Subgrid_Heterogeneity.m) is hosted on the CSIRO data portal and can be found at *https://doi.org/10.25919/cmn7-1j48*. Please contact tyler.rohr@csiro.au for any further data access inquiries.

Acknowledgments

This research was supported by the Centre for Southern Hemisphere Oceans Research (CSHOR), a partnership between the Commonwealth Scientific and Industrial Research Organisation (CSIRO) and the Qingdao National Laboratory for Marine Science, and the Australian Antarctic Program Partnership through the Australian Government's Antarctic Science Collaboration Initiative.

References

Adjou, M., Bendtsen, J., & Richardson, K. (2012, January). Modeling the influence from ocean transport, mixing and grazing on phytoplankton diversity. *Ecological Modelling*, *225*, 19–27. doi: 10.1016/j.ecolmodel.2011.11.005

Aksnes, D., & EGGE, J. (1991, February). A Theoretical Model for Nutrient Uptake

in Phytoplankton. *Marine Ecology-Progress Series*, *70*, 65–72. doi: 10.3354/meps070065

Aldebert, C., & Stouffer, D. (2018, December). Community dynamics and sensitivity to model structure: towards a probabilistic view of process-based model predictions. *Journal of The Royal Society Interface*, *15*, 20180741. doi: 10.1098/rsif.2018.0741

Alver, M. O., Broch, O. J., Melle, W., Bagøien, E., & Slagstad, D. (2016). Validation of an Eulerian population model for the marine copepod Calanus finmarchicus in the Norwegian Sea. *Journal of Marine Systems*, *C*(160), 81–93. Retrieved 2021-08-10, from `https://www.infona.pl//resource/bwmeta1.element.elsevier-ccc8cb9c-f8aa-31bb-9e36-b87db0d09727` doi: 10.1016/j.jmarsys.2016.04.004

Anderson, T., Gentleman, W. C., & Sinha, B. (2010, October). Influence of grazing formulations on the emergent properties of a complex ecosystem model in a global ocean general circulation model. *Progress In Oceanography*, *87*, 201–213. doi: 10.1016/j.pocean.2010.06.003

Anderson, T. R. (2005, November). Plankton functional type modelling: Running before we can walk? *Journal of Plankton Research*, *27*(11), 1073–1081. (Publisher: Oxford Academic) doi: 10.1093/plankt/fbi076

Anugerahanti, P., Kerimoglu, O., & Smith, S. (2021, July). Enhancing Ocean Biogeochemical Models With Phytoplankton Variable Composition. *Frontiers in Marine Science*, *8*. doi: 10.3389/fmars.2021.675428

Archibald, K. M., Siegel, D. A., & Doney, S. C. (2019). Modeling the Impact of Zooplankton Diel Vertical Migration on the Carbon Export Flux of the Biological Pump. *Global Biogeochemical Cycles*, *33*(2), 181–199. Retrieved 2022-02-03, from `https://onlinelibrary.wiley.com/doi/abs/10.1029/2018GB005983` doi: 10.1029/2018GB005983

Audzijonyte, A., Pethybridge, H., Porobic, J., Gorton, R., Kaplan, I., & Fulton, E. A. (2019). Atlantis: A spatially explicit end-to-end marine ecosystem model with dynamically integrated physics, ecology and socio-economic modules. *Methods in Ecology and Evolution*, *10*(10), 1814–1819. Retrieved 2021-11-09, from `https://onlinelibrary.wiley.com/doi/abs/10.1111/2041-210X.13272` (_eprint: https://onlinelibrary.wiley.com/doi/pdf/10.1111/2041-210X.13272) doi: 10.1111/2041-210X.13272

Aumont, O., & Bopp, L. (2006). Globalizing Results from Ocean in Situ Iron Fertilization Studies. *Global Biogeochemical Cycles*, *20*(2). (tex.copyright: Copyright 2006 by the American Geophysical Union.) doi: 10.1029/2005GB002591

Aumont, O., Ethé, C., Tagliabue, A., Bopp, L., & Gehlen, M. (2015, August). PISCES-v2: An ocean biogeochemical model for carbon and ecosystem studies. *Geoscientific Model Development*, *8*. doi: 10.5194/gmd-8-2465-2015

Bandara, K., Varpe, , Wijewardene, L., Tverberg, V., & Eiane, K. (2021). Two hundred years of zooplankton vertical migration research. *Biological Reviews*, *96*(4), 1547–1589. Retrieved 2021-11-09, from `https://onlinelibrary.wiley.com/doi/abs/10.1111/brv.12715` (_eprint: https://onlinelibrary.wiley.com/doi/pdf/10.1111/brv.12715) doi: 10.1111/brv.12715

Beardsell, A., Gravel, D., Berteaux, D., Gauthier, G., Clermont, J., Careau, V., ... Bêty, J. (2021). Derivation of Predator Functional Responses Using a Mechanistic Approach in a Natural System. *Frontiers in Ecology and Evolution*, *9*, 115. Retrieved 2021-09-23, from `https://www.frontiersin.org/article/10.3389/fevo.2021.630944` doi: 10.3389/fevo.2021.630944

Behrenfeld, M. J., Doney, S. C., Lima, I., Boss, E. S., & Siegel, D. A. (2013). Annual cycles of ecological disturbance and recovery underlying the subarctic Atlantic spring plankton bloom. *Global Biogeochemical Cycles*, *27*(2), 526–540. Retrieved 2022-03-08, from `https://`

onlinelibrary.wiley.com/doi/abs/10.1002/gbc.20050 (_eprint: https://onlinelibrary.wiley.com/doi/pdf/10.1002/gbc.20050) doi: 10.1002/gbc.20050

Blanchard, J. L., Heneghan, R. F., Everett, J. D., Trebilco, R., & Richardson, A. J. (2017, March). From Bacteria to Whales: Using Functional Size Spectra to Model Marine Ecosystems. *Trends in Ecology & Evolution*, *32*(3), 174–186. doi: 10.1016/j.tree.2016.12.003

Brander, K. M. (2007, December). Global fish production and climate change. *Proceedings of the National Academy of Sciences*, *104*(50), 19709–19714. doi: 10.1073/pnas.0702059104

Butenschön, M., Clark, J., Aldridge, J. N., Allen, J. I., Artioli, Y., Blackford, J., ... Torres, R. (2016, April). ERSEM 15.06: a generic model for marine biogeochemistry and the ecosystem dynamics of the lower trophic levels. *Geoscientific Model Development*, *9*(4), 1293–1339. Retrieved 2021-08-10, from https://gmd.copernicus.org/articles/9/1293/2016/ doi: 10.5194/gmd-9-1293-2016

Campbell, H. (2021). The consequences of checking for zero-inflation and overdispersion in the analysis of count data. *Methods in Ecology and Evolution*, *12*(4), 665–680. Retrieved 2021-11-09, from https://onlinelibrary.wiley.com/doi/abs/10.1111/2041-210X.13559 (_eprint: https://onlinelibrary.wiley.com/doi/pdf/10.1111/2041-210X.13559) doi: 10.1111/2041-210X.13559

Campbell, J. (1995, August). The lognormal distribution as a model for bio-optical variability in the sea. *Journal of Geophysical Research Atmospheres*, *100*. doi: 10.1029/95JC00458

Caperon, J. (1967). Population Growth in Micro-Organisms Limited by Food Supply. *Ecology*, *48*(5), 715–722. Retrieved 2022-04-01, from https://onlinelibrary.wiley.com/doi/abs/10.2307/1933728 (_eprint: https://onlinelibrary.wiley.com/doi/pdf/10.2307/1933728) doi: 10.2307/1933728

Chen, B., Laws, E. A., Liu, H., & Huang, B. (2014). Estimating microzooplankton grazing half-saturation constants from dilution experiments with non-linear feeding kinetics. *Limnology and Oceanography*, *59*(3), 639–644. doi: 10.4319/lo.2014.59.3.0639

Chenillat, F., Rivière, P., & Ohman, M. D. (2021, May). On the sensitivity of plankton ecosystem models to the formulation of zooplankton grazing. *PLOS ONE*, *16*(5), e0252033. Retrieved 2021-05-27, from https://journals.plos.org/plosone/article?id=10.1371/journal.pone.0252033 doi: 10.1371/journal.pone.0252033

Chow-Fraser, P., & Sprules, W. G. (1992, April). Type-3 functional response in limnetic suspension-feeders, as demonstrated by in situ grazing rates. *Hydrobiologia*, *232*(3), 175–191. doi: 10.1007/BF00013703

Christian, J. R., Denman, K. L., Hayashida, H., Holdsworth, A. M., Lee, W. G., Riche, O. G. J., ... Swart, N. C. (2021, October). Ocean biogeochemistry in the Canadian Earth System Model version 5.0.3: CanESM5 and CanESM5-CanOE. *Geoscientific Model Development Discussions*, 1–68. Retrieved 2022-01-05, from https://gmd.copernicus.org/preprints/gmd-2021-327/ doi: 10.5194/gmd-2021-327

Clerc, C., Aumont, O., & Bopp, L. (2021, July). Should we account for mesozooplankton reproduction and ontogenetic growth in biogeochemical modeling? *Theoretical Ecology*. Retrieved 2021-07-20, from https://doi.org/10.1007/s12080-021-00519-5 doi: 10.1007/s12080-021-00519-5

Denny, M. (2014). Buzz Holling and the Functional Response. *The Bulletin of the Ecological Society of America*, *95*(3), 200–203. Retrieved 2021-09-23, from https://onlinelibrary.wiley.com/doi/abs/10.1890/0012-9623-95.3.200

(_eprint: https://esajournals.onlinelibrary.wiley.com/doi/pdf/10.1890/0012-9623-95.3.200) doi: 10.1890/0012-9623-95.3.200

Doney, S. C. (1999). Major challenges confronting marine biogeochemical modeling. *Global Biogeochemical Cycles*, *13*(3), 705–714. doi: 10.1029/1999GB900039

Druon, J.-N., Hélaouët, P., Beaugrand, G., Fromentin, J.-M., Palialexis, A., & Hoepffner, N. (2019, March). Satellite-based indicator of zooplankton distribution for global monitoring. *Scientific Reports*, *9*(1), 4732. Retrieved 2021-11-09, from https://www.nature.com/articles/s41598-019-41212-2 (Bandiera_abtest: a Cc_license_type: cc_by Cg_type: Nature Research Journals Number: 1 Primary_atype: Research Publisher: Nature Publishing Group Subject_term: Ecological modelling;Ecosystem ecology;Marine biology Subject_term_id: ecological-modelling;ecosystem-ecology;marine-biology) doi: 10.1038/s41598-019-41212-2

Dunn, R. P., & Hovel, K. A. (2020, January). Predator type influences the frequency of functional responses to prey in marine habitats. *Biology Letters*, *16*(1), 20190758. (Publisher: Royal Society) doi: 10.1098/rsbl.2019.0758

Dutkiewicz, S., Hickman, A. E., Jahn, O., Gregg, W. W., Mouw, C. B., & Follows, M. J. (2015, July). Capturing optically important constituents and properties in a marine biogeochemical and ecosystem model. *Biogeosciences*, *12*(14), 4447–4481. doi: 10.5194/bg-12-4447-2015

Edwards, A. M., & Yool, A. (2000, June). The role of higher predation in plankton population models. *Journal of Plankton Research*, *22*(6), 1085–1112. Retrieved 2022-04-04, from https://doi.org/10.1093/plankt/22.6.1085 doi: 10.1093/plankt/22.6.1085

Edwards, C., Powell, T., & Batchelder, H. (2000, January). The stability of an NPZ model subject to realistic levels of vertical mixing. *Journal of Marine Research*, *58*. doi: 10.1357/002224000321511197

Edwards, C. A., Batchelder, H. P., & Powell, T. M. (2000, September). Modeling microzooplankton and macrozooplankton dynamics within a coastal upwelling system. *Journal of Plankton Research*, *22*(9), 1619–1648. (Publisher: Oxford Academic) doi: 10.1093/plankt/22.9.1619

Evans, G. T., & Parslow, J. S. (1985, January). A Model of Annual Plankton Cycles. *Biological Oceanography*, *3*(3), 327–347. (Publisher: Taylor & Francis) doi: 10.1080/01965581.1985.10749478

Eyring, V., Bony, S., Meehl, G. A., Senior, C. A., Stevens, B., Stouffer, R. J., & Taylor, K. E. (2016, May). Overview of the Coupled Model Intercomparison Project Phase 6 (CMIP6) experimental design and organization. *Geoscientific Model Development*, *9*(5), 1937–1958. (Publisher: Copernicus GmbH) doi: 10.5194/gmd-9-1937-2016

Falls, M., Bernardello, R., Castrillo, M., Acosta, M., Llort, J., & Galí, M. (2022, July). Use of genetic algorithms for ocean model parameter optimisation: a case study using PISCES-v2_rc for North Atlantic particulate organic carbon. *Geoscientific Model Development*, *15*(14), 5713–5737. Retrieved 2022-08-08, from https://gmd.copernicus.org/articles/15/5713/2022/ (Publisher: Copernicus GmbH) doi: 10.5194/gmd-15-5713-2022

Fasham, M. J. R. (1995, July). Variations in the seasonal cycle of biological production in subarctic oceans: A model sensitivity analysis. *Deep Sea Research Part I: Oceanographic Research Papers*, *42*(7), 1111–1149. doi: 10.1016/0967-0637(95)00054-A

Fasham, M. J. R., Ducklow, H. W., & McKelvie, S. M. (1990, August). A nitrogen-based model of plankton dynamics in the oceanic mixed layer. *Journal of Marine Research*, *48*(3), 591–639. doi: 10.1357/002224090784984678

Flato, G., Marotzke, J., Abiodun, B., Braconnot, P., Chou, S. C., Collins, W., ... Rummukainen, M. (2013). *Evaluation of climate models*. Cambridge University Press. (Pages: 741) doi: 10.1017/CBO9781107415324.020

Flynn, K. J., & Mitra, A. (2016). Why Plankton Modelers Should Reconsider Using Rectangular Hyperbolic (Michaelis-Menten, Monod) Descriptions of Predator-Prey Interactions. *Frontiers in Marine Science*, *3*. (Publisher: Frontiers) doi: 10.3389/fmars.2016.00165

Follows, M. J., & Dutkiewicz, S. (2011). Modeling Diverse Communities of Marine Microbes. *Annual Review of Marine Science*, *3*(1), 427–451. Retrieved 2022-04-28, from `https://doi.org/10.1146/annurev-marine-120709-142848` (_eprint: https://doi.org/10.1146/annurev-marine-120709-142848) doi: 10.1146/annurev-marine-120709-142848

Franks, P., & Chen, C. (1996, July). Plankton production in tidal fronts: A model of Georges Bank in summer. *Journal of Marine Research*, *54*(4), 631–651. doi: 10.1357/0022240963213718

Franks, P., & Chen, C. (2001, January). A 3-D prognostic numerical model study of the Georges bank ecosystem. Part II: Biological–Physical model. *Deep Sea Research Part II: Topical Studies in Oceanography*, *48*(1), 457–482. doi: 10.1016/S0967-0645(00)00125-9

Franks, P., Wroblewski, J. S., & Flierl, G. R. (1986, April). Behavior of a simple plankton model with food-level acclimation by herbivores. *Marine Biology*, *91*(1), 121–129. doi: 10.1007/BF00397577

Frost, B. W. (1972). Effects of Size and Concentration of Food Particles on the Feeding Behavior of the Marine Planktonic Copepod Calanus Pacificus1. *Limnology and Oceanography*, *17*(6), 805–815. (tex.copyright: © 1972, by the Association for the Sciences of Limnology and Oceanography, Inc.) doi: 10.4319/lo.1972.17.6.0805

Frost, B. W. (1975). A threshold feeding behavior in Calanus pacificus1. *Limnology and Oceanography*, *20*(2), 263–266. (tex.copyright: © 1975, by the Association for the Sciences of Limnology and Oceanography, Inc.) doi: 10.4319/lo.1975.20.2.0263

Fussmann, G. F., & Blasius, B. (2005, March). Community response to enrichment is highly sensitive to model structure. *Biology Letters*, *1*(1), 9–12. (Publisher: Royal Society) doi: 10.1098/rsbl.2004.0246

Gentleman, W. C., Leising, A., Frost, B., Strom, S., & Murray, J. (2003, November). Functional responses for zooplankton feeding on multiple resources: A review of assumptions and biological dynamics. *Deep Sea Research Part II: Topical Studies in Oceanography*, *50*(22), 2847–2875. doi: 10.1016/j.dsr2.2003.07.001

Gentleman, W. C., & Neuheimer, A. B. (2008, November). Functional responses and ecosystem dynamics: How clearance rates explain the influence of satiation, food-limitation and acclimation. *Journal of Plankton Research*, *30*(11), 1215–1231. doi: 10.1093/plankt/fbn078

Giske, J., Rosland, R., Berntsen, J., & Fiksen, (1997, February). Ideal free distribution of copepods under predation risk. *Ecological Modelling*, *95*(1), 45–59. Retrieved 2022-08-04, from `https://www.sciencedirect.com/science/article/pii/S0304380096000270` doi: 10.1016/S0304-3800(96)00027-0

Gismervik, I. (2005, September). Numerical and functional responses of choreo- and oligotrich planktonic ciliates. *Aquatic Microbial Ecology*, *40*(2), 163–173. doi: 10.3354/ame040163

Gismervik, I., & Andersen, T. (1997, October). Prey switching by Acartia clausi: Experimental evidence and implications of intraguild predation assessed by a model. *Marine Ecology Progress Series*, *157*, 247–259. doi: 10.3354/meps157247

Gross, T., Ebenhöh, W., & Feudel, U. (2004, April). Enrichment and foodchain stability: The impact of different forms of Predator–Prey interaction. *Journal of Theoretical Biology*, *227*(3), 349–358. doi: 10.1016/j.jtbi.2003.09.020

Hajima, T., Watanabe, M., Yamamoto, A., Tatebe, H., Noguchi, M. A., Abe, M., ... Kawamiya, M. (2020, May). Development of the MIROC-ES2L Earth

system model and the evaluation of biogeochemical processes and feedbacks. *Geoscientific Model Development*, *13*(5), 2197–2244. Retrieved 2022-03-10, from https://gmd.copernicus.org/articles/13/2197/2020/ (Publisher: Copernicus GmbH) doi: 10.5194/gmd-13-2197-2020

Hansen, P. J., Bjørnsen, P. K., & Hansen, B. W. (1997). Zooplankton grazing and growth: Scaling within the 2-2,-Mm body size range. *Limnology and Oceanography*, *42*(4), 687–704. doi: 10.4319/lo.1997.42.4.0687

Hansen, P. J., Bjørnsen, P. K., & Hansen, B. W. (2014, August). Maximum ingestion and maximum clearance rate of Zooplankton determined experimentally. Retrieved 2021-05-11, from https://doi.pangaea.de/10.1594/PANGAEA.834800 (Publisher: PANGAEA type: dataset) doi: 10.1594/PANGAEA.834800

Harrison, C. S., Long, M. C., Lovenduski, N. S., & Moore, J. K. (2018, April). Mesoscale Effects on Carbon Export: A Global Perspective. *Global Biogeochemical Cycles*, *0*(0). doi: 10.1002/2017GB005751

Hauck, J., Völker, C., Wang, T., Hoppema, M., Losch, M., & Wolf-Gladrow, D. A. (2013). Seasonally different carbon flux changes in the Southern Ocean in response to the southern annular mode. *Global Biogeochemical Cycles*, *27*(4), 1236–1245. (tex.copyright: © 2013 The Authors. Global Biogeochemical Cycles published byWiley on behalf of the American Geophysical Union.) doi: 10.1002/2013GB004600

Heneghan, R. F., Everett, J. D., Sykes, P., Batten, S. D., Edwards, M., Takahashi, K., ... Richardson, A. J. (2020, November). A functional size-spectrum model of the global marine ecosystem that resolves zooplankton composition. *Ecological Modelling*, *435*, 109265. Retrieved 2021-08-10, from https://www.sciencedirect.com/science/article/pii/S0304380020303355 doi: 10.1016/j.ecolmodel.2020.109265

Herman, A. W., & Platt, T. (1983, January). Numerical modelling of diel carbon production and zooplankton grazing on the Scotian shelf based on observational data. *Ecological Modelling*, *18*(1), 55–72. Retrieved 2022-08-04, from https://www.sciencedirect.com/science/article/pii/0304380083900753 doi: 10.1016/0304-3800(83)90075-3

Hernández-García, E., & López, C. (2004, September). Sustained plankton blooms under open chaotic flows. *Ecological Complexity*, *1*(3), 253–259. doi: 10.1016/j.ecocom.2004.05.002

Hirst, A. G., & Bunker, A. J. (2003). Growth of marine planktonic copepods: Global rates and patterns in relation to chlorophyll a, temperature, and body weight. *Limnology and Oceanography*, *48*(5), 1988–2010. doi: 10.4319/lo.2003.48.5.1988

Holling, C. S. (1959a, May). The Components of Predation as Revealed by a Study of Small-Mammal Predation of the European Pine Sawfly1. *The Canadian Entomologist*, *91*(5), 293–320. (Publisher: Cambridge University Press) doi: 10.4039/Ent91293-5

Holling, C. S. (1959b, July). Some Characteristics of Simple Types of Predation and Parasitism. *The Canadian Entomologist*, *91*(7), 385–398. doi: 10.4039/Ent91385-7

Holling, C. S. (1965). The Functional Response of Predators to Prey Density and its Role in Mimicry and Population Regulation. *The Memoirs of the Entomological Society of Canada*, *97*(S45), 5–60. doi: 10.4039/entm9745fv

Ivlev, V. (1961). *Experimental ecology of the feeding of fishes*. New Haven: Yale University Press.

Jeschke, J. M., Kopp, M., & Tollrian, R. (2004). Consumer-food systems: Why type I functional responses are exclusive to filter feeders. *Biological Reviews*, *79*(2), 337–349. doi: 10.1017/S1464793103006286

Kane, A., Moulin, C., Thiria, S., Bopp, L., Berrada, M., Tagliabue, A., ... Bad-

ran, F. (2011, June). Improving the parameters of a global ocean biogeochemical model via variational assimilation of in situ data at five time series stations. *Journal of Geophysical Research*, *116*(C6), C06011. Retrieved 2022-08-08, from http://doi.wiley.com/10.1029/2009JC006005 doi: 10.1029/2009JC006005

Kroodsma, D. A., Mayorga, J., Hochberg, T., Miller, N. A., Boerder, K., Ferretti, F., ... Worm, B. (2018, February). Tracking the global footprint of fisheries. *Science*, *359*(6378), 904–908. Retrieved 2021-06-01, from https://science.sciencemag.org/content/359/6378/904 doi: 10.1126/science.aao5646

Lampert, W. (2005, April). Vertical distribution of zooplankton: density dependence and evidence for an ideal free distribution with costs. *BMC Biology*, *3*(1), 10. Retrieved 2022-08-04, from https://doi.org/10.1186/1741-7007-3-10 doi: 10.1186/1741-7007-3-10

Lancelot, C., Spitz, Y., Gypens, N., Ruddick, K., Becquevort, S., Rousseau, V., ... Billen, G. (2005, March). Modelling diatom and Phaeocystis blooms and nutrient cycles in the Southern Bight of the North Sea: The MIRO model. *Marine Ecology Progress Series*, *289*, 63–78. doi: 10.3354/meps289063

Laufkötter, C., Vogt, M., Gruber, N., Aita-Noguchi, M., Aumont, O., Bopp, L., ... Völker, C. (2015, December). Drivers and Uncertainties of Future Global Marine Primary Production in Marine Ecosystem Models. *Biogeosciences*, *12*(23), 6955–6984. doi: 10.5194/bg-12-6955-2015

Law, R. M., Ziehn, T., Matear, R. J., Lenton, A., Chamberlain, M. A., Stevens, L. E., ... Vohralik, P. F. (2017, July). The carbon cycle in the Australian Community Climate and Earth System Simulator (ACCESS-ESM1) – Part 1: Model description and pre-industrial simulation. *Geoscientific Model Development*, *10*(7), 2567–2590. doi: 10.5194/gmd-10-2567-2017

Laws, E. A., Falkowski, P. G., Smith, W. O., Ducklow, H., & McCarthy, J. J. (2000). Temperature Effects on Export Production in the Open Ocean. *Global Biogeochemical Cycles*, *14*(4), 1231–1246. (tex.copyright: Copyright 2000 by the American Geophysical Union.) doi: 10.1029/1999GB001229

Leising, A. W., Gentleman, W. C., & Frost, B. W. (2003, November). The threshold feeding response of microzooplankton within Pacific high-nitrate low-chlorophyll ecosystem models under steady and variable iron input. *Deep Sea Research Part II: Topical Studies in Oceanography*, *50*(22), 2877–2894. doi: 10.1016/j.dsr2.2003.07.002

Le Quéré, C., Buitenhuis, E. T., Moriarty, R., Alvain, S., Aumont, O., Bopp, L., ... Vallina, S. M. (2016, July). Role of Zooplankton Dynamics for Southern Ocean Phytoplankton Biomass and Global Biogeochemical Cycles. *Biogeosciences*, *13*(14), 4111–4133. doi: 10.5194/bg-13-4111-2016

Long, M. C., Moore, J. K., Lindsay, K., Levy, M., Doney, S. C., Luo, J. Y., ... Sylvester, Z. T. (2021). Simulations With the Marine Biogeochemistry Library (MARBL). *Journal of Advances in Modeling Earth Systems*, *13*(12), e2021MS002647. Retrieved 2022-01-05, from https://onlinelibrary.wiley.com/doi/abs/10.1029/2021MS002647 doi: 10.1029/2021MS002647

Lotka, A. J. (1910, March). Contribution to the Theory of Periodic Reactions. *The Journal of Physical Chemistry*, *14*(3), 271–274. (Publisher: American Chemical Society) doi: 10.1021/j150111a004

Malchow, H., Hilker, F. M., Sarkar, R. R., & Brauer, K. (2005, November). Spatiotemporal patterns in an excitable plankton system with lysogenic viral infection. *Mathematical and Computer Modelling*, *42*(9), 1035–1048. doi: 10.1016/j.mcm.2004.10.025

Matear, R. J. (1995, July). Parameter optimization and analysis of ecosystem models using simulated annealing: A case study at Station P. *Journal of Marine Research*, *53*(4), 571–607. doi: 10.1357/0022240953213098

Maury, O. (2010, January). An overview of APECOSM, a spatialized mass balanced "Apex Predators ECOSystem Model" to study physiologically structured tuna population dynamics in their ecosystem. *Progress in Oceanography*, *84*(1), 113–117. doi: 10.1016/j.pocean.2009.09.013

Mayzaud, P., & Poulet, S. A. (1978). The importance of the time factor in the response of zooplankton to varying concentrations of naturally occurring particulate matter 1. *Limnology and Oceanography*, *23*(6), 1144–1154. (tex.copyright: © 1978, by the Association for the Sciences of Limnology and Oceanography, Inc.) doi: 10.4319/lo.1978.23.6.1144

Mayzaud, P., Tirelli, V., Bernard, J. M., & Roche-Mayzaud, O. (1998, June). The influence of food quality on the nutritional acclimation of the copepod Acartia clausi. *Journal of Marine Systems*, *15*(1), 483–493. doi: 10.1016/S0924-7963(97)00039-0

McCauley, E., & Murdoch, W. W. (1987, January). Cyclic and Stable Populations: Plankton as Paradigm. *The American Naturalist*, *129*(1), 97–121. Retrieved 2021-08-20, from `https://www.journals.uchicago.edu/doi/abs/10.1086/284624` (Publisher: The University of Chicago Press) doi: 10.1086/284624

Menden-Deuer, S., & Lessard, E. J. (2000). Carbon to volume relationships for dinoflagellates, diatoms, and other protist plankton. *Limnology and Oceanography*, *45*(3), 569–579. Retrieved 2022-04-18, from `https://onlinelibrary.wiley.com/doi/abs/10.4319/lo.2000.45.3.0569` (_eprint: https://onlinelibrary.wiley.com/doi/pdf/10.4319/lo.2000.45.3.0569) doi: 10.4319/lo.2000.45.3.0569

Michaelis, L., & Menten, M. (1913). Die Kinetik der Invertinwirkung. *Biochem Z*, *49*, 333–369.

Moloney, C. L., & Field, J. G. (1989). General allometric equations for rates of nutrient uptake, ingestion, and respiration in plankton organisms. *Limnology and Oceanography*, *34*(7), 1290–1299. Retrieved 2021-04-09, from `https://aslopubs.onlinelibrary.wiley.com/doi/abs/10.4319/lo.1989.34.7.1290` (_eprint: https://aslopubs.onlinelibrary.wiley.com/doi/pdf/10.4319/lo.1989.34.7.1290) doi: https://doi.org/10.4319/lo.1989.34.7.1290

Monod, J. (1949, October). The growth of bacterial cultures. *Annual Review of Microbiology*, *3*(1), 371–394. (Publisher: Annual Reviews) doi: 10.1146/annurev.mi.03.100149.002103

Moore, J. K., Lindsay, K., Doney, S. C., Long, M. C., & Misumi, K. (2013, August). Marine Ecosystem Dynamics and Biogeochemical Cycling in the Community Earth System Model [CESM1(BGC)]: Comparison of the 1990s with the 2090s under the RCP4.5 and RCP8.5 Scenarios. *Journal of Climate*, *26*(23), 9291–9312. doi: 10.1175/JCLI-D-12-00566.1

Moriarty, R., Buitenhuis, E. T., Le Quéré, C., & Gosselin, M.-P. (2013, July). Distribution of known macrozooplankton abundance and biomass in the global ocean. *Earth System Science Data*, *5*(2), 241–257. doi: 10.5194/essd-5-241-2013

Moriarty, R., & O'Brien, T. (2012, September). Mesozooplankton biomass in the global ocean. *Earth System Science Data Discussions*, *5*, 893–919. doi: 10.5194/essdd-5-893-2012

Morozov, A. (2010). Emergence of Holling type III zooplankton functional response: Bringing together field evidence and mathematical modelling. *Journal of Theoretical Biology*, *265*(1), 45–54. doi: 10.1016/j.jtbi.2010.04.016

Morozov, A., & Arashkevich, E. (2008). Patterns of Zooplankton Functional Response in Communities with Vertical Heterogeneity: a Model Study. *Mathematical Modelling of Natural Phenomena*, *3*(3), 131–148. Retrieved 2022-08-04, from `https://www.mmnp-journal.org/articles/mmnp/abs/2008/03/mmnp20083p131/mmnp20083p131.html` (Number: 3 Publisher: EDP Sciences)

doi: 10.1051/mmnp:2008061

Morozov, A., & Arashkevich, E. (2010, January). Towards a correct description of zooplankton feeding in models: Taking into account food-mediated unsynchronized vertical migration. *Journal of Theoretical Biology*, *262*(2), 346–360. Retrieved 2022-04-21, from https://www.sciencedirect.com/science/article/pii/S0022519309004536 doi: 10.1016/j.jtbi.2009.09.023

Morozov, A., Arashkevich, E., Reigstad, M., & Falk-Petersen, S. (2008, October). Influence of spatial heterogeneity on the type of zooplankton functional response: A study based on field observations. *Deep Sea Research Part II: Topical Studies in Oceanography*, *55*(20), 2285–2291. doi: https://doi.org/10.1016/j.dsr2.2008.05.008

Neelin, J. D., Bracco, A., Luo, H., McWilliams, J. C., & Meyerson, J. E. (2010, December). Considerations for parameter optimization and sensitivity in climate models. *Proceedings of the National Academy of Sciences*, *107*(50), 21349–21354. Retrieved 2021-10-13, from https://www.pnas.org/content/107/50/21349 (Publisher: National Academy of Sciences Section: Physical Sciences) doi: 10.1073/pnas.1015473107

Oaten, A., & Murdoch, W. W. (1975, May). Functional Response and Stability in Predator-Prey Systems. *The American Naturalist*, *109*(967), 289–298. (Publisher: The University of Chicago Press) doi: 10.1086/282998

Ohman, M. D. (1990). The Demographic Benefits of Diel Vertical Migration by Zooplankton. *Ecological Monographs*, *60*(3), 257–281. (tex.copyright: © 1990 by the Ecological Society of America) doi: 10.2307/1943058

Oke, P. R., Griffin, D. A., Schiller, A., Matear, R. J., Fiedler, R., Mansbridge, J., ... Ridgway, K. (2013, May). Evaluation of a near-global eddy-resolving ocean model. *Geoscientific Model Development*, *6*, 591–615. doi: 10.5194/gmd-6-591-2013

Pearre, S. (2003, February). Eat and run? The hunger/satiation hypothesis in vertical migration: history, evidence and consequences. *Biological Reviews*, *78*(1), 1–79. Retrieved 2022-08-04, from https://www.cambridge.org/core/journals/biological-reviews/article/abs/eat-and-run-the-hungersatiation-hypothesis-in-vertical-migration-history-evidence-and-consequences/50A1C5DC5D56B93197B31BB386B72CC6 (Publisher: Cambridge University Press) doi: 10.1017/S146479310200595X

Peters, R. H., & Downing, J. A. (1984). Empirical analysis of zooplankton filtering and feeding rates1. *Limnology and Oceanography*, *29*(4), 763–784. Retrieved 2021-04-09, from https://aslopubs.onlinelibrary.wiley.com/doi/abs/10.4319/lo.1984.29.4.0763 (_eprint: https://aslopubs.onlinelibrary.wiley.com/doi/pdf/10.4319/lo.1984.29.4.0763) doi: https://doi.org/10.4319/lo.1984.29.4.0763

Pierson, J. J., Frost, B. W., & Leising, A. W. (2013, February). Foray foraging behavior: seasonally variable, food-driven migratory behavior in two calanoid copepod species. *Marine Ecology Progress Series*, *475*, 49–64. Retrieved 2022-08-04, from https://www.int-res.com/abstracts/meps/v475/p49-64/ doi: 10.3354/meps10116

Ray, S., Sandip, M., Mukherjee, J., M, R., Mandal, S., & Saikia, S. (2011, January). Body Size versus Rate Parameters of Zooplankton and Phytoplankton: Effects on Aquatic Ecosystems. In *Zooplankton and Phytoplankton: Types, Characteristics and Ecology* (pp. 219–228). (Journal Abbreviation: Zooplankton and Phytoplankton: Types, Characteristics and Ecology)

Raymont, J. E. G. (2014). *Plankton & Productivity in the Oceans: Volume 1: Phytoplankton*. Elsevier.

Real, L. A. (1977, March). The Kinetics of Functional Response. *The American Naturalist*, *111*(978), 289–300. (Publisher: The University of Chicago Press) doi: 10.1086/283161

Real, L. A. (1979). Ecological Determinants of Functional Response. *Ecology*, *60*(3), 481–485. (Publisher: Ecological Society of America) doi: 10.2307/1936067

Richardson, A. J., & Verheye, H. M. (1998, January). The relative importance of food and temperature to copepod egg production and somatic growth in the southern Benguela upwelling system. *Journal of Plankton Research*, *20*(12), 2379–2399. Retrieved 2021-07-05, from `https://doi.org/10.1093/plankt/20.12.2379` doi: 10.1093/plankt/20.12.2379

Saiz, E., & Calbet, A. (2007). Scaling of feeding in marine calanoid copepods. *Limnology and Oceanography*, *52*(2), 668–675. Retrieved 2021-04-09, from `https://aslopubs.onlinelibrary.wiley.com/doi/abs/10.4319/lo.2007.52.2.0668` (_eprint: https://aslopubs.onlinelibrary.wiley.com/doi/pdf/10.4319/lo.2007.52.2.0668) doi: https://doi.org/10.4319/lo.2007.52.2.0668

Sarnelle, O., & Wilson, A. E. (2008). Type Iii Functional Response in Daphnia. *Ecology*, *89*(6), 1723–1732. (tex.copyright: © 2008 by the Ecological Society of America) doi: 10.1890/07-0935.1

Schartau, M., & Oschlies, A. (2003a, November). Simultaneous data-based optimization of a 1D-Ecosystem model at three locations in the North Atlantic: Part II—Standing stocks and nitrogen fluxes. *Journal of Marine Research*, *61*, 794–820. doi: 10.1357/002224003322981156

Schartau, M., & Oschlies, A. (2003b, November). Simultaneous data-based optimization of a 1D-Ecosystem model at three locations in the North Atlantic: Part I—Method and parameter estimates. *Journal of Marine Research*, *61*, 765–793. doi: 10.1357/002224003322981147

Schartau, M., Wallhead, P., Hemmings, J., Löptien, U., Kriest, I., Krishna, S., ... Oschlies, A. (2017, March). Reviews and syntheses: Parameter identification in marine planktonic ecosystem modelling. *Biogeosciences*, *14*(6), 1647–1701. doi: 10.5194/bg-14-1647-2017

Scherrer, K. J. N., Harrison, C. S., Heneghan, R. F., Galbraith, E., Bardeen, C. G., Coupe, J., ... Xia, L. (2020, November). Marine wild-capture fisheries after nuclear war. *Proceedings of the National Academy of Sciences*. (Publisher: National Academy of Sciences Section: Biological Sciences tex.copyright: Copyright © 2020 the Author(s). Published by PNAS.. https://creativecommons.org/licenses/by-nc-nd/4.0/This open access article is distributed under Creative Commons Attribution-NonCommercial-NoDerivatives License 4.0 (CC BY-NC-ND).) doi: 10.1073/pnas.2008256117

Shigemitsu, M., Okunishi, T., Nishioka, J., Sumata, H., Hashioka, T., Aita, M. N., ... Yamanaka, Y. (2012). Development of a one-dimensional ecosystem model including the iron cycle applied to the Oyashio region, western subarctic Pacific. *Journal of Geophysical Research: Oceans*, *117*(C6). (tex.copyright: ©2012. American Geophysical Union. All Rights Reserved.) doi: 10.1029/2011JC007689

Smith, S., Pahlow, M., Merico, A., Acevedo-Trejos, E., Yoshikawa, C., Sasai, Y., ... Honda, M. (2015, April). Flexible Phytoplankton Functional Type (FlexPFT) model: Size-scaling of traits and optimal growth. *Journal of Plankton Research*, *38*, 977–992.

Solomon, M. E. (1949). The Natural Control of Animal Populations. *Journal of Animal Ecology*, *18*(1), 1–35. Retrieved 2021-09-23, from `https://www.jstor.org/stable/1578` (Publisher: [Wiley, British Ecological Society]) doi: 10.2307/1578

Steele, J. (1974). Stability of plankton ecosystems. In M. B. Usher & M. H. Williamson (Eds.), *Ecological Stability* (pp. 179–191). Boston, MA: Springer US. doi: 10.1007/978-1-4899-6938-5_12

Steele, J. H., & Henderson, E. W. (1992, January). The role of predation in plankton models. *Journal of Plankton Research*, *14*(1), 157–172. Retrieved 2022-04-

04, from https://doi.org/10.1093/plankt/14.1.157 doi: 10.1093/plankt/14.1.157

Stock, C. A., Dunne, J. P., Fan, S., Ginoux, P., John, J., Krasting, J. P., ... Zadeh, N. (2020). Ocean Biogeochemistry in GFDL's Earth System Model 4.1 and Its Response to Increasing Atmospheric CO2. *Journal of Advances in Modeling Earth Systems*, *12*(10), e2019MS002043. Retrieved 2022-01-05, from https://onlinelibrary.wiley.com/doi/abs/10.1029/2019MS002043 doi: 10.1029/2019MS002043

Stock, C. A., Dunne, J. P., & John, J. G. (2014, January). Global-scale carbon and energy flows through the marine planktonic food web: An analysis with a coupled Physical–Biological model. *Progress in Oceanography*, *120*, 1–28. doi: 10.1016/j.pocean.2013.07.001

Stock, C. A., Powell, T. M., & Levin, S. A. (2008, November). Bottom–up and Top–down forcing in a simple size-structured plankton dynamics model. *Journal of Marine Systems*, *74*(1), 134–152. doi: 10.1016/j.jmarsys.2007.12.004

Strom, S. L., & Morello, T. (1998, January). Comparative growth rates and yields of ciliates and heterotrophic dinoflagellates. *Journal of Plankton Research*, *20*(3), 571–584. Retrieved 2021-04-09, from https://doi.org/10.1093/plankt/20.3.571 doi: 10.1093/plankt/20.3.571

Taylor, K. E., Stouffer, R. J., & Meehl, G. A. (2012, April). An Overview of CMIP5 and the Experiment Design. *Bulletin of the American Meteorological Society*, *93*(4), 485–498. (Publisher: American Meteorological Society) doi: 10.1175/BAMS-D-11-00094.1

Tittensor, D. P., Eddy, T. D., Lotze, H. K., Galbraith, E. D., Cheung, W., Barange, M., ... Walker, N. D. (2018, April). A protocol for the intercomparison of marine fishery and ecosystem models: Fish-MIP v1.0. *Geoscientific Model Development*, *11*(4), 1421–1442. doi: 10.5194/gmd-11-1421-2018

Tittensor, D. P., Novaglio, C., Harrison, C. S., Heneghan, R. F., Barrier, N., Bianchi, D., ... Blanchard, J. L. (2021, October). Next-generation ensemble projections reveal higher climate risks for marine ecosystems. *Nature Climate Change*, 1–9. Retrieved 2021-10-25, from https://www.nature.com/articles/s41558-021-01173-9 doi: 10.1038/s41558-021-01173-9

Tjiputra, J. F., Schwinger, J., Bentsen, M., Morée, A. L., Gao, S., Bethke, I., ... Schulz, M. (2020, May). Ocean biogeochemistry in the Norwegian Earth System Model version 2 (NorESM2). *Geoscientific Model Development*, *13*(5), 2393–2431. Retrieved 2022-03-08, from https://gmd.copernicus.org/articles/13/2393/2020/ doi: 10.5194/gmd-13-2393-2020

Totterdell, I. J. (2019, October). Description and evaluation of the Diat-HadOCC model v1.0: The ocean biogeochemical component of HadGEM2-ES. *Geoscientific Model Development*, *12*(10), 4497–4549. (Publisher: Copernicus GmbH) doi: 10.5194/gmd-12-4497-2019

Truscott, J. E., & Brindley, J. (1994, September). Ocean plankton populations as excitable media. *Bulletin of Mathematical Biology*, *56*(5), 981–998. doi: 10.1016/S0092-8240(05)80300-3

Truscott, J. E., Brindley, J., Brindley, J., & Gray, P. (1994, June). Equilibria, stability and excitability in a general class of plankton population models. *Philosophical Transactions of the Royal Society of London. Series A: Physical and Engineering Sciences*, *347*(1685), 703–718. (Publisher: Royal Society) doi: 10.1098/rsta.1994.0076

Uye, S. (1986, July). Impact of copepod grazing on the red-tide flagellate Chattonella antiqua. *Marine Biology*, *92*(1), 35–43. doi: 10.1007/BF00392743

van Leeuwen, E., Jansen, V. a. A., & Bright, P. W. (2007). How Population Dynamics Shape the Functional Response in a One-Predator–Two-Prey System. *Ecology*, *88*(6), 1571–1581. (tex.copyright: © 2007 by the Ecological Society of America) doi: 10.1890/06-1335

Vichi, M., Pinardi, N., & Masina, S. (2007, January). A generalized model of pelagic biogeochemistry for the global ocean ecosystem. Part I: Theory. *Journal of Marine Systems*, *64*(1), 89–109. doi: 10.1016/j.jmarsys.2006.03.006

Volterra, V. (1927). *Variazioni e fluttuazioni del numero d'individui in specie animali conviventi*. C. Ferrari. (tex.googlebooks: 1ai9PgAACAAJ)

Wang, H., Morrison, W., Singh, A., & Weiss, H. H. (2009, June). Modeling inverted biomass pyramids and refuges in ecosystems. *Ecological Modelling*, *220*(11), 1376–1382. doi: 10.1016/j.ecolmodel.2009.03.005

Ward, B. A., Friedrichs, M. A. M., Anderson, T. R., & Oschlies, A. (2010, April). Parameter optimisation techniques and the problem of underdetermination in marine biogeochemical models. *Journal of Marine Systems*, *81*(1), 34–43. doi: 10.1016/j.jmarsys.2009.12.005

Wirtz, K. W. (2013, January). How fast can plankton feed? Maximum ingestion rate scales with digestive surface area. *Journal of Plankton Research*, *35*(1), 33–48. Retrieved 2021-04-09, from `https://doi.org/10.1093/plankt/fbs075` doi: 10.1093/plankt/fbs075

Yool, A., Palmiéri, J., Jones, C. G., de Mora, L., Kuhlbrodt, T., Popova, E. E., ... Sellar, A. A. (2021, June). Evaluating the physical and biogeochemical state of the global ocean component of UKESM1 in CMIP6 historical simulations. *Geoscientific Model Development*, *14*(6), 3437–3472. Retrieved 2022-01-05, from `https://gmd.copernicus.org/articles/14/3437/2021/` doi: 10.5194/gmd-14-3437-2021